

**Distribution and transportation
pathways of marine particulate
matter off Northwest Africa**

**Dissertation zur Erlangung
des Doktorgrades am
Fachbereich 5 – Geowissenschaften
der Universität Bremen**

Gutachter

Herr Prof. Dr. Gerold Wefer

Frau Dr. habil. Uta Passow

vorgelegt von Nicolas Nowald

Bremen, Mai 2004

When I think of the floor of the deep sea, the single, overwhelming fact that possesses my imagination is the accumulation of sediments. I see always the steady, unremitting, downward drift of materials from above, flake upon flake, layer upon layer – a drift that has continued for hundreds of millions of years, that will go on for as long as there are seas and continents ...

For the sediments are the materials of the most stupendous snowfall the earth has ever seen...

Rachael Carson

The Sea around Us (1951)

<i>Table of contents</i>	<i>Page</i>
Abstract	1
Zusammenfassung	3
1. Introduction	5
The global carbon cycle	5
Particulate matter in the ocean: distribution, formation and fate	7
1.1 Scientific goals	12
1.2 Study Area	14
Atmospheric settings	14
Oceanographic settings	14
1.3 Methods	16
1.3.1 Deep-sea camera system ParCa	17
Image analysis	18
Determination of particle parameter	19
1.3.2 Remotely operated vehicle (ROV)	21
Cherokee ROV	21
Winch and tether	21
Surface control units	22
Stereoscopic camera system	23
Deployment procedure	24
Image analysis	24
2. References	26
3. Publications	31
3.1 Manuscript 1:	31
The vertical distribution of particulate matter in the upwelling system off Cape Blanc (NW-Africa) obtained by high-resolution camera profiles and implications for rapid, vertical mass transfer	

3.2 Manuscript 2:	65
The abundance and size of marine particles off the NW-African coast (Dakhla, Cape Bojador) and the detection of a massive lateral intrusion	
3.3 Manuscript 3:	95
Observation of accumulation of marine particulate matter at the lower boundary of the mixed layer off NW-Africa (20°49'N / 17°58'W)	
4. Summary of research	117
5. Conclusions and outlook	120
Danksagung	

Abstract

The ocean off NW-Africa is strongly influenced by a large coastal upwelling system. Cold and nutrient rich deep-water is conveyed to the ocean surface along a broad belt, resulting in an enhanced growth of primary producers. Resulting particle fluxes and respectively, the transfer of carbon from the atmosphere to the deep-sea in the form of particulate matter, plays a key role in the global carbon cycle and hence, the global climate. The amount of material transferred from the sea surface to the ocean bottom is in the first instance quantified by the use of sediment traps, moored in different depths of the water column. Nevertheless, little is known about the in-situ distribution of particles in the water column and its transportation pathways in this specific region.

In this study a profiling camera system and a from the ships undulations decoupled remotely operated vehicle (ROV) was used for in-situ observations on the distribution, transport processes and sinking behaviour of marine particulate matter. Between the regional areas of investigation Cape Blanc, Dakhla and Cape Bojador significant differences could be observed with respect to distribution and transportation patterns. These differences are primarily related to the different primary production conditions between the investigation areas. Primary production is the most important factor for the abundance of particulate matter, where highest particle concentrations in the entire water column were seen off Cape Blanc. Next to primary production, water depth, currents and density gradients are factors influencing the particle distribution patterns. With respect to the prevailing transport processes, the Cape Blanc region is characterised by predominant, vertically orientated transport patterns. In addition to the continuous supply of large, relatively fast sinking particle aggregates a sinking event could be documented for the first time in-situ in the water column. These events deliver huge amounts of particulate matter from the ocean surface to the seafloor within several days. The observed transport processes off Cape Blanc emphasize a very close coupling between surface and deep-sea. Although vertical transport is important off Dakhla and Cape Bojador as well, it is not as pronounced and intense compared to the Cape Blanc region. Off Cape Bojador, large amounts of material from the shelf or upper slope areas are laterally advected towards the open ocean. This advection process could be observed in-situ with aid of the particle camera. However, similar processes could not be detected off Cape Blanc or Dakhla.

The vertical distribution of particles, acquired with aid of the profiling camera system, showed significant differences. Particle concentrations measured at the lower boundary of the euphotic zone, decreased from 200 down to 50 particles per litre within a few metres. The

applied horizontal transects up to a maximum length of 20 m with the ROV, showed no significant changes on short spatial scales. The observation of sinking particles revealed that particles sink with changing velocities in different water depths. The evaluation of particle trajectories in a particle minimum zone around 100 m depth showed a distinct vertical sinking direction. In contrast, particles are reduced in their sinking speeds in a particle maximum layer 75 m deeper. The reduction of the sinking velocities, lead to an accumulation of large amounts of material at the border of the upper mixed layer to the midwater column.

Zusammenfassung

Die Region vor der NW-Afrikanischen Küste wird durch ein großes Auftriebsgebiet charakterisiert. Kaltes, nährstoffreiches Wasser gelangt in einem breiten Auftriebsgürtel an die Meeresoberfläche und fördert dort das Wachstum von Primärproduzenten. Diese besondere Situation machte die NW-Afrikanische Küste zum Ziel intensiver Forschungsarbeiten, u.a. mit Blick auf die vertikalen Partikel Flüsse. Der Partikel Fluss, also der Transport von organisch gebundenem Kohlenstoff aus der Atmosphäre in das Sediment, spielt eine besondere Rolle im globalen Kohlenstoffhaushalt und nimmt somit Einfluss auf das weltweite Klima. Die Bilanzierung der Menge des aus dem Oberflächenwasser exportierten Materials erfolgte in erster Linie mit Hilfe von Sinkstofffallen. Allerdings ist bislang wenig darüber bekannt, wie das partikuläre Material in dieser Region in der Wassersäule verteilt ist, bzw. welche Transportprozesse und –wege hier eine Rolle spielen.

Mit Hilfe einer profilierenden Tiefseekamera und eines von den Schiffsbewegungen entkoppelten Tauchrobotersystems (ROV), wurden in-situ Studien an Partikeln hinsichtlich ihrer Verteilung, Transportprozesse und Sinkverhalten durchgeführt. Es zeigen sich deutliche Unterschiede im Hinblick auf Verteilung und Transport von Partikeln in den einzelnen Untersuchungsgebieten. Diese sind Kap Blanc im Süden, Dakhla und Kap Bojador weiter nördlich. Die Ursachen liegen in erster Linie in den unterschiedlichen Produktivitätsbedingungen der einzelnen Gebiete. Die Primärproduktion ist der maßgeblichste Steuerungsfaktor für Partikelverteilungen im Oberflächenwasser und diese ist am höchsten vor Kap Blanc. Dort wurden mit Abstand die höchsten Konzentrationen in der gesamten Wassersäule gemessen. Als weitere Steuerfaktoren für Partikelverteilungsmuster werden Wassertiefe, Strömungen und Dichtegradienten angeführt. Hinsichtlich der Transportprozesse lässt sich feststellen, dass das Gebiet vor Kap Blanc von einer sehr starken, deutlich vertikal ausgerichteten Transportrichtung geprägt wird. Abgesehen von einem kontinuierlichen Transfer großer, schnell sinkender Partikelaggregate konnte erstmalig ein Absinkereignis direkt in der Wassersäule dokumentiert werden. Bei solchen Ereignissen werden große Mengen Materials innerhalb weniger Tage absedimentiert. Die Region vor Kap Blanc zeigt somit eine sehr enge Kopplung zwischen Wasseroberfläche und Meeresboden. Obwohl der vertikale Transport auch vor Dakhla and Kap Bojador eine Rolle spielt, ist dieser doch deutlich geringer ausgeprägt. Hinzu kommt, dass große Mengen von lateral advektiertem Material vom Schelf oder oberen Kontinentalhang in die distale Region vor Kap Bojador eingetragen werden. Auch dieser Prozess konnte zum ersten Mal mit der Kamera in-situ erfasst werden. Hinweise auf vergleichbare Mechanismen gibt es vor Kap Blanc nicht.

Die mit Hilfe des profilierenden Kamerasystems erfassten vertikalen Partikelkonzentrationen zeigen deutliche Schwankungen. Am unteren Bereich der euphotischen Zone, verringert sich die Konzentration von 200 auf bis zu 50 Partikel pro Liter innerhalb weniger Meter. Im Gegensatz dazu, ließen die mit dem ROV unternommen Horizontaltransekte bis zu 20 m Gesamtlänge in verschiedenen Wassertiefen keine signifikanten Unterschiede erkennen. Die Beobachtung von sinkenden Partikelaggregaten zeigte hingegen überraschende Erkenntnisse. Partikuläres Material sinkt in verschiedenen Wassertiefen unterschiedlich schnell. Während in einer Partikelminimumzone bei ungefähr 100 m Wassertiefe die Sinktrajektorien von Partikeln eine klare vertikale Fallrichtung aufzeigten, so kommt es in einer Partikelmaximumzone bei ~175 m zu einem „Abbremsen“ der sinkenden Aggregate und somit zu einer Akkumulation an der Grenze von der durchmischten Zone zur mittleren Wassersäule.

1. Introduction

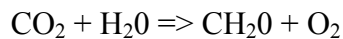
Since the beginning of the industrial revolution in the middle of the 19th century, mankind influenced his environment to a high degree. The population explosion, related to fast progresses in technology and medicine, enabled humanity to change the face and climate of the planet. Of special importance became the anthropogenic release of so called greenhouse gases, like carbon dioxide (CO₂). The burning of fossil fuels and changing land utilisation increased the CO₂ content of the atmosphere from 290 ppm back in 1850 to far above 370 ppm today. Carbon dioxide partially prevents the re-radiation of sunrays to space, resulting in a worldwide global warming. Melting of the polar caps, floods in the Far East or the declining glaciers are discussed to be the result of global warming via increasing greenhouse gas emissions into the atmosphere. The demand of predictions and estimations about the future climate on the part of society and politics became a significant domain in science. Intense researches on global climate changes were undertaken for more than 20 years. While the climate is a global phenomenon, a complete picture can only be drawn when taking into account the world oceans. Two main branches of marine geology focus on research of the climate of present and past. Palaeoclimatology focuses on the reconstruction and understanding of the climate of earth history. Particle flux studies try to quantify the amount of marine particulate matter, formerly produced in the surface waters, embedded into the ocean sediments. It has been established past the last two decades that sinking marine particulate matter is one of the most influencing factors with respect to the global carbon cycle and hence, a potential control factor of earth climate.

The global carbon cycle

Oceans and atmosphere represent the largest gas exchange interface on earth. Both environments aim to reach a steady equilibrium of their gas budgets. Increasing CO₂ in the atmosphere lead to increased CO₂ concentrations in the oceans and vice versa. The significance of this gas exchange processes with respect to the global carbon cycle, might be demonstrated in the following example. Approximately 6 gt of carbon in the form of CO₂ are released by human activity every year. A third of these emissions is currently absorbed by the world's oceans (Clarke et al., 2001). This emphasizes the importance of the oceans as a sink for CO₂. The amount of gas exchanged between these two environments is controlled by two natural mechanisms. First, the *Solubility pump* (e.g. Dyrssen, 2001) and second the *Biological pump* (Broecker, 1982). The first is driven by physical and chemical processes. The uptake of CO₂ by the surface waters is caused via diffusion and mixing and focused to small areas of

the oceans, such as the Polar North Atlantic Ocean and the Polar South Atlantic Ocean. The low water temperatures in these regions have two effects. CO₂ uptake is enhanced because solubility increases at low temperatures. Second, a decrease of temperature result in an increase of the water mass density causing it to sink into deeper parts of the ocean where it is conveyed along the ocean bottom through the deep-sea. Deep water formation is a temporary sink of CO₂ with retention times of about 1000 years (Chisholm, 2000).

The uptake of CO₂ by the *Biological pump* occurs during photosynthesis in the upper, light flooded parts of the water column. Inorganic carbon is converted into organic carbon by autotroph marine organisms, known as phytoplankton. This process is called primary production and can be described by the following, simplified equation:



Posthumously, the organisms start to sink into deeper parts of the water column in the form of marine particulate matter. However, 3/4 of this organic matter formed in the ocean surface waters is already remineralised in the upper 1000 m of the water column by consumption and bacterial respiration. Only 1/4 of the decayed material reaches the deeper parts of the water column on its further descent towards the sea floor. Depending on the oceanic region, 0.03 % to 1 % of the organic carbon produced in the surface waters are finally embedded in the sediment (Berger et al., 1989). These sediments act as a long term sink of carbon. While CO₂ is removed from the surface waters via phytoplankton growth or primary production respectively, the production of calcium carbonate (CaCO₃) by specific calcifying organisms, increase the CO₂ content of the oceans. This process is called the *Carbonate pump* and follows the equation:



Biological pump and *Carbonate pump* are thus processes that act in opposite directions. Next to the composition of particulate matter the amount and speed with which particulate matter is transferred from the ocean surface to the deep-sea sediments, is the decisive process for the withdrawal of CO₂ from the atmosphere.

Particulate matter in the ocean: distribution, formation and fate

Particulate matter can be described as non-living, macroscopically resolvable flakes from any organic and inorganic sources (Fig. 1). Particulate matter is ubiquitous in the world oceans and even present in fresh water lakes and rivers. These flakes form the ocean sediments by sinking from the ocean surface to the deep sea floor. The flakes reminded the observers in the submersible *Kurushio* of a snow fall in the open ocean and were described as *Marine snow* since then (Suzuki and Kato, 1953). Later, the term *Marine snow* was used to determine a size classification of particulate matter. Any particle or flake of a size > 0.5 mm in diameter, is classified as *Marine snow* (Fowler and Knauer, 1986).

The sources of marine particulate matter are manifold. As described in the chapter before, the most important organic source of marine particulate matter are autotroph organisms, which use sunlight and inorganic carbon to form organic matter. Coccolithophorids and diatoms are the most common species of this phytoplankton group. They are the backbone of the marine food chain, from which a large variety of secondary, organic marine particles derive. These are in the first instance the carcasses and excrements of zooplankton organisms, which feed on marine algae, such as copepods, pteropods or foraminifers. Inorganic sources of marine particles are primarily related to the input of material from the continents. Apart from smaller sources, such as ice rafted debris or coastal erosion, the main sources of anorganic, terrigenous particles are the rivers and wind transported dust. A total of 20×10^9 t of anorganic, lithogenic material is discharged by the rivers every year into the oceans (Milliman and Syvitsky, 1992). The input of wind transported material is only a small fraction, compared to those of rivers. The global, annual aeolian dust input into the oceans was estimated to range between 2.0 bt y^{-1} (Schütz and Sebert, 1987) and 2.15 bt y^{-1} (Penner and Zhang, 2004). However, dust input is of special interest because it is transported over long distances, taking influence on ecosystems on intercontinental scales (Swap et al., 1992).

As complex as the large variety of particle sources, is their distribution in the oceans. Their spatial abundance in the sunlit ocean surface around the globe is mainly a function of the primary production conditions. Primary production is described as the total amount of carbon in grams converted into organic material per square meter of sea surface per year. The primary production conditions differ decisively, dependant on the prevailing season and oceanic region. Increased particulate matter concentrations are observed in higher productive regions such as the upwelling system off California. Here, MacIntyre et al. (1995) reported concentrations of 100 particles per litre where mean primary production is far above 250 g C

$\text{m}^{-2} \text{y}^{-1}$. In comparison, 40 particles per litre were measured in the lower productive Mediterranean Sea (Gorsky et al., 1992) with a mean primary production between 100 and $150 \text{ g C m}^{-2} \text{y}^{-1}$.

Fig. A

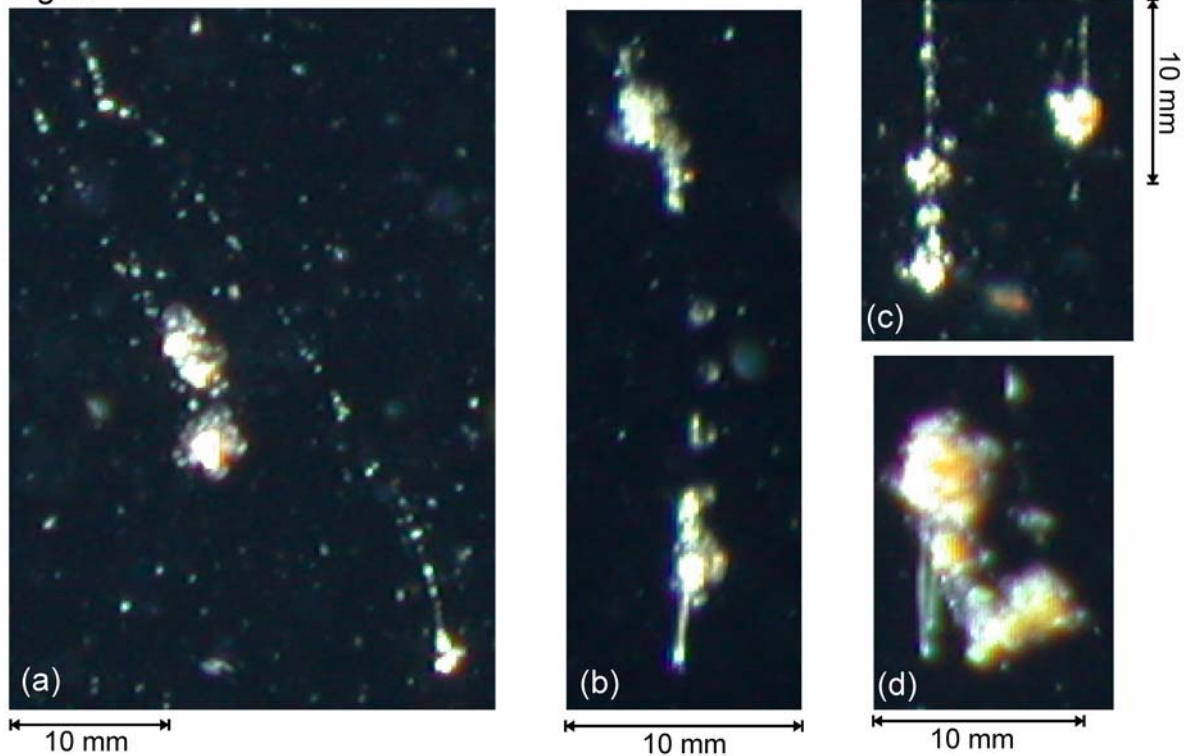


Fig. B

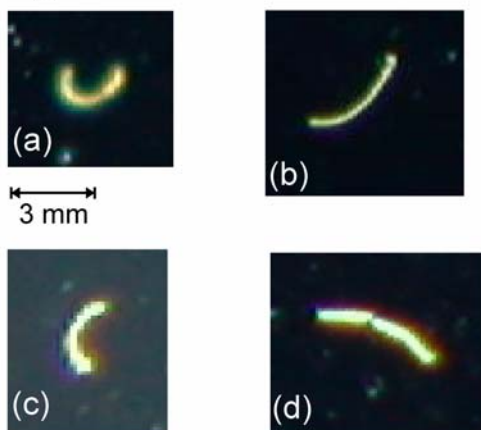


Fig. C

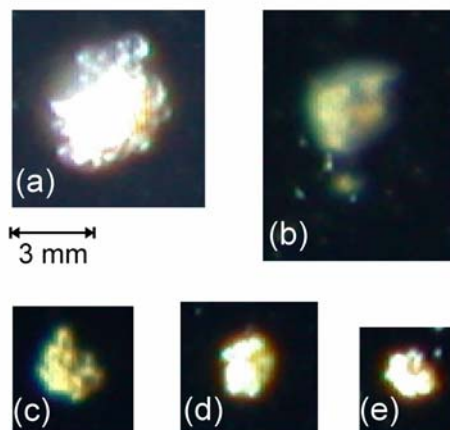


Fig. 1: Detrital particles obtained off Cape Timeris, NW-Africa. Fig. A (a-d) shows typical large, coagulated aggregates known as *Stringers*. They consist of a large variety of detrital and often still living material, mainly agglutinated by transparent exopolymer particles (TEP). Usually the largest and heaviest particles are located at the bottom or head of the aggregate (a, c). Aggregates (b) and (d) include some sort of spiculae, possibly originating from forminifera. Fig. B are fecal pellets from macro crustaceans like *euphasiids* or *sergestids*. Fig. C are possibly mineral grains, partially eroded (c). The bubbles seen on Table 3a could not be identified. They might be either gas bubbles or attached eggs.

This non-uniform distribution in the ocean surface is extruded into the vertical. As a direct result of the primary production conditions, the majority of particles are concentrated in the surface waters. When following a typical, vertical particle concentration profile, many studies report an abrupt change in the particle abundance between 100 m and 200 m of the water column (e.g. Asper et al., 1992; Honjo et al., 1984; Ratmeyer and Wefer, 1996; Walsh and Gardner, 1992). Particle concentrations often decrease by a factor of 5 within several metres of the water column in this specific depth. The first hundred metres of the water column underlie drastic changes with respect to turbulences, temperature, chemistry, intensity of light and many other factors (Lampitt, 1996). Consumption, degradation and solubilisation processes are most intense in this water layer. In addition, gradients in the density structure are reported to accumulate particles in depths, when sinking from a low density layer into higher dense waters (Alldredge and Crocker, 1995; MacIntyre et al., 1995). Thus, the rapid changes in the particle abundances are a function of the rates of production and loss of particulate matter in the highly dynamic, sunlit ocean surface. As soon as the particles leave the euphotic zone, the material encounters reduced intensities of physical, biological and chemical degradation. The comparably lower alteration processes are well reflected in constant or slightly decreasing particle concentrations between the euphotic zone and the seafloor. The so-called midwater column comprises the largest segment of the water column. Shortly above the ocean bottom concentration peaks can be observed. The material has reached the *Benthic Boundary Layer* (BBL) (Thomsen, 2003), where particulate matter is resuspended from the ocean floor by bottom near currents. The BBL is usually well pronounced along the shelf and slope areas, where bottom near currents are stronger compared to the open ocean areas. Large amounts of material can be kept in suspension for a serious amount of time, where they again underlie the decomposing processes before the final settlement in the seabed.

With aid of new technologies like remotely operated vehicles (ROV) or autonomous underwater vehicles (AUV), appropriate tools exist now for investigations of the horizontal distribution of particulate matter in the ocean. Before the introduction of these technologies, acquiring high resolution horizontal transects was difficult. Recent studies from Yu et al. (2002) or Cunningham et al. (2003) showed that the horizontal distribution of i.e. the planktonic community or smallest suspended particles, underlie similar distinct variations as the vertical distribution on spatial scales of several kilometres. The processes, responsible for generating horizontal distribution patterns are probably very complex and still not sufficiently understood. Comparable studies will conceivably play a major role within the next years.

The considerably well-preserved remnants of marine organisms in the deep-sea sediments lead to the conclusion that there must be a close coupling between ocean surface and seafloor. Although this assumption was first made by Lohmann (1908), it was a wide belief until the late 1970 that the distance between surface and sediment was large enough to decouple both ecosystems. This belief was mainly related to the fact that the material forming particulate matter was so small that it would take months to years to reach the ocean bottom. According to Stokes Law, marine organisms such as diatoms or coccolithophorids and a large fraction of the aeolian, wind-transported dust would sink at neglectable rates. However, sinking velocities estimated from deployed sediment trap results, were in the range between 50 m d⁻¹ and 150 m d⁻¹ (e.g. Alldredge, 1979; Alldredge and Gotschalk, 1988; Shanks and Trent, 1980). Extremely high sinking speeds of almost 3000 m d⁻¹ were reported by Lampitt (1985) in the North Atlantic Ocean.

While the knowledge that accurate settling speeds is crucial for understanding flux dynamics, estimates of settling velocities using sediment traps are only a rough estimation. The time difference is measured for a clearly recognisable sinking event that is observed in different water depths. However, the time resolution of sediment trap studies is no better than the sampling interval (typically 1-3 weeks per collection interval). Furthermore, this method is not able to determine, which particle populations drive the vertical flux. Hence, in-situ observations of the sinking behaviour of individual particles are required. Due to the difficulties, such in-situ observation studies about the sinking behaviour of marine particles are quite rare and were mainly accomplished by Scuba dives or ROV's deployments (Alldredge and Gotschalk, 1988; Pilskaln et al., 1998). Sinking speeds are controlled by particle shape, density, porosity, composition and size. Size and sinking behaviour is discussed widely (Alldredge and Gotschalk, 1988, 1989). While Alldredge and Gotschalk (1988) and Pilskaln et al. (1998) found a clear size/sinking rate relationship, no such connection was found by Diercks and Asper (1997). Azetsu-Scott and Passow (in press) showed ascending particles, when the material contained a certain amount of transparent exopolymer particles (TEP). These contradictory findings emphasize the complexity of particle dynamics in the water column and confirm the necessity for further in-situ studies.

The small temporal delay of material from the surface trapped in different water depths is related to the coagulation of small, single particles, to large coagulated aggregates, resulting in a higher density and hence faster settling speeds. The coagulation processes of particulate matter are a complex field of study and in the first instance controlled by biological and physical processes. A detailed overview on aggregation processes of marine

particles is given in Alldredge and Jackson (1995). Sticky exudations of marine organisms such as filtration webs from appendicularians (Hamner and Robison, 1992) or TEP produced by diatoms (Logan et al., 1995; Passow and Alldredge, 1995), interact with the surrounding particles to form aggregates of significant sizes and sinking rates. The driving forces for such coagulation are physical processes. Aggregates grow in size via differential settlement, where fast sinking particles collide with slower sinking ones. Another important, physical aggregation processes is due to mixing processes in surface waters. Internal waves, wind driven and tidal shear increase the collision rates of particles (Lueck and Osborn, 1985). Pure biological aggregation occurs mainly in the form of the ingestion and excretion of phytoplankton by feeding zooplankton. These exudations, known as fecal pellets, were thought to be the major transport vehicle of material to the sea floor. But the amount of trapped pellets was so small that this assumption could not be maintained. It has now become accepted that the transfer of elements and nutrients from the ocean surface to the deep sea, occurs in the form of large, coagulated marine snow aggregates. The importance of a close coupling between ocean surface and deep-sea, was described by Lampitt (1985). Food consumption and replication of the benthos rely on the episodically supply of material from above. More recent studies describe the importance of marine aggregates as a food source and residence for the zooplankton fauna (Kiorboe, 2000; 2001).

When thinking of a marine snowfall, the idea suggests the image of a continuous supply of material to the ocean bottom. The transportation processes however, are far more complex. Apart from the prevailing continuous flux of material, the rapid but episodic delivery of particulate matter on short temporal scales is strongly associated with phytoplankton blooms (Alldredge and Gotschalk, 1989; MacKenzie et al., 2002; Waite et al., 2000). Blooms trigger mass sedimentation events after the abrupt extinction of the phytoplankton organisms. The sticky exudates of diatoms for instance, initiate a chain reaction by entraining any material in the water column on their fast descent to the deep-sea. Another trigger for rapid particle transfer is the fallout of wind transported, lithogenic material from the continents into the ocean. Dust particles with higher density interact with the biogenic particles in the water column. This so called *particle loading* process (Ramaswamy et al., 1991) is responsible for a comparably fast delivery of the particles from the ocean surface to the sea floor. While the described processes imply a predominantly vertical transport direction, material is reported to be laterally advected from the slope areas towards the open ocean (e.g. Freudenthal et al., 2001; Gardner and Walsh, 1990; Neuer et al.,

1997). The advected plumes of material can be transported over long distances, providing another significant transportation process in the oceans.

1.1 Scientific goals

The region off NW-Africa is subject to many palaeoclimatic, oceanographic and particle fluxes studies. Although a lot of scientific progress for our understanding of this highly dynamic part of the eastern, subtropical North Atlantic was made, little is known about the vertical distribution and little about the transport processes of particulate matter in this region. The manuscripts presented in this thesis, focus on the description of the distribution and transportation mechanisms of marine particulate matter. It is subject of further investigations, which particle populations are responsible for the vertical transport and the way the material is transferred to the deep sea.

Major tools for these studies were a vertically profiling photo camera system (ParCa), developed at the University of Bremen (Ratmeyer and Wefer, 1996) and a remotely operated vehicle (ROV) equipped with video cameras. For studies on the distribution and transport of particles in the ocean, non-destructive methods are necessary. Due to their fragile nature, marine aggregates are not preserved in the sample cups of sediment traps or water samplers. In addition, cameras are the only possibility to obtain in-situ information of particles such as their abundance, size, shape, orientation in the water column or sinking behaviour. Hence, a focal point was the determination of particle parameters, which could detect and describe the transport process on the basis of photo- and videosequences.

The scientific goals are summarised in three following questions:

- 1.) How is particulate matter distributed along the NW-African coast and which processes are responsible for generating the observed particle abundance patterns ?
- 2.) What are the key transport processes and pathways of marine particulate matter in the investigation area ?
- 3.) Which statements with respect to the flux of particulate matter can be made on the basis of the in-situ observations and measurements ?

The results are presented in the following three publications:

Manuscript 1: The vertical distribution of particulate matter in the upwelling system off Cape Blanc (NW-Africa) obtained by high-resolution camera profiles and implications for rapid, vertical mass transfer

The manuscript describes the results from 6 vertical camera profiles obtained in the highly dynamic upwelling system off Cape Blanc. The camera profiles were deployed in order to obtain information about the vertical particle distribution and transport processes in a high productivity area. The acquisition of profiles in a time window as small as possible was of major importance in order to allow a comparison of the particle distributions between the single profiles. In the methodical part of the manuscript, a detailed description of the parameters extracted from the camera images is given. Apart from the common particle parameters, such as the change of the particle abundance with depth, several new approaches for the visualisation of particle distribution and transport relevant parameters were applied. These were in the first instance the generation of high resolution datasets of the vertical size distribution of particulate matter, information about the in-situ orientation of marine particles and the comparison of satellite derived chlorophyll concentrations with the particle abundances in the very ocean surface. With aid of the camera profiles, several transportation processes were investigated and a transport model was developed.

Manuscript 2: The abundance and size of marine particles off the NW-African coast (Dakhla, Cape Bojador) and the detection of a massive lateral intrusion

The successful concept and strategy of camera deployments and data extraction was continued for further studies on particle distribution and transportation processes off NW-Africa. The presented camera profiles were obtained along two transects in lower productive areas, compared to the profiles of the first manuscript. The additional extraction of the particle volume concentrations and water column turbidity provided further insights of the sedimentation of particles in low productive areas. The size distribution turned out to be the crucial parameter for the detection of transport processes in the water column. While there is no clear taxonomy for particulate matter, a proposal for a nomenclature of marine particles is presented in this publication on the basis of their size distribution and shape.

Manuscript 3: Observation of accumulation of marine particulate matter at the lower boundary of the mixed layer off NW-Africa (20°49'N / 17°58'W)

A ROV that is decoupled from the ships undulations was used to study the horizontal distribution of particles at a station off Cape Blanc. These observations were applied with aid of a common and an additional stereoscopic video camera system providing 3-D vision. The challenging part of this study was the adaption of the image analysis on the video sequences, to extract reasonable and reproducible datasets. Several horizontal transects were applied for

the comparison of particle distributions in different water depths but the focus was laid on observations of the sinking behaviour of marine particles.

1.2 Study area

Study area is the eastern, subtropical North Atlantic Ocean between 30°N and 20°N. Investigation areas are the continental slope areas off the Mauritanian and Moroccan coast. The sites are located within or at the border of the northwest African upwelling system, which is the result of a close coupling of the prevailing atmospheric and oceanographic conditions.

Oceanographic settings

The dominating surface current of the study area is the Canary Current (Fig. 2a). The Canary Current diverges from the eastward flowing Azores current, which is part of the subtropical gyre circulation system (Siedler and Onken, 1996). Three large branches separate from the Azores Current, where the Canary Current is the most eastern and coastal nearest. It turns around 35°N to the south, flowing along the NW-African coast from Cape Ghir in the north, passing the Canary Islands to Cape Verde to the south with velocities up to 20 cm s⁻¹ (Johnson and Stevens, 2000). The Canary Current splits up around 10°N into the westward flowing North Equatorial Current (NEC) and the eastward flowing Equatorial Counter Current (ECC). South of Liberia, the ECC becomes the Guinea Current (GC) (Mittelstaedt, 1983). Underneath the Canary Current, two important water masses can be identified between 200 m and 500 m depth. The southward flowing North Atlantic Central Water (NACW) and the northward flowing South Atlantic Central Water (SACW) (Sarnthein et al., 1982). The SACW with its high nutrient content, provides a significant part of the source water for upwelling in this specific region (Hughes and Barton, 1974).

Atmospheric settings

The area of investigation is influenced by two major wind systems. The Saharan Air Layer (SAL) and the trade winds (Fig. 2b). The SAL originates from the African Easterly Jet, a mid-tropospheric wind system (Prospero, 1990). The SAL predominantly occurs in the hot periods of the summer, where extremely hot and dust laden *Harmattan* winds originate in the Saharan desert. Large amounts of this dust is lifted into heights between 1 km and 6 km via thermal convection processes (Tetzlaff and Wolter, 1980) and transported towards the open ocean with the SAL. While the dominant wind direction is westwards, a branch of the SAL turns to the north, taking influence on the Canary Islands. (Sarnthein et al., 1981). The

SAL is responsible for the long range transport of Saharan dust (Middleton et al., 2001; Schütz et al., 1990) towards the Caribbean Sea.

The SAL is underlayed by the trade wind system. The trade winds are part of the Hadley Circulation system, blowing southwest. They are a near surface wind system, which main direction is along the NW-African shore and it is the driving force for the Canary Current. An important characteristic of the trade winds is their latitudinal shift. The trade wind belt moves from 10°N and 25°N in the winter, to 20°N and 30°N in summer. Responsible for this is the seasonal movement of the Inter Tropical Convergence Zone (ITCZ). The trade winds are responsible for a significant import of material from the northern Sahara and the Atlas mountains.

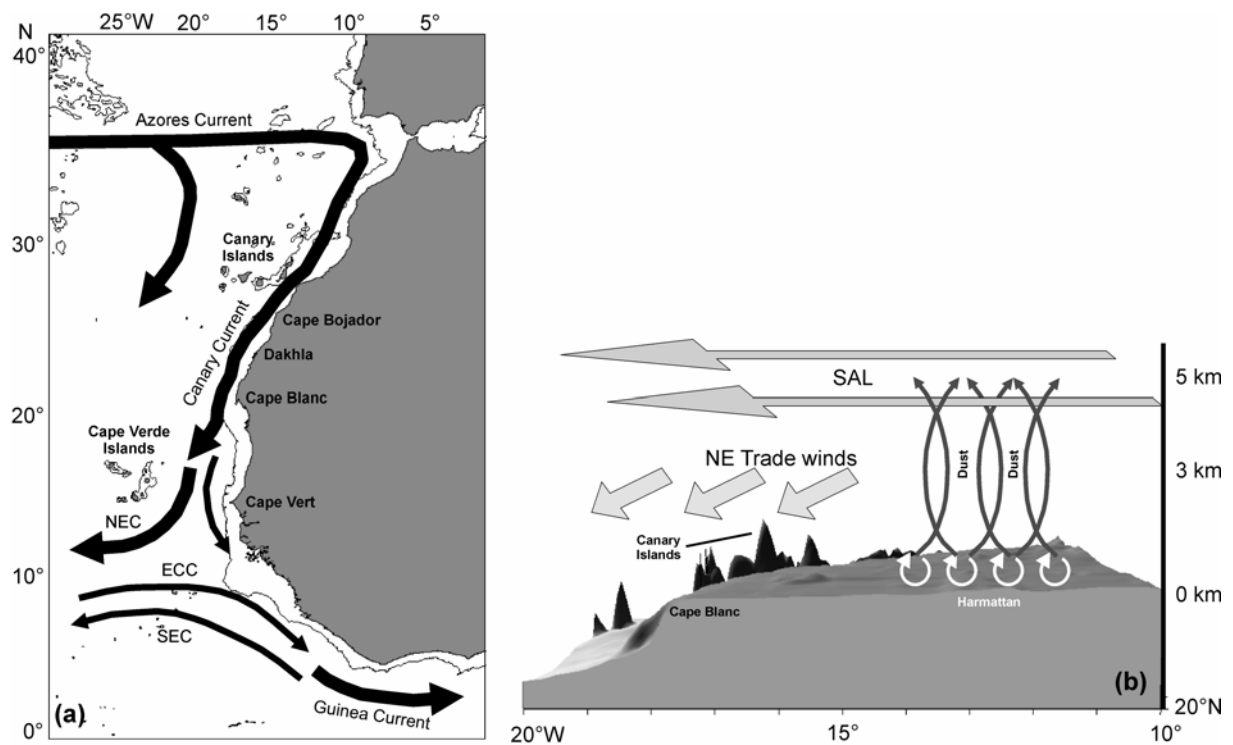


Fig. 2: Schematic views of the prevailing current and wind systems in the area of investigation. (a) North Equatorial Current (NEC), Equatorial Counter Current (ECC), South Equatorial Current (SEC) – modified after Sarnheim (1982) and Mittelstaedt (1983). Thin lines represent the 2000 m depth contours. (b) Saharan Air Layer (SAL) and the NE trade winds are the dominating wind systems.

The upwelling of nutrient rich, cold water is strongly coupled to the persistent blowing trade winds. Trade winds and the Ekman drift displace the surface water, conveying nutrient rich waters from the deep. Although the width of the upwelling belt is only 50 km – 70 km and limited to the continental shelf (Mittelstaedt, 1991), large filaments of chlorophyll enriched

water are laterally advected several hundreds of kilometres towards the open ocean in the region off Cape Blanc.

1.3 Methods

Two different, optical in-situ methodologies were used – a profiling photo camera (ParCa) and a ROV. Both methods differ with respect to their possibilities and limitations of in-situ particle observations.

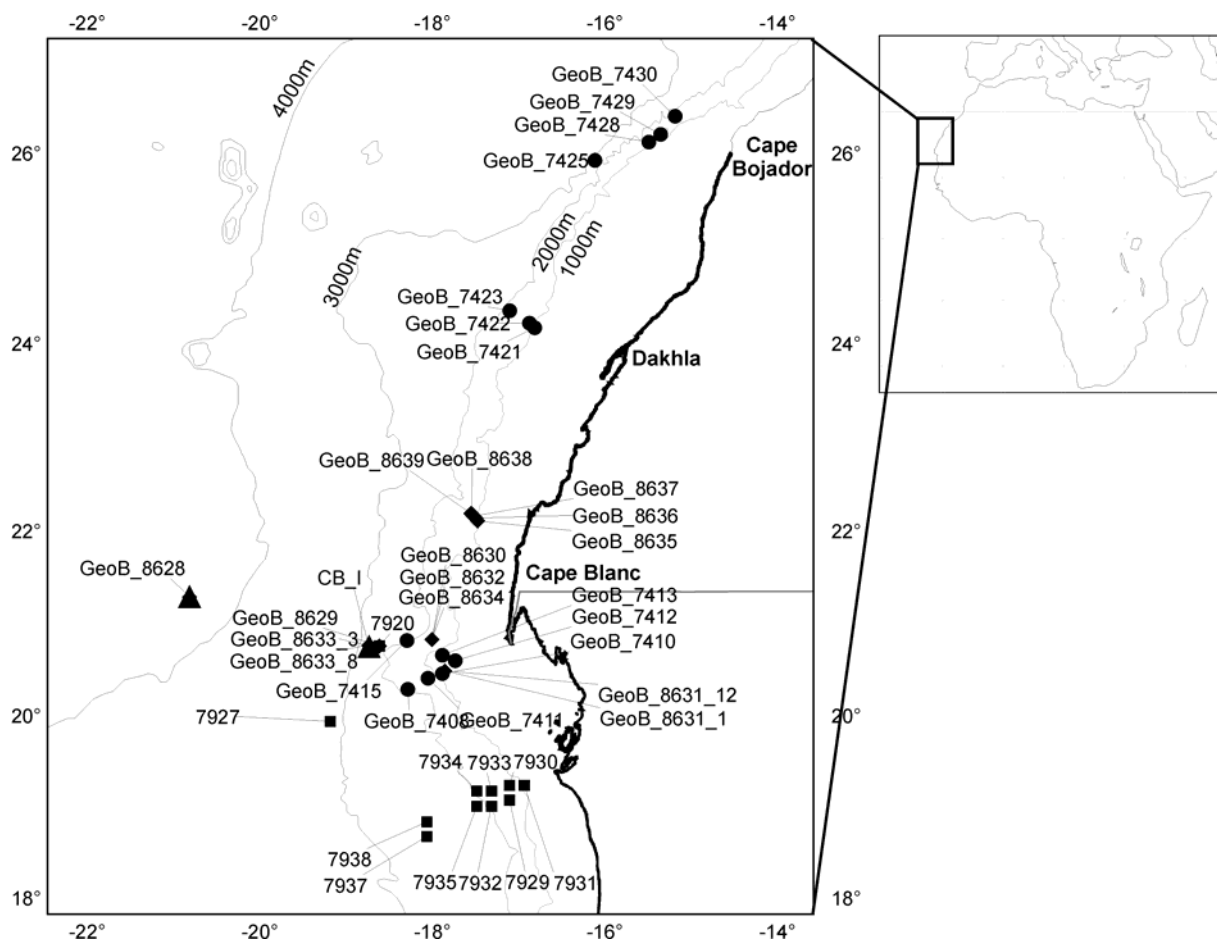


Fig. 3: Investigation area and ParCa deployment sites. Profiles obtained during cruise POS-272 are marked as circles; cruise M53-1c profiles as squares and M58-2b profiles as rhombi. Large triangles mark the position of the trap location CB and CB-i.

The ParCa system was deployed along a number of transects in order to acquire the vertical distribution of particulate matter off the NW-African coast (Fig. 3). The camera system acquired the spatial distribution of particulate matter in the water column. ParCa was deployed during RV Poseidon and RV Meteor cruises POS 272 (2001), M53-1b (2002) and

M58-2 (2003) on 34 locations. Profiling depths ranged between 250 m on the upper slope, down to depths of 4000 m in the deep-sea plains.

ROV's, decoupled from the ships undulations, offer excellent possibilities for in-situ observations in the water column. The motion of particles can be tracked with video cameras over temporal scales long enough, to allow conclusive statements regarding their sinking behaviour. Another advantage is the possibility of horizontal transects in any depth of interest. While little is known about the horizontal distribution of particles, the ROV was used for several horizontal transects. The ROV was deployed at 4 stations during RV Meteor cruise M58-2b (2003) and a total of 13 h of video sequences were acquired. In the frame of this thesis, video observations from one dive were evaluated and published.

1.3.1 Deep-sea camera system ParCa

The ParCa system was developed in 1996 at the University of Bremen and continuously improved since then (Fig. 4a). Although a comprehensive overview of the system is given in Ratmeyer and Wefer (1996), a short description of the camera and its functionality is presented here.

The camera was designed and improved in consideration of similar systems used by Honjo et al. (1984) or Asper (1987). ParCa consists of a modified 70 mm middle format camera with a film capacity of 30.5 m of a light sensitive, black/white Tri-X Pan film. A perpendicular to the camera mounted strobe, fires a collimated light beam illuminating a known sample volume for statistical analysis of the images (Fig. 4b). The camera is lowered at a winch speed of 0.3 m s^{-1} , acquiring images at 10 m intervals. The system can operate in depths down to 6000 m and power source is a 24 V/38 Ah rechargeable lead battery. Communication with the ship is provided by a microcontroller and adapted software. A telemetry unit allows full control over the system via the ships coaxial wire. The camera is triggered by the pressure sensor of a CTD probe for accurate trigger depths.

The analog ParCa system was replaced by a digital photo camera in 2002. The camera optic provides 3.2 Megapixel at a picture resolution of 2048 x 1536 pixel. Up to 320 single frames can be stored on a 512 Megabyte flashcard. The main advantage of the new system is that the images are direct available in a digital format, ready for the image analysis. This enabled the quick evaluation of the camera profiles during an ongoing cruise, which was not possible with the analog system. The camera produces 24 bit RGB colour images and an additional particle parameter used for further studies. Apart from the camera itself and

changes in the controller software, all other devices and their illumination setup are identical to the analog ParCa system.

Image analysis

The image processing procedure used for the evaluation of the camera pictures, are described in detail in Ratmeyer and Wefer (1996) or Nowald (1999). Changes in the image processing of the ParCa frames were in the first instance provided for the digital ParCa system. The raw images cannot be evaluated by an image analysis software, without the application of several image filters. The basic difficulties of the image processing between both systems do not considerably differ. They lie in the separation of the background from the foreground or so to speak, the particles. This is done with aid of several morphological filter operations, which were applied to the frames to allow an automated, statistical analysis. These procedures were used for the analog as well as for the digital camera, using the imaging software *Optimas*.

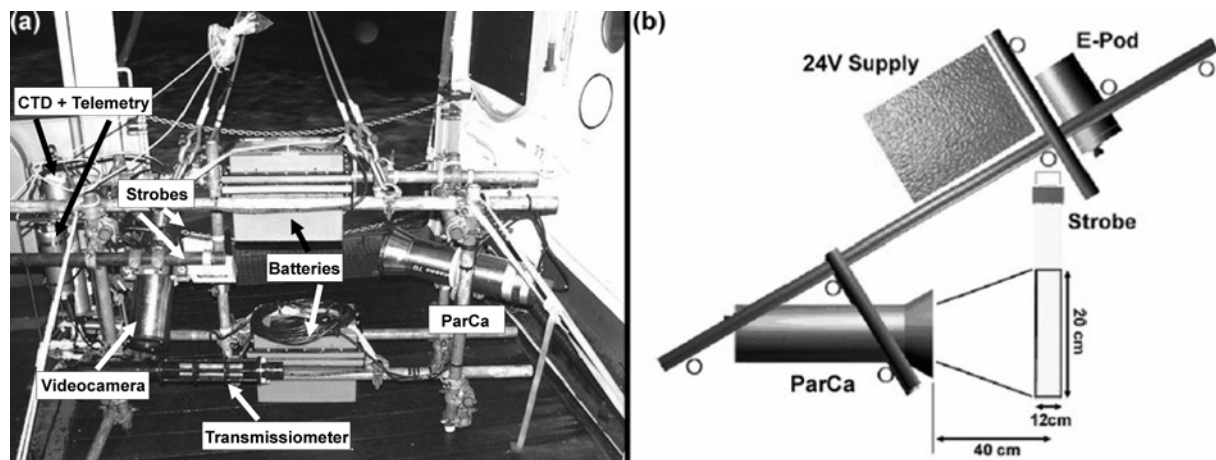


Fig. 4: ParCa (right) onboard RV Poseidon with additional Videocamerasystem mounted to the left (a). Schematic setup of the ParCa devices and resulting sample volume (b).

The main goal since the introduction of the digital camera system was to make particle datasets available for shipboard use as quickly as possible after the recovery. With aid of these profiles, specific depths of interest, such as particle maxima, could be detected. Afterwards the ROV could operate in these depths previously determined as particle relevant. The major problem of the image processing is the amount of time needed, to evaluate the images of an entire camera profile. For a 2000 m profile, the analysis takes about 2 h, which is too much because the ROV was usually deployed right after the particle camera. Thus, a

compromise between a representative, statistical evaluation of the images and the amount of time that is needed for the analysis had to be found. The problem was solved by several steps. First, the 24-bit RGB colour images were converted into 8 bit grey scale pictures. The processing of grey scale images is significantly faster, because 8 bit images comprise only 2^8 or 256 grey scales (0 = black; 255 = white). In comparison, a 24-bit RGB image comprises 1677216 red, 1677216 green and 1677216 blue scales. The time consuming morphological filter operations were likewise discarded for reasons of a faster processing. These operations are important in this respect that they eliminate weakly lighted particles, which disturb and falsify the statistical evaluation. Without the morphological filters, the standard procedure would assign large areas of the background to foreground particles, leading to unacceptable results. To prevent this, the software was adjusted in a manner that it only measured well-lit, bright shining particles with a grey value above 150. Although a certain amount of particles was hence missed by the analysis software, it leads to satisfying results. In addition, the timeframe of the preliminary analysis could be reduced from 2 h to 0.5 h for a profile of 2000 m length.

Determination of particle parameter

A major focus during this thesis was laid on the determination of parameters, describing and detecting transportation and distribution patterns of particulate matter. The extraction procedures are described in detail in the corresponding manuscripts. Nevertheless, a short summary is given here.

Usually, camera profiles are used for the documentation of the change of the particle concentration with depth. The potential of camera profiles however, lie in the choice and visualisation of parameters, extracted from the pictures with aid of an image analysis software. Several approaches of the extraction and visualisation of new parameters were applied and described in manuscript 1 and 2 (p. 31 & 65).

The particle images were used to distinguish between three particle classes. The first class are macroscopically resolvable, spherically shaped particles. They are above the cameras resolution ($>180 \mu\text{m}$) and usually not larger than 2 mm (Fig. 5a). The second class are large, coagulated aggregates, described as *Stringers* (Shanks, 2002; Syvitsky et al., 1995). They consist of at least two coherent, macroscopically resolvable particles and are the largest particle class obtained ($>2 \text{ mm}$) (Fig. 5b). The third class are smallest, suspended particles, beyond the cameras resolution. These particulates are responsible for the turbidity of the water column and were described with aid of the mean grey value of the image background

(Fig. 5c). Apart from the class of the large, coagulated aggregates, the remaining classes were extracted automatically from the images.

The abundance of large, coagulated aggregates had to be extracted manually, because the image analysis software is not able to distinguish between a large aggregate and spherically shaped particles. The distinction between several particle classes, were considered to lead to a more differentiated view of particle distributions in the water column.

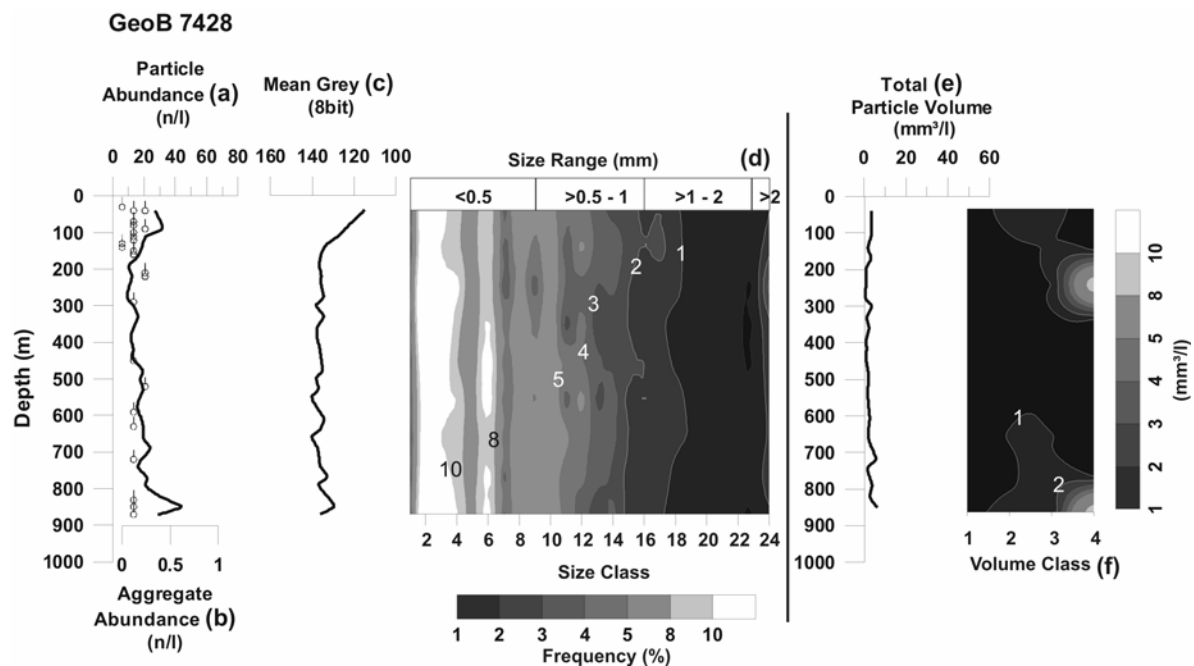


Fig. 5: Comprehensive presentation of extracted particle parameter: a) abundance of spherically shaped particles, b) abundance of large, coagulated aggregates, c) mean grey as a mean for the turbidity, d) size distribution, e) & f) particle volumes

Of special interest was the visualisation of the vertical size distribution of marine particulate matter. Abrupt or unusual changes in the particle size distribution with depth are probably related to an alteration of the material and might reflect a change in the transport mechanism. The camera acquires a broad range of particles (>180 μm - >2 mm) and thus, high-resolution size classification had to be applied. A low-resolution size classification might have missed events of interest. The equivalent diameters of each particle measured on the image were therefore allocated to one of 24 size classes (Manuscript 1 & 2; p. 31 & 65). Their frequencies in percent down the profile, was visualised with aid of colour or grey scale encoding (Fig. 5d).

A similar approach was applied to the particle volumes. The volume of each single particle was calculated after the equation for spheres:

$$V = (4 / 3) * \pi * r^3$$

All volumes calculated from the particles were added, resulting in the total particle volume in a litre of seawater (Fig. 5e). Afterwards each particle volume was allocated to one of 4 volume classes and their change with depth was encoded in grey scales as described for the size distribution (Fig. 5f). Particle abundances might not be a measure of the distributions of particulate matter, because particles break apart and re-aggregate. The same total amount of particulate matter mass can be distributed in a few big or in a number of small particles. Hence, the change of the particle volumes with depth is considered to be another important parameter for the detection of a possible alteration of material during transport.

1.3.2 Remotely operated vehicle (ROV)

The ROV system consists of three major components: the vehicle, the surface control units and the winch.

Cherokee ROV

The *Cherokee* is a commercially available, 1000 m deep diving, open frame system. Dimensions are 140 x 90 x 80 cm (L x W x H) and weight in air is approximately 250 kg (Fig. 6). The ROV has a payload of 50 kg for the integration and mounting of additional, scientific devices. The vehicle is propelled by four thrusters, supplied by a 12 kW at 440 VAC power distribution unit. Maximum velocity is 1.5 m s⁻¹ forward and 1 m s⁻¹ backwards. The standard equipment consists of a hydraulic, 5-function manipulator and a scanning sonar, operating at 325/675 Hz. Four dimmable, 250 W halogen headlights provide a sufficient lighting of the environment for a standard analog video camera, mounted onto a pan & tilt unit. For operations above the sea floor, the *Cherokee* is equipped with an altimeter with a resolution of 0.1 m. Autodepth and auto heading functions, facilitate the control of the ROV. Video and data telemetry supplies 4 video, 4 RS232 and 4 RS485 channels. 3 video channels are used for the applied in-situ studies.

Winch and tether

The winch has a storage capacity of 1000 m for the 27 mm thick tether cable. It is electrically powered (1.5 kW), dimensions are 2.3 x 1.3 x 1.4 (L x B x H) and total weight is

~1.8 t. The synthetic cable armour contains an aramid-inlay and is buoyancy compensated. Data and video telemetry is provided by 4 multi mode fibre lines. Power supply is provided by 12 x 220 V lines. The winch has an electrical slip ring for the transmission of power and the analog data streams, such as heading or depth during spooling.

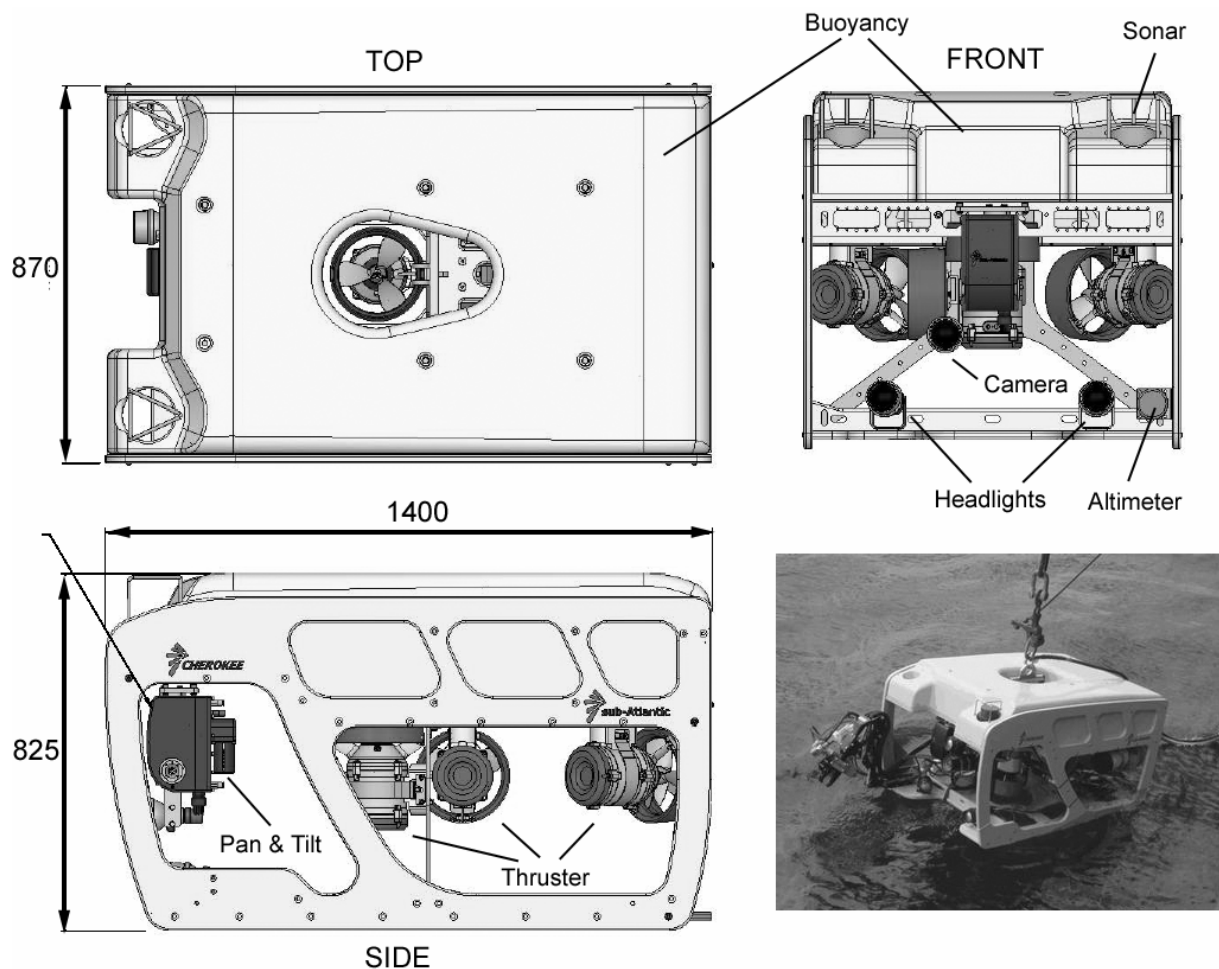


Fig. 6: Schematic view of the *Cherokee* ROV and basic components. Dimensions are given in mm. Lower right: *Cherokee* during deployment with the 5-function manipulator visible on the starboard side.

Surface control units

Three 19" racks belong to the topside control equipment (Fig. 7a). For piloting purpose, two racks are necessary for a proper and reasonable display of the essential sensors, such as cameras, sonar and navigation information. Flying the ROV is done by a special control panel, providing a comfortable flying along all 3 spatial axes. A third rack was developed for the storage of the devices for the stereoscopic camera system (see next section).

Additionally, this rack accommodates two Mini-DV Recorders for the storage of the video sequences obtained during the dives.

Stereoscopic camera system

With a common video system, the information of the spatial z-axis is lost. It is not possible to determine, which particles are in the front and which are in the back. This information however, is crucial for a proper observation of sinking particles in a 3 dimensional environment.

In addition to the standard video camera system, a stereoscopic camera system was developed by the marine technology group of the University of Bremen and used during the in-situ observations. It consists of two pencil cameras, mounted onto a second pan & tilt unit (Fig. 7b). The cameras are adjusted so that the lines of sights are slightly converging. Both video signals are transferred independently to the surface control units. Here, two transscaler convert the analog, composite video signals into 640 x 480 VGA signals. The VGA signals are displayed on two LCD displays, mounted into a helmet (Head Mounted Display – HMD). The result is a 3 dimensional view of the particles in the water column. To make the 3-D vision as realistic and as efficient as possible, the pan & tilt unit can either be controlled by a joystick or simply by moving the head. An infrared sensor transfers the information about the position of the helmet to the downside mounted pan & tilt unit.

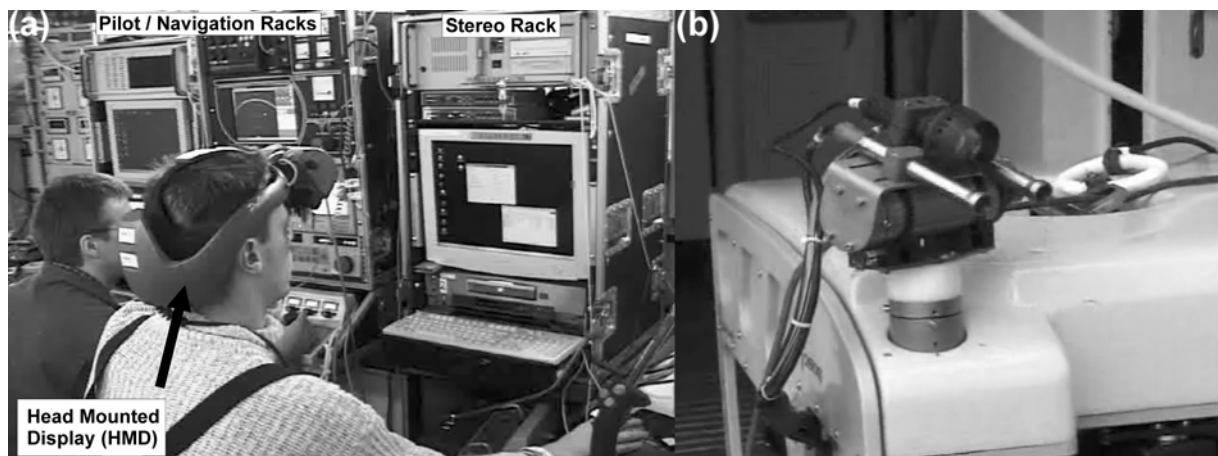


Fig. 7: (a) The two piloting control racks (left & middle) onboard RV Poseidon providing video screens, sonar screen and additional navigation information. On the right side, the stereo rack and HMD. (b) The stereo pencil cameras mounted onto a pan & tilt unit with additional headlight on top.

Deployment procedure

The Cherokee is deployed without a *Tether Management System* (TMS) in a *free flying* modus. The more tether is hogged down, the stronger is the drag on the wire, making the system inoperational at a certain tether length. To prevent this, the ROV tether was attached to a ship wire in 10 m intervals with cable ties. Between the first connection of the tether to the ships wire, approximately 50 m were paid out, providing the actual operation radius of the ROV. The ships wire was connected to a depressor weight and lowered simultaneously with the ROV tether to the operation depth. Using this procedure, it takes about 45 min to deploy the system to the maximum diving depth of 1000 m. Operation time ranged between 6 h to 8 h with a minimum crew of six persons during deployment and recovery.



Fig. 8. The *Adelie* video software was used for sighting sequences of interest. In addition, it provided the grabbing of single frames for the subsequent image analysis. The image shows a filtration structure of a giant appendicularian (*Bathochordaeus*). Identification was provided by Dr. W. Hamner, University of California Los Angeles

Image analysis

The videotapes were evaluated using the *Ifremer* video software *Adelie* (Fig. 8). The DV recorder was connected via Firewire interface to a PC. The software was used for video

sighting and frame grabbing purposes. Single images were acquired from the DV tapes and subsequently stored to the PC's hard disk. The image analysis and data extraction was done with the *Optimas* software. The ROV was used to acquire the horizontal distribution of particles along several transects in specific depth and for in-situ observation of the sinking behaviour of marine aggregates. For data extraction procedures refer to manuscript 1 (p. 31), which includes a complete and detailed description of the applied measurements.

2. References

- Allredge, A.L., 1979, The chemical composition of macroscopic aggregates in two neritic seas: *Limnology and Oceanography*, v. 24, p. 855-866.
- Allredge, A.L., and Crocker, K.M., 1995, Why do sinking mucilage aggregates accumulate in the water column?: *The Science of the Total Environment*, v. 165, p. 15-22.
- Allredge, A.L., and Gotschalk, C., 1988, In situ settling behaviour of marine snow: *Limnology and Oceanography*, v. 33, p. 339-351.
- Allredge, A.L., and Gotschalk, C., 1989, Direct observation of the mass flocculation of diatom blooms: characteristics, settling velocities and formation of diatom aggregates: *Deep Sea Research I*, v. 36, p. 159-171.
- Allredge, A.L., and Jackson, G.A., 1995, Aggregation in marine system: *Deep Sea Research II*, v. 42, p. 1-7.
- Asper, V.L., 1987, Measuring the flux and sinking speed of marine snow aggregates: *Deep Sea Research I*, v. 34, p. 1-17.
- Asper, V.L., Honjo, S., and Orsi, T.H., 1992, Distribution and transport of marine snow aggregates in the Panama Basin: *Deep Sea Research I*, v. 39, p. 939-952.
- Azetsu-Scott, K., and Passow, U., in press, Ascending marine particles: Significance of transparent exopolymer particles (TEP) in the upper ocean: *Limnology and Oceanography*.
- Berger, W., Smetacek, V., and Wefer, G., 1989, Ocean productivity and paleoproductivity - An overview, *in* Berger, W., Smetacek, V., and Wefer, G., eds., *Productivity in the ocean: Present and past*: New York, Wiley, p. 139-153.
- Broecker, W.S., 1982, Ocean Chemistry During Glacial Times: *Geochim Cosmochim Acta*, v. 46, p. 1698-1705.
- Chisholm, 2000, Oceanography: Stirring times in the Southern Ocean: *Nature*, v. 407, p. 685-687.
- Clarke, A., Church, J., and Gould, J., 2001, Ocean processes and climate phenomena, *in* Siedler, G., Church, J., and Gould, J., eds., *Ocean Circulation and Climate: Observing and Modelling the Global Ocean*: London, Academic Press, pp. 11-30.
- Cunningham, A., McKee, D., Craig, S., Tarran, G., and Widdicombe, C., 2003, Fine-scale variability in phytoplankton community structure and inherent optical properties measured from an autonomous underwater vehicle: *Journal of Marine Systems*, v. 43, p. 51-59.
- Diercks, A.R., and Asper, V.L., 1997, In situ settling speeds of marine snow aggregates below the mixed layer: Black Sea and Gulf of Mexico: *Deep Sea Research I*, v. 44, p. 385-398.
- Dyrssen, D.W., 2001, The biogeochemical cycling of carbon dioxide in the oceans - perturbations by man: *The Science of the Total Environment*, v. 277, p. 106.
- Fowler, S.W., and Knauer, G.A., 1986, Role of large particles in the transport of elements and organic compounds through the oceanic water column: *Progress in Oceanography*, v. 16, p. 147-194.
- Freudenthal, T., Neuer, S., Meggers, H., Davenport, R., and Wefer, G., 2001, Influence of lateral particle advection and organic matter degradation on sediment accumulation and stable nitrogen isotope ratios along a productivity gradient in the Canary Islands region: *Marine Geology*, v. 177, p. 93-109.
- Gardner, W.D., and Walsh, I.D., 1990, Distribution of macroaggregates and fine-grained particles across a continental margin and their potential role in fluxes: *Deep Sea Research I*, v. 37, p. 401-411.
- Gorsky, G., Aldorf, C., Kage, M., Picheral, M., Garcia, Y., and Favole, J., 1992, Vertical distribution of suspended aggregates determined by a new underwater video profiler: *Annales de l'Institut océanographique*, v. 68, p. 275-280.

- Hamner, W.M., and Robison, B.H., 1992, In situ observations of giant appendicularians in Monterey Bay: *Deep Sea Research*, v. 39, p. 1299-1313.
- Honjo, S., Doherty, K.W., Agrawal, Y.C., and Asper, V.L., 1984, Direct optical assessment of large amorphous aggregates (marine snow) in the deep ocean: *Deep Sea Research* i, v. 31, p. 67-76.
- Hughes, P., and Barton, E.D., 1974, Stratification and water mass structure in the upwelling area northwest Africa in April/May 1969: *Deep Sea Research I*, v. 21, p. 611-628.
- Johnson, J., and Stevens, I., 2000, A fine resolution model of the eastern North Atlantic between the Azores, the Canary Islands and the Gibraltar Strait: *Deep Sea Research I*, v. 47, p. 875-899.
- Kiorboe, T., 2000, Colonisation of marine snow aggregates by invertebrate zooplankton: Abundance, scaling and possible role: *Limnology and Oceanography*, v. 45, p. 479-484.
- Kiorboe, T., 2001, Formation and fate of marine snow: small-scale processes with large-scale implications: *Scientia Marina*, v. 65, p. 57-71.
- Lampitt, R.S., 1985, Evidence for the seasonal deposition of detritus to the deep-sea floor and its subsequent resuspension: *Deep Sea Research I*, v. 32, p. 885-897.
- Lampitt, R.S., 1996, Snow Falls in the Open Ocean, in Summerhayes, C.P., and Thorpe, S.A., eds., *Oceanography - An Illustrated Guide*: London, Manson Publishing, p. 96-112.
- Logan, B.E., Passow, U., Alldredge, A.L., Grossart, H.-P., and Simon, M., 1995, Rapid formation and sedimentation of large aggregates is predictable from coagulation rates (half-lives) of transparent exopolymer particles (TEP): *Deep Sea Research II*, v. 42, p. 203-214.
- Lohmann, H., 1908, On the relationship between pelagic deposits and marine plankton: *Int. Rev. Ges. Hydrobiol. Hydrogr.*, v. 1, p. 309-323.
- Lueck, R.G., and Osborn, T.R., 1985, Turbulence measurements with a submarine: *J. Phys. Oceanogr.*, v. 15, p. 1502-1520.
- MacIntyre, S., Alldredge, A.L., and Gotschalk, C., 1995, Accumulation of marine snow at density discontinuities in the water column: *Limnology and Oceanography*, v. 40, p. 449-468.
- MacKenzie, L., Sims, I., Beuzenberg, V., and Gillespie, P., 2002, Mass accumulation of mucilage caused by dinoflagellate polysaccharide exudates in Tasman Bay, New Zealand: *Harmful Algae*, v. 1, p. 69-83.
- Middleton, N.J., Betzer, P.R., and Bull, P.A., 2001, Long range transport of 'giant' aeolian quartz grains: linkage with discrete sedimentary sources and implications for protective particle transfer: *Marine Geology*, v. 177, p. 411-417.
- Milliman, J.D., and Syvitsky, J.P.M., 1992, Geomorphic/Tectonic control of sediment discharge to the ocean: The importance of small mountainous rivers: *Journal of Geology*, v. 100, p. 520-540.
- Mittelstaedt, E., 1983, The Upwelling Area Off Northwest Africa - A Description of Phenomena Related to Coastal Upwelling: *Progress in Oceanography*, v. 12, p. 307-331.
- Mittelstaedt, E., 1991, The ocean boundary along the northwest African coast: Circulation and oceanographic properties at the sea surface: *Progress in Oceanography*, v. 26, p. 307-355.
- Neuer, S., Ratmeyer, V., Davenport, R., Fischer, G., and Wefer, G., 1997, Deep water particle flux in the Canary Island region: seasonal trends in relation to long-term satellite derived pigment data and lateral sources: *Deep-Sea Research I*, v. 44, p. 1451-1466.
- Nowald, N., 1999, Die Erfassung der vertikalen Verteilung partikulären Materials im Ozean mit Hilfe von Kamerasystem und digitaler Bildanalyse [Diploma thesis]: Bremen, University of Bremen.

- Passow, U., and Alldredge, A.L., 1995, Aggregation of a diatom bloom in a mesocosm: The role of transparent exopolymer particles (TEP): *Deep Sea Research II*, v. 42, p. 99-109.
- Penner, J.E., and Zhang, Y., 2004, Projections of climate forcing by sulfate, organic aerosols, dust, and sea salt, IPCC Model Intercomparison Workshop: Seattle.
<http://ams.confex.com/ams/annual2000/11global/program.htm>
- Pilskaln, C.H., Lehmann, C., Paduan, J.B., and Silver, M.W., 1998, Spatial and temporal dynamics in marine aggregate abundance, sinking rate and flux: Monterey Bay, central California: *Deep Sea Research II*, v. 45, p. 1803-1837.
- Prospero, J.M., 1990, Mineral-aerosol transport to the North Atlantic and North Pacific: The impact of African and Asian sources, *in* Knap, A.H., ed., *The long-range atmospheric transport of natural and contaminant substances*: Dordrecht, Mathematical and Physical Sciences. Kluwer Academic Publishers, p. 19-52.
- Ramaswamy, V., Nair, R.R., Manganini, S., Haake, B., and Ittekott, V., 1991, Lithogenic fluxes to the deep Arabian Sea measured by sediment traps: *Deep Sea Research I*, v. 38, p. 169-184.
- Ratmeyer, V., and Wefer, G., 1996, A high resolution camera system (ParCa) for imaging particles in the ocean: System design and results from profiles and a three-month deployment: *Journal of Marine Research*, v. 54, p. 589-603.
- Sarnthein, M., Tetzlaff, G., Koopmann, B., Wolter, K., and Pflaumann, U., 1981, Glacial and interglacial wind regimes over the eastern subtropical Atlantic and North-West Africa: *Nature*, v. 293, p. 193-196.
- Sarnthein, M., Thiede, J., Pflaumann, H., Erlenkeuser, H., Fütterer, D., Koopmann, D., Lange, H., and Seibold, E., 1982, Atmospheric and oceanic circulation patterns off Northwest Africa during the past 25 million years, *in* von Rad, H., Hinz, K., Sarnthein, M., and Seibold, E., eds., *Geology of the Northwest African Continental Margin*: Berlin, Springer, p. 584-604.
- Schütz, L., and Seibert, M., 1987, Mineral aerosol and source identification: *Journal of Aerosol Science*, v. 18, p. 1-10.
- Schütz, L.W., Prospero, J.M., Buat-Menard, P., Carvalho, R.A.C., Cruzado, A., Harriss, R., Heidam, N.Z., and Jaenicke, R., 1990, The long-range transport of mineral aerosols: group report, *in* Knap, A.H., ed., *The long-range atmospheric transport of natural and contaminant substances*: Dordrecht, Mathematical and Physical Sciences. Kluwer Academic Publishers, p. 197-229.
- Shanks, A.L., 2002, The abundance, vertical flux, and still-water and apparent sinking rates of marine snow in a shallow coastal water column: *Continental Shelf Research*, v. 22, p. 2045-2064.
- Shanks, A.L., and Trent, J.D., 1980, Marine snow: sinking rates and potential role in vertical flux: *Deep Sea Research I*, v. 27A, p. 137-143.
- Siedler, G., and Onken, R., 1996, Eastern Recirculation, *in* Krauss, W., ed., *The Warmwatersphere of the North Atlantic Ocean*: Berlin, Stuttgart, Gebrüder Bornträger, p. 339-364.
- Suzuki, N., and Kato, K., 1953, Studies on suspended materials (marine snow) in the sea. Part 1. Sources of marine snow: *Bulletin of the faculty of Fisheries of Hokkaido University*, v. 4, p. 132-135.
- Swap, R., Garstang, M., Greco, S., Talbot, R., and Kallberg, P., 1992, Saharan dust in the Amazon Basin: *Tellus*, v. 44b, p. 133-149.
- Syvitsky, J.P.M., Asprey, K.W., and Leblanc, K.W.G., 1995, In-situ characteristics of particles settling within a deep-water estuary: *Deep Sea Research II*, v. 42, p. 223-256.

- Tetzlaff, G., and Wolter, K., 1980, Meteorological patterns and the transport of mineral dust from the North African continent, *in* Sarnthein, M., Seibold, E., and Rognon, P., eds., *Palaeoecology of Africa*: Rotterdam, Balkema, A.A., p. 31-42.
- Thomsen, J., 2003, The benthic boundary layer, *in* Wefer, G., Billet, D., Hebbeln, D., Jorgensen, B.B., Schlüter, S., and van Weering, T.C.E., eds., *Ocean Margin System*: Berlin Heidelberg New York, Springer Verlag, p. 143-155.
- Waite, A.M., Safi, K.A., Hall, J.A., and Nodder, S.D., 2000, Mass sedimentation of picoplankton embedded in organic aggregates: *Limnology and Oceanography*, v. 45, p. 87-97.
- Walsh, I.D., and Gardner, W.D., 1992, A comparison of aggregate profiles with sediment trap fluxes: *Deep Sea Research I*, v. 39, p. 1817-1834.
- Yu, X., Dickey, T.D., Bellingham, J., Manov, D., and Streitlien, K., 2002, The application of autonomous underwater vehicles for interdisciplinary measurements in Massachusetts and Cape Bays: *Continental Shelf Research*, v. 22, p. 2225-2245.

3. Publications

3.1 The vertical distribution of particulate matter in the upwelling system off Cape Blanc (NW-Africa) obtained by high-resolution camera profiles, and implications for rapid, vertical mass transfer

submitted to Deep-Sea Research

Nicolas Nowald, Volker Ratmeyer and Gerold Wefer

University of Bremen, Department of Geosciences, Klagenfurterstrasse, 28359 Bremen

Abstract

During the RV POSEIDON cruise 272 in April 2001, 6 vertical profiles were obtained along two transects with the deep-sea particle camera system ParCa. The camera was deployed on the middle and upper slope areas in the highly productive upwelling region off Cape Blanc (NW-Africa). Middle and upper slope profiles show significant differences in the distribution of particulate matter in the water column. The highest concentrations of particulate matter on the middle slope were observed in the upper 200 m of the water column ($\sim 200 \text{ n l}^{-1}$), and these amounts decreased steadily down to the seafloor ($\sim 30 \text{ n l}^{-1}$). In contrast, the highest concentrations on the upper slope were seen just above the ocean floor. Particle concentrations here exceeded those observed in the euphotic zone by a factor of two, and the profiles indicate intense resuspension and re-aggregation processes in the benthic boundary layer (BBL). Although the upper-slope profiles are characterised by increased particle concentrations in the BBL, no indications for the lateral advection of particulate matter from the upper slope towards the open ocean were observed. In fact, two major vertical transport mechanisms can be described for the Cape Blanc region. The first case is a continuous flux of particulate matter mainly driven by large, coagulated particle aggregates. These aggregates were observed in high concentrations in the entire water column, providing a steady, vertical flux of material from the ocean surface to the seafloor. Because these aggregates sink relatively fast and their sinking trajectory is almost vertical, their lateral advection is presumed to be small. Thus, we conclude a predominant in-situ deposition of particulate matter on the middle- and upper-slope areas. The second case is the rapid mass transfer of large amounts of particulate matter on short temporal scales. During such a “sinking event”, the size spectrum of particles in the water column is distinctively altered. Material initially produced in the surface waters sinks at higher rates than the particulate matter in the mid-water zone and scavenges the more abundant small particles on its way down through the water column. This results in increased particle sizes within the sinking cloud and a depletion of small particles in the water column above. High concentrations of large particle aggregates ($>2 \text{ mm}$) in the sinking particle cloud indicate a vertical delivery of particulate matter at rates higher than 35 m d^{-1} .

1. Introduction

In the region off Cape Blanc/Mauritania, intense upwelling occurs throughout the year (Nykjaer and Van Camp, 1994). The atmospheric and oceanographic conditions are responsible for a high primary production of particulate matter in the euphotic zone along the coast. Although the upwelling belt is only about 50 to 70 km wide (Van Camp et al., 1991), large filaments of chlorophyll-enriched water are advected almost 300 km towards the open ocean (Hernandez-Guerra and Nykjaer, 1997).

During recent decades, the upwelling system off the NW African coast has been the subject of many palaeoclimatic, oceanographic and particle flux studies. The Cape Blanc region has been characterised by extremely high sedimentation rates of more than $18 \text{ g cm}^{-2} \text{ k.y}^{-1}$ during the last 5000 years (de Menocal et al., 2000) and is strongly influenced by wind-transported dust from the continent (Ratmeyer et al., 1999; Schütz et al., 1981). Long-term monitoring of particle fluxes, carried out with sediment-trap moorings by Fischer et al. (1996a) and Romero et al. (2002), showed distinct year-to-year flux variations. Other oceanic regions, such as the Canary Islands or the Sargasso Sea, reflect rather clear seasonal flux patterns (Neuer et al., 1997; Conte et al., 2001).

Although significant scientific progress for our understanding of this highly dynamic upwelling system has been made, still little is known about the in-situ distribution of particulate matter in this region. Our knowledge of the shape, size and vertical distribution of particles in the ocean is mainly based on non-destructive optical methods, like camera profiles. Since the introduction of this method by Honjo et al. (1984), studies on the vertical distribution of particulate matter have been carried out in many oceanic regions, including the Black Sea (Diercks and Asper, 1997), the Gulf of Mexico (Gardner and Walsh, 1990; Walsh and Gardner, 1992), the Panama Basin (Asper et al., 1992b), the Monterey Bay (MacIntyre et al., 1995), the Mediterranean Sea (Gorsky et al., 1992), and the equatorial Atlantic Ocean (Ratmeyer and Wefer, 1996). However, the number of publications is comparably low, and our knowledge of the in-situ distribution of particles in the ocean is based on few studies.

The export of particulate matter from the ocean surface to the deep-sea occurs in the form of large, coagulated aggregates, known as marine snow. Marine snow, or by definition particulate matter $>0.5 \text{ mm}$ (Fowler and Knauer, 1986; McCave, 1975), is formed of small particles from organic and inorganic sources. The aggregation of particulate matter is a complex field of study, controlled by biological and physical processes (Alldredge et al., 1995; Jackson, 1990, 2001; Passow and Alldredge, 1995). Sticky exudations of microorganisms, phytodetritus, and lithogenic material from the continents, form complex

and fragile aggregates when they collide as a direct result of wave energy (Lampitt, 1996) and/or gravitational processes (Alldredge and McGillivray, 1991). The result of aggregate growth is increased density and hence, faster sinking velocities (Alldredge and Gotschalk, 1988; Asper, 1987; Asper et al., 1992b; Pilskaln et al., 1998). While more than 3/4 of the organic material produced in the euphotic zone is already remineralised in the upper water column, only large, fast sinking aggregates have a chance to reach the seafloor. So their contribution to the mass transfer of nutrients and elements from the ocean surface to the seafloor is mainly a function of their vertical distribution, composition, size, and sinking rate (Asper, 1987; Gardner and Walsh, 1990; MacIntyre et al., 1995; Walsh and Gardner, 1992).

To study the vertical distribution of particulate matter and its role with respect to particle fluxes in the Cape Blanc region, 6 vertical camera profiles were obtained within the dynamic upwelling belt. These profiles were acquired against the background of three major scientific questions:

- 1.) How is particulate matter distributed along the upper and middle slope areas off Cape Blanc?
- 2.) Which factors and mechanisms are responsible for generating particle abundance patterns in the water column?
- 3.) What are the key transport processes and pathways of particulate matter in highly dynamic upwelling systems?

Apart from the changing particle concentration with depth, additional parameters are necessary for our understanding regarding the generation of particle distribution patterns and transport processes. For this purpose, we extracted the vertical size distribution of particles and their orientation in the water column. Another objective was to determine the abundance of large, coagulated particle aggregates. These large, comet shaped aggregates were reported by Alldredge and Gotschalk (1988), Syvitsky et al. (1995) and Gentien et al. (1995), and their abundance is of special interest due to their key role in rapid vertical mass transfer. In addition to the camera images, we used satellite-derived chlorophyll pigment concentrations and compared them with the particle distributions in the ocean surface. In this approach, we examined the extent to which primary production is associated with the in-situ particle abundance in the surface waters.

2. Methods

2.1 Investigation area

The study area is located ~80 km southwest of Cape Blanc/Mauritania, within the highly dynamic upwelling belt. The investigation area is a rectangle of approximately 80 km x 60 km. Along two transects, a total of 6 vertical camera profiles were obtained (Fig. 1). Profile depths range between 240 m on the lower shelf down to 1930 m in the middle slope areas. The particle camera was lowered at a winch speed of 0.3 m s^{-1} from the surface to the seafloor, acquiring images from the entire water column at depth intervals of 10 m. The temporal delay between the first (GeoB 7408) and the last camera profile (GeoB 7415) is 38 h. Primary production conditions in the upper water column change rapidly on short temporal scales. Thus, a small time window is necessary to evaluate the coherence of the particle distribution in the area of investigation. A detailed station list is presented in Table 1.

Table 1: ParCa station list: positions, deployment times and depths

Station	Position		Date	Deploy time downcast		Depths (m)	
	Lat.	Lon.		Time	(UTC)	Water	Profile
GeoB 7408	20°17.1'N	18°14.8'W	06.04.01	06.00 - 08.00		1860	1820
GeoB 7410	20°26.94'N	17°50.85'W	06.04.01	19.40 - 20.10		635	620
GeoB 7411	20°23.6'N	18°01.1'W	06.04.01	21.20 - 22.30		1213	1180
GeoB 7412	20°35.7'N	17°41.9'W	07.04.01	01.30 - 02.00		241	241
GeoB 7413	20°38.9'N	17°50.7'W	07.04.01	06.30 - 07.00		509	480
GeoB 7415	20°48.6'N	18°15.7'W	07.04.01	18.00 - 20.00		1933	1930

2.2 Camera system description

The datasets presented in this study were obtained with the deep-sea camera system ParCa, described in Ratmeyer and Wefer (1996). The optical setup is based on camera systems used by Honjo et al. (1984), Asper (1987), and others. ParCa employs a modified, programmable PHOTOSEA 70 middle format camera. Compared to standard 35 mm camera systems, the 6x6 cm sized negatives provide images with a much higher resolution. ParCa is equipped with a light-sensitive KODAK TRI-X Pan film for enhanced results in low light situations. Up to 350 single frames can be stored in the camera's magazine. A strobe, mounted perpendicular to the camera, shoots a collimated light beam of 12 cm width, illuminating a total sample volume of 0.025 m^3 . Power supply is provided by a 24V/38Ah battery. All system components are mounted in a galvanised frame, with a total weight of approximately 200 kg. In contrast to the ParCa system in Ratmeyer and Wefer (1996), the improved version is equipped with a SeaBird 36 telemetry unit and a SeaBird 19 CTD. The CTD transmits the pressure values to ParCa's controller and triggers it at specific depth

intervals. The telemetry unit provides full control over the system and trigger depth information, while it is being lowered on the ship's coaxial wire.

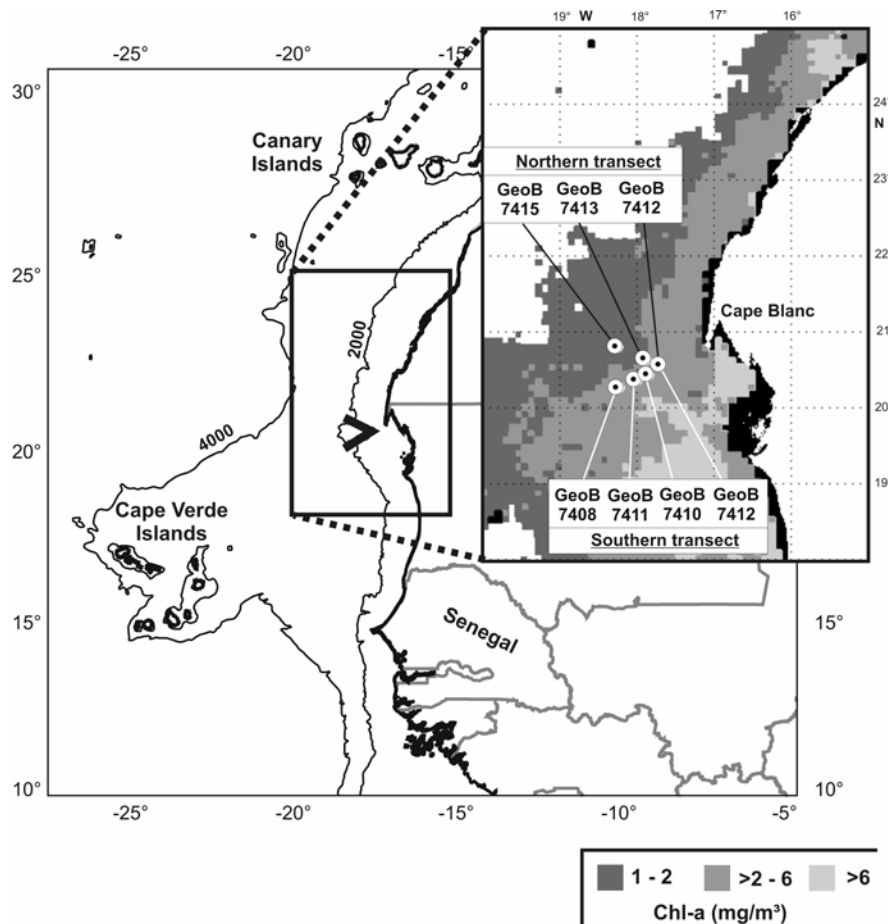


Fig.1: Map of ParCa stations during RV Poseidon cruise 272. ParCa was deployed at six stations along two transects ~ 80 km southwest off Cape Blanc. Chlorophyll pigment concentrations were averaged for the month of April 2001.

2.2 Image capturing and data extraction

Two subsamples from the 6x6 cm negatives were digitised after recovery and film development, using an ADIMEC MX12 CCD 8-bit grey scale camera (1024x1024 pixel resolution) and an IC PCI Imaging Technology frame-grabber card. Subsamples were taken because digitalisation of the entire negative would result in a poor size/resolution relationship. To obtain smaller particles, the negative was magnified before digitalisation. The calibrated frame width of a digitised subsample picture is 187 x 187 cm, resulting in a sample volume of 4.19 l. The smallest measurable particle size with this image analysis setup is 180 μm . Within the digital image analysis software OPTIMAS, the automated image processing and data extraction procedure was provided by an adapted OPTIMAS macro file. This macro was used

to export the datasets of particle abundance, particle size and particle orientation to a worksheet for further data preparation.

2.2.1 Particle abundance

The image analysis software recognises particles as areas in the 2-dimensional frames. The abundance of single, small particles was computed by counting the number of areas, i.e., particles, on each subsample image (Fig. 2). An 8-bit grey-scale threshold (Burdick, 1997; Parker, 1997) was used to distinguish between the background and the particles in the foreground. Zooplankton and large-particle aggregates were excluded from the measurement by being cut away from the image.

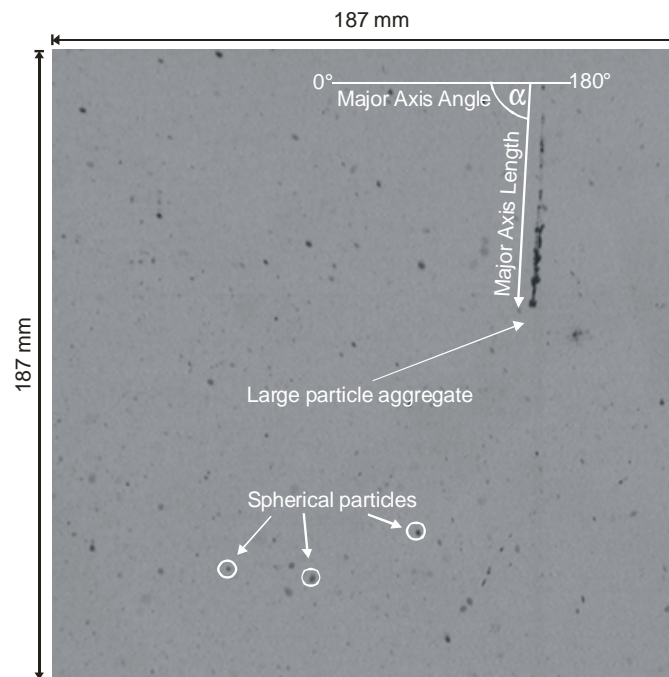


Fig.2: Calibrated ParCa image showing small, spherically shaped particles and large, coagulated aggregates. The orientation of particulate matter is defined by the Major Axis Angle and the Major Axis Length.

The size of spherically shaped particles is calculated as their Equivalent Spherical Diameter (ESD). An algorithm computes all areas, however they are shaped, to regular, geometrical circles and extracts the ESD. The inaccuracy, when transforming, i.e., ellipsoidal areas to circles, is a function of the ratio between the two ellipsoidal axes. Because most of the particles are comparatively small, the ratio between the two axes is small, and therefore the error in the computation can be ignored.

2.2.2 Aggregate abundance

Because the software is not able to distinguish between spherical particles and large, coagulated particle aggregates, the aggregate abundance dataset was created by viewing each subsample image and counting aggregates manually (Fig. 2). The size of large aggregates at profile GeoB 7415 was likewise measured manually, using the Major Axis Length extraction tool (Chapter 2.2.4). The determination of what is a particle aggregate and what is not is subjective. By our definition, an aggregate had to consist of at least two coherent particles, regardless of its size. In general, they looked like flakes or were comet-shaped. These characteristic shapes made them easy to identify. We think that other investigators would obtain results similar to ours, and that this method leads to a representative dataset for the distribution of large, coagulated aggregates in the water column.

2.2.3 Particle-size distribution

For investigations of the vertical size distribution of particulate matter, 24 size classes were defined ranging from $\leq 185 \mu\text{m}$ to $>2000 \mu\text{m}$ (Tab. 2). For illustrating the change of particle sizes with depth, the particle concentrations of each size class were averaged over a depth interval of 100 m. The concentrations of the different size classes were calculated as their frequencies in percent. The colour spectra encoding was carried out using the Kriging method, where blue colours represent low, and white to yellow colours high frequencies.

Table 2: Size classifications and ranges for spherical particles

Size Class	1	2	3	4	5	6	7	8	9	10	11	12	13	14	15	16	17	18	19	20	21	22	23	24
Range (μm)	≤ 185	245	269	296	324	356	391	429	471	517	623	684	751	825	905	994	1091	1198	1315	1443	1584	1739	1909	> 2000
Range (mm)	$\leq 0,5$									$> 0,5 - \leq 1$						$> 1 - \leq 2$					> 2			

2.2.4 Particle and aggregate orientation

The digital image analysis software provides tools for the extraction of parameters for the determination of the orientation of objects in a 2-dimensional frame. The first parameter is the Major Axis Length, and second is the Major Axis Angle. The Major Axis Length is the longest axis, measurable within a screen object from one edge to the other. The Major Axis Angle gives the angle of the Major Axis of a screen object from the horizontal in degrees, measured counterclockwise. If a particle has a Major Axis Angle of 0° or 180° , it would be orientated horizontally, or parallel to the ocean bottom. At 90° , the Major Axis of a particle would be orientated perpendicular to the seafloor (Fig. 2).

2.2.5 Chlorophyll pigment concentrations and particle abundance in the surface water

Chlorophyll-a concentrations were obtained by SeaWiFS satellite images for a comparison of the camera-derived in-situ particle abundance and pigment concentrations at the ocean surface. Data extraction was provided by a SUN workstation using the IDL image processing software. The daily chlorophyll values from all available images from April 2001 were averaged. Chlorophyll concentrations that are congruent with the ParCa deployment sites are presented in Table 3. These data were compared with the averaged particle concentrations of the camera profiles of the upper 30 m of the water column. The chlorophyll signal might be reflected down to this still light-flooded and high-productive depth. At least two images were obtained within this depth range in all profiles to ensure a representative comparison. Due to a malfunction of the camera, an exception was made for site GeoB 7408. The particle concentration presented in Table 3 for this site is from 60 m, because the first image of this profile was obtained at this depth.

Table 3: Chlorophyll-a pigment concentrations averaged for the period of April 2001 and averaged particle concentrations of the upper 30 m of the water column

Transect	South				North	
Station	GeoB 7408	GeoB 4711	GeoB 7410	GeoB 7412	GeoB 7413	GeoB 7415
Chl-a (mg m ⁻³) April 2001	3.43	3.43	3.43	3.31	3.20	1.45
Particle abundance (n/l) ≤ 30m	(168 at 60m)	79.73	115.07	106.59	73.53	58.81

2.2.6 Methodical limitations and general considerations

In this study, we describe new parameters extracted directly from the images in order to examine factors influencing particle abundance patterns and transport processes. Most studies presenting vertical camera profiles describe the changing particle concentrations with depth in comparison with other datasets, for example from CTD probes. Pilskaln et al. (1998) underlined the necessity of the simultaneous measurement of many parameters, coincident in time and space, in order to understand processes influencing particle fluxes and particle distribution patterns. Additional CTD data would increase the significance of the particle profiles, but these are not available. However, the images provide more information than just the numbers of particles visible on a frame. We present high-resolution size distribution datasets, particle concentrations, large-particle aggregate concentrations, and information about the orientation of particles in the marine environment as extracted from the images. We think that the evaluated image datasets are a meaningful method to explain and to support known mechanisms responsible for the vertical distribution of particulate matter, and that they provide new insights of particle transport mechanisms in the Cape Blanc region.

SeaWiFS satellite images were used for a quantitative comparison of particle abundances and chlorophyll pigment concentrations in the upper water column. The intention was to examine to what extent particle abundance is mirrored by the chlorophyll concentration in surface waters. For this purpose, we used the averaged chlorophyll concentration for the period of April 2001. However, the best way to compare the two parameters would be the simultaneous temporal acquisition of both datasets. Due to a massive sandstorm this was not possible, and no satellite images are available for the time period of the camera deployment. Thus, the chlorophyll datasets presented are used as approximate guide values to describe possible connections of the two parameters. One has to keep in mind that the satellite measures the area-wide surface distribution of chlorophyll pigments and doesn't penetrate more than 5 m below the ocean surface. By contrast, camera profiles obtain the vertical distribution of macroscopically resolvable particles in the water column.

The first image was usually taken at a depth of 10 m, which is deeper than the satellite sensor penetration. In addition, we averaged the particle concentration over the upper 30 m to visualise general trends of the particle distribution of the surface water. Thus, it might be difficult to say whether differences or conformities between camera and satellite data are meaningful. Keeping these limitations in mind, we used the two methods for an initial, careful examination of a possible connection between chlorophyll concentrations and particulate matter in the ocean surface layer.

The composition of particulate matter is as complex as the processes influencing their distribution in the water column. Several different types of marine snow were described by Alldredge (1979, 1998) and Silver et al. (1998). The composition varies depending on the location as well as the prevailing season. These results are based on in-situ collection by scuba dives or Remotely Operated Vehicle operations. Images do not provide any information about the compositional properties. Nevertheless, we could clearly distinguish between large, coagulated aggregates and spherically shaped particles. Usually, particulate matter is divided into two classes: smaller marine snow and marine snow. As this classification is based only on the size of the particulate matter, it gives no information regarding single particles or coagulated aggregates. A particle smaller marine snow could theoretically consist of more than one component. On the other hand, a particle of the marine snow size class could be just a single particle. In this study we pursue a different approach: we do not distinguish between smaller marine snow and marine snow, but between large coagulated aggregates, and spherical particles regardless of their size. An aggregate is, by definition, not a grain and therefore cannot be characterised by a size class. In fact, it consists of a variety of particles of

different sizes, materials, and origins and is formed by the repetitive collision and coalescence of smaller ones (McCave, 1984; O'Melia, 1972). Due to the resolution limits of the digital images, it is not possible to ascertain whether a spherical particle is an aggregate or not. Thus, we only designated particles to be aggregates when they obviously consisted of at least two coherent particles. These aggregates are thought to contribute a large amount to the vertical flux and so aggregates and spherical particles were regarded as two different populations.

Transportation can be described as the shift of material over time and space. Regarding particle profiles, time is a parameter, which cannot be taken into account. Vertical profiles represent a snapshot of the distribution of particulate matter at a certain location at a specific time. Research on transport processes is usually done by investigating the size distribution of, for instance, sediments or trap material. In this study, we use changes in the in-situ size distribution with depth to make statements about possible transport processes of particles and aggregates in the water column. It has to be kept in mind that the camera system obtains only particles larger than 180 μm , and that smaller particles are excluded from the measurements due to the image resolution.

3. Results

3.1 Particle abundance and distribution patterns

The Cape Blanc profiles are divided into a northern and a southern transect, where profile GeoB 7412 is the most eastern station of both transects. The most noticeable feature of all profiles is the large variety of particle abundance patterns and the distinct differences in the particle concentrations (Fig. 3a-c and Fig. 4a-d).

Particle concentrations range between a minimum of 8 n l^{-1} at station GeoB 7411 at 1150 m depth, and more than 250 n l^{-1} at a depth of 630 m at station GeoB 7410. The highest concentrations were expected in the ocean surface, but this was only the case at site GeoB 7413. The highest concentrations were measured at either at the bottom of the upper mixed layer, around 200 m depth (GeoB 7408 – Fig. 4a; GeoB 7411 – Fig. 4b), or just above the seafloor (GeoB 7410 – Fig. 4c, GeoB 7412 – Fig. 4d). At profile GeoB 7415 (Fig. 3a), high values are also found within a mid-water maximum, between 650 m and 800 m. Particle concentrations in the ocean surface waters (<30 m) of the northern transect (Fig. 3), decrease constantly from 106.59 n l^{-1} at site GeoB 7412 close to the coast, to 73.53 n l^{-1} (GeoB 7413), down to 58.81 n l^{-1} at site GeoB 7415, farther offshore. In contrast, no such decreasing trend was observed for the southern transect (Fig. 4a-d). Here, concentrations range between 90 n l^{-1} (GeoB 7411) and 150 n l^{-1} at station GeoB 7408, with no coherence with respect to the

distance from the coast. Increasing concentration near the ocean bottom is found at all sites except GeoB 7415. At the shallower sites GeoB 7410 (Fig. 4c) and GeoB 7412 (Fig. 4d), abundances are more than twice as high above the ocean floor ($> 200 \text{ n l}^{-1}$) in comparison to the entire water column above. The trend of decreasing numbers of particles in the ocean surface layer with increasing distance from the coast observed for the northern transect, is seen in the near-bottom areas in the southern transect. Concentrations above the seafloor decrease from more than 250 n l^{-1} at site GeoB 7412, down to 173 n l^{-1} at site GeoB 7411 and 119 n l^{-1} at station GeoB 7408.

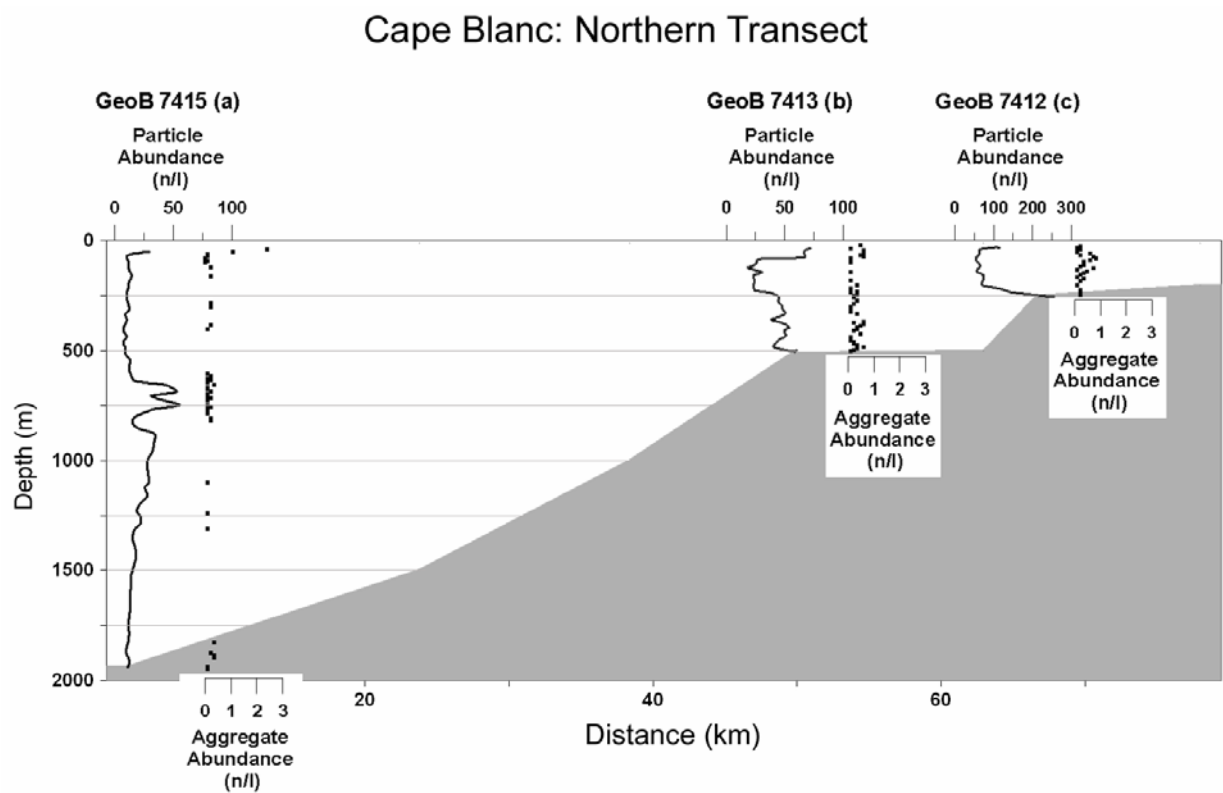


Fig.3 a-c: Vertical distribution of spherical particles and large aggregates along the northern transect. All lines are fitted with a 5-point running average. Site GeoB 7415 (3a) is characterised by a mid-water maximum between 650 and 800 m. This maximum of spherical particles corresponds with increased numbers of large aggregates in this specific depth.

The diversity of particle abundance patterns is more distinct at depths $< 1000 \text{ m}$ (GeoB 7410, GeoB 7412, GeoB 7413). The profile depths of GeoB 7410 (Fig. 4c) and GeoB 7413 (Fig. 3b) are identical, but particle distributions differ significantly. The temporal difference of the deployment is only 6 h and the distance between the two stations is less than 30 kilometres. Profile GeoB 7410 is characterised by changing particle concentrations down to a

depth of 530 m. Below this depth, particle concentrations increase significantly and a large maximum at more than 100 m above the seafloor is well visible. In contrast, site GeoB 7413 shows a well pronounced particle minimum between 100 m and 250 m, with no great changes in the concentration below it.

Similarities in the distribution of particles were only found at profiles obtained at depths greater than 1000 m. GeoB 7408 (Fig. 4a) and GeoB 7411 (Fig. 4b) have comparable abundance progression curves. Due to a malfunction of ParCa, there are picture gaps in the intervals 630 m–1090 m, 1200 m–1270 m, 1700 m–1720 m, and 1760 m–1790 m at site GeoB 7408. Nevertheless, both stations are characterised by a particle maximum around 200 m, with rapidly decreasing concentrations from $\sim 200 \text{ n l}^{-1}$ down to less than 100 n l^{-1} within only several tenths of meters. Below 200 m the particle abundances decrease slightly down to just above the seafloor at both stations.

3.2 Chlorophyll pigment concentrations and comparison with particle abundances in the surface water

The chlorophyll pigment concentrations computed for the positions of the camera profiles (Tab. 3) are usually higher than 3 mg m^{-3} . Chlorophyll values range between 3.20 mg m^{-3} and 3.43 mg m^{-3} . The only exception is site GeoB 7415. At this site, a minimum concentration of 1.45 mg m^{-3} is measured. This is less than half of the concentration observed at the neighbouring sites. The decreasing particle abundances with increasing distance from the coast in the upper 30 m presented for the northern transect are well reflected in the chlorophyll concentrations. Pigment concentrations decrease from 3.31 mg m^{-3} at site GeoB 7412, down to 3.20 mg m^{-3} at site GeoB 7413 and 1.45 mg m^{-3} at site GeoB 7415. In comparison, chlorophyll concentrations remain constant in the southern transect and highest concentrations of 3.43 mg m^{-3} were measured for each of the sites GeoB 7408, GeoB 7410 and GeoB 7411. In contrast to the consistent chlorophyll concentrations, the particle abundances in the southern transect vary distinctively between 79.73 n l^{-1} at site GeoB 7411 and 168 n l^{-1} at station GeoB 7408.

3.3 Aggregate abundances

The abundance of large, coagulated aggregates (Fig. 3a-c and Fig. 4a-d) is much smaller in comparison to spherical particles. Maximum values of 2.39 n l^{-1} were found at stations GeoB 7410 at 80 m depth (Fig. 4c), or GeoB 7415 (Fig. 3a) at 40 m depth. The concentration of spherical particles often exceeds those of large aggregates by a factor of 400

(i.e., GeoB 7411, 180 m depth – Fig. 4b). In all evaluated profiles, the highest concentrations of large aggregates are found in the upper 200 m of the water column. In this upper water stratum, an anticorrelation between coagulated aggregates and spherical particles is found at site GeoB 7411. The same might be true for profile GeoB 7408 (Fig. 4a), but it is not as obvious as described for GeoB 7411 (Fig. 4b). Aggregate concentration decreases constantly from the ocean surface down to 200 m, while the opposite is observed for the concentration of spherical particles. Their numbers increase down to 200 m water depth. Below 200 m, aggregate abundances remain more or less constant with no significant changes. The only exception is profile GeoB 7410 (Fig. 4c). Aggregate abundance decreases in the mid-water column, between 200 m and 530 m, where particle concentration increases slightly. Within the distinct near-bottom particle maximum (530 m-620 m), the increasing particle abundances correspond with increasing aggregate concentration. The aggregate distribution of profile GeoB 7415 (Fig 3a) is notable. The highest aggregate concentrations are found in the upper 200 m. This coincides with the aggregate distribution observed in all camera profiles, but aggregates do not appear in all depths at this specific site. They are mainly concentrated within the mid-water particle maximum between 650 m and 800 m.

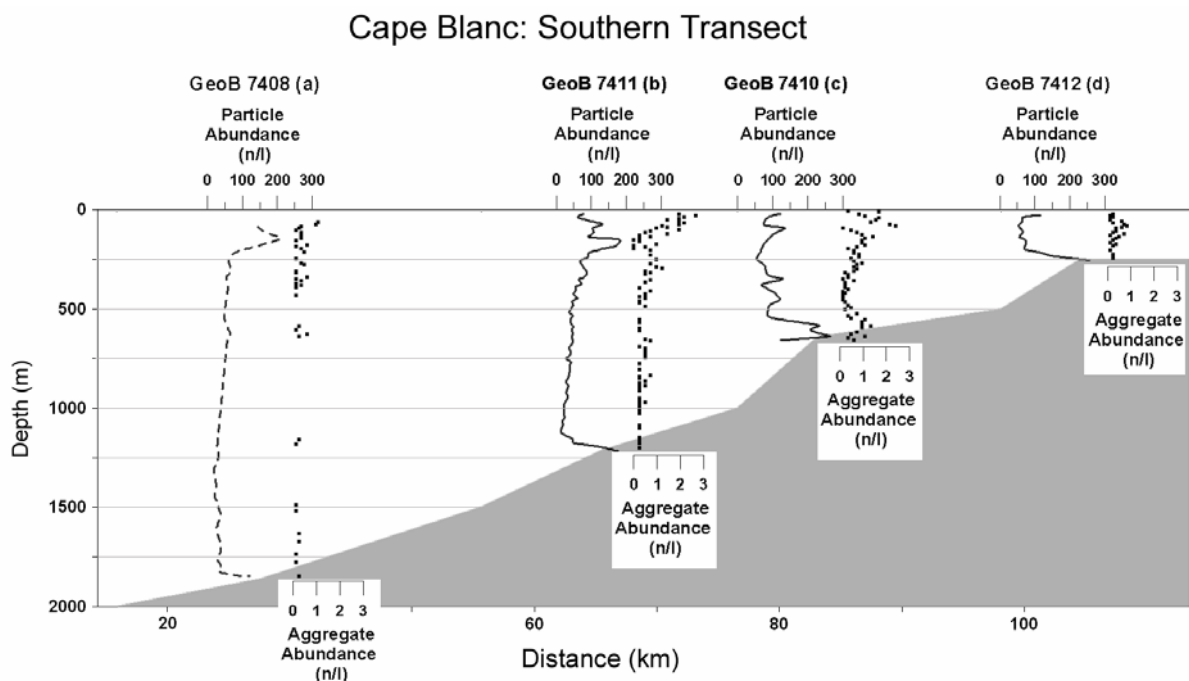


Fig.4 a-d: Vertical distribution of spherical particles and large aggregates along the southern transect. All lines are fitted with a 5-point running average. GeoB 7408 is presented in dashed lines, due to picture gaps in the profile (see Chapter 3.1 for details).

3.4 Size distribution

In this chapter, we describe the particle-size distribution of profiles GeoB 7411 and GeoB 7415. We think that the size distributions at these two stations reflect the major transport mechanisms and processes off Cape Blanc. Thus, the focus was centered on these profiles and they are described in detail in Chapter 4.

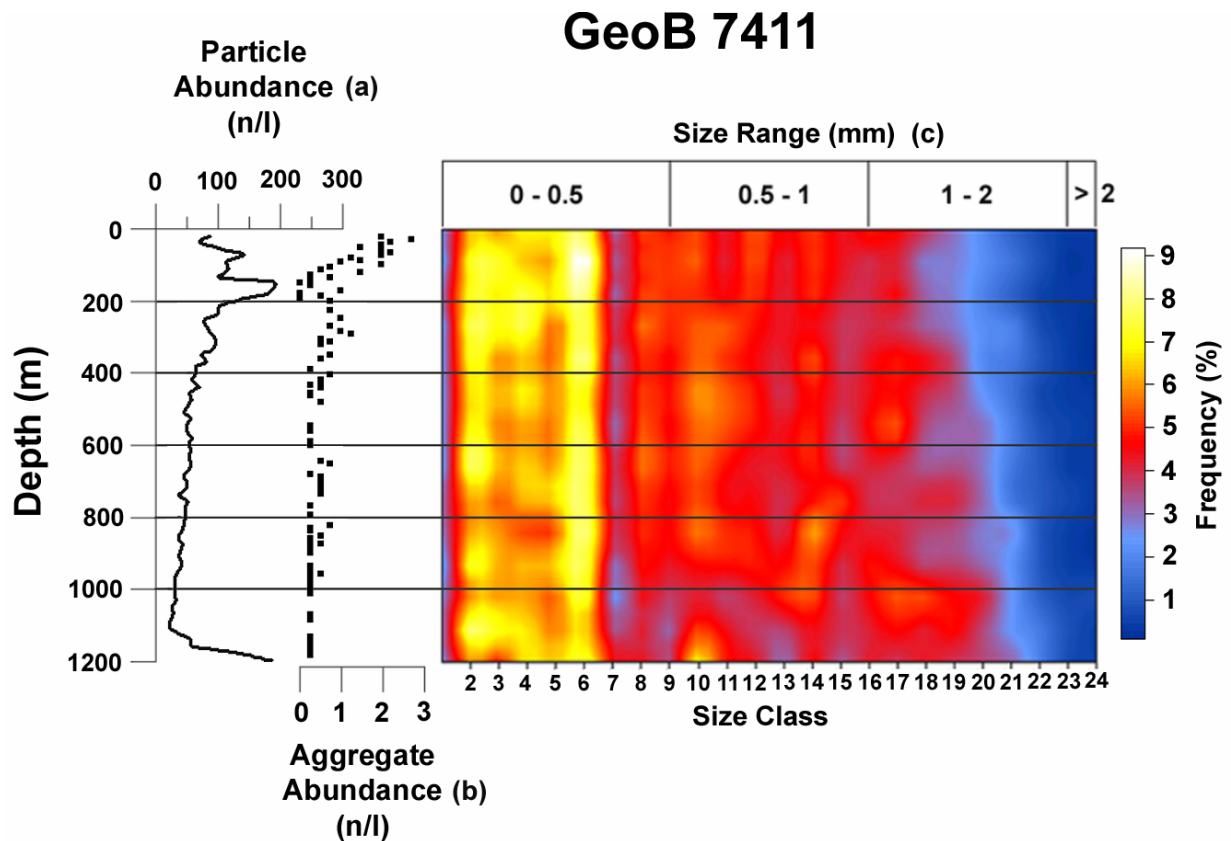


Fig.5 a-c: Particle and aggregate concentration in comparison with the vertical size distribution of spherical particles at site GeoB 7411. The abundance of particles >1 mm, increases with increasing water depth. Note the anticorrelation of small, spherical particles and large aggregates in the upper 200 m.

3.4.1 GeoB 7411

Smaller particles (size class 1-7) are distributed in high concentrations throughout the water column (Fig. 5c). However, the highest concentrations are found in the upper 200 m, corresponding with the high concentration of particles and aggregates in these depths (Fig. 5a-b). Below 200 m, their distribution becomes patchier and frequencies show only slight changes. Medium sized particles (0.5 mm-1 mm) appear to be distributed evenly in the GeoB 7411 profile. The only exception is observed above the ocean bottom between 1100 m and 1200 m. In this depth range, size classes 8, 9, 12 and 13 are depleted. In comparison, size

classes 10 and 11 are characterised by high frequencies around 8%. These changes might correspond with the increasing particle concentrations above the seafloor in this specific depth. Significant changes in the size distribution are only observed for the large particle sizes (>1 mm). While the concentration of spherical particles decreases with depth, their size increases constantly.

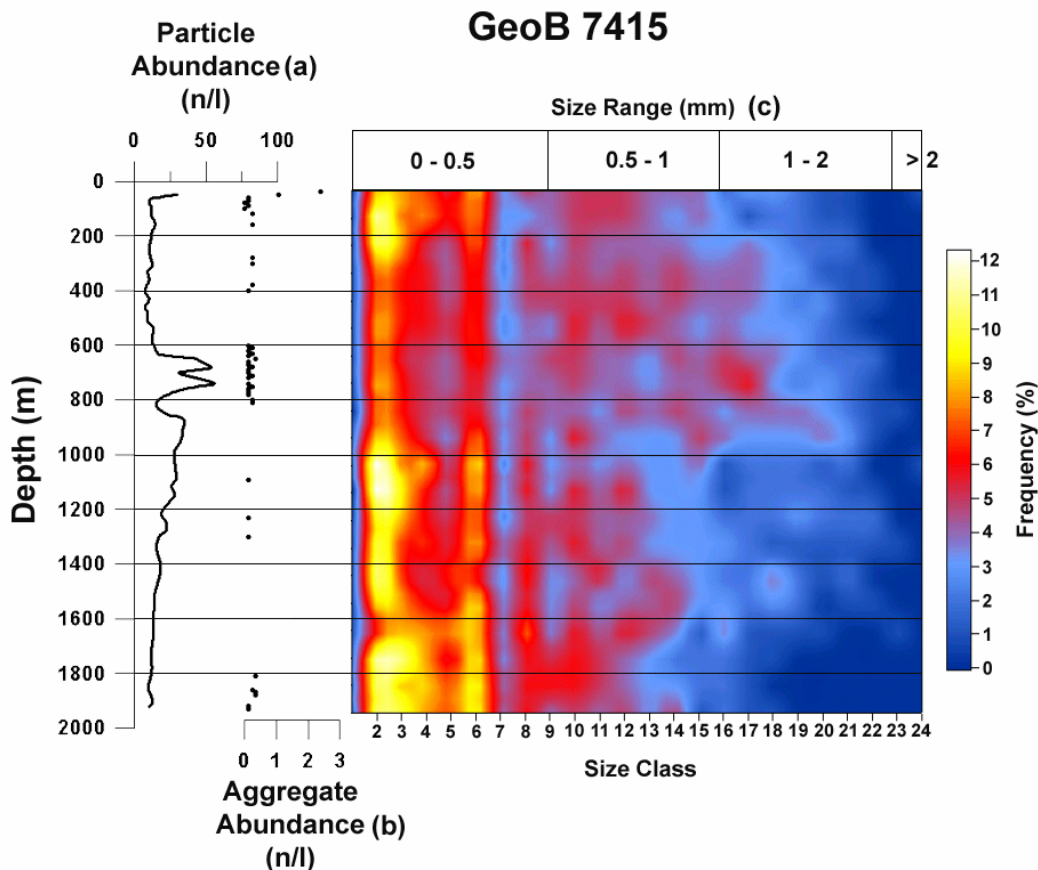


Fig.6 a-c: Particle and aggregate concentration in comparison with the vertical size distribution of spherical particles at site GeoB 7415. High concentration of large aggregates and increased particle sizes (>1mm), corresponds with the mid-water particle maximum between 650 and 800 m depth.

3.4.2 GeoB 7415

With respect to the size distribution, the optical profile of station GeoB 7415 can be divided into two parts (Fig. 6c). The water column down to the bottom of the particle mid-water maximum at 900 m is dominated by medium sized particles (0.5 mm-1.2 mm). In the remaining water column, higher concentrations of smaller particles are observed (size classes 1-6). Especially the fraction >825 μm (size class >14) is almost absent below 900 m. Apart from the upper 300 m of the water column, where particles of size classes 1-6 are dominant, a

depletion of the fraction between 140 μm and 391 μm (size classes 1-7) can be observed down to a depth of 900 m. Within the particle maximum between 650 m and 800 m, the frequency of the size fraction ranging from 905 μm to 1443 μm (size class 15-20) is increased and shows the highest values of large particles in this profile. Below the mid-water particle maximum, the fraction $\leq 0,5$ mm, smaller than the marine snow size range, is enriched and dominates the size fraction down to the seafloor.

Note that in the depth range between 650 m and 800 m the mid-water maximum of spherical particles (Fig. 6a) corresponds well with increased frequencies of the large fraction (>1 mm – Fig. 6c) and large, coagulated aggregates (Fig. 6b).

3.5 Particle and macro aggregate orientation

Figure 7a shows the orientation of the major axes of all particulate matter >3 mm in length at site GeoB 7415, both spherical particles and coagulated aggregates. No preferred orientation of particulate matter is observed and Major Axis Angles scatter in all directions. Figure 7b shows the same dataset with spherical particles and macro aggregates plotted independently. This results in a very different image. Major Axis Angles of large aggregates range between 80° and 110° . While spherical particles have no preferred orientation in the water column, large aggregates are more or less orientated perpendicular to the seafloor.

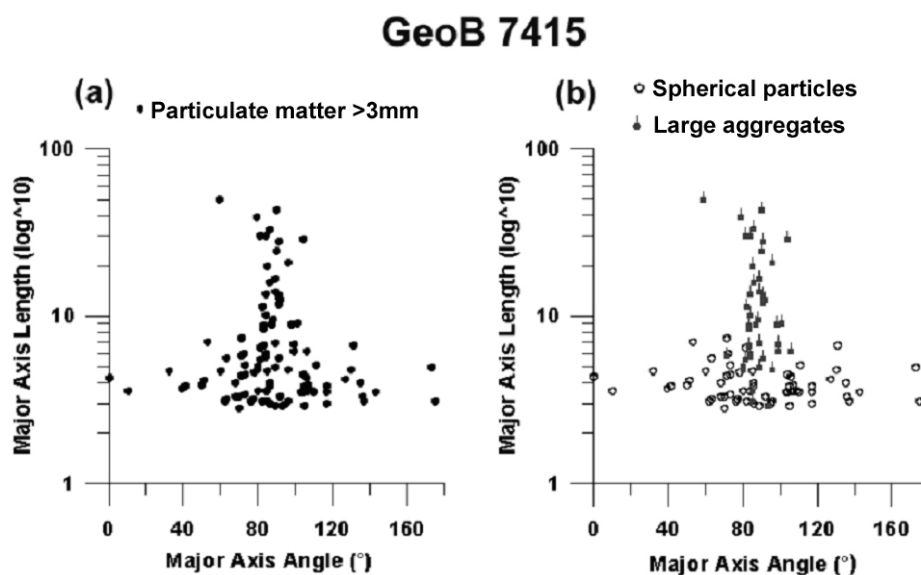


Fig.7a-b: Orientation of all particulate matter >3 mm in length in the water column at site GeoB 7415 (7a). Fig. 7b shows the same dataset with the difference that spherical particles and large, particle aggregates are plotted independently.

4. Discussion

4.1 Particle abundances and primary production at the ocean surface

The ocean surface, or the euphotic zone, can be described as the “production facility” for particulate matter. Particle concentrations are usually highest in the upper water column as a direct result of the primary production intensity. Thus, the production intensity must control the concentration of particulate matter in the ocean surface to a high degree, and it is apparent that a linkage between the two parameters must exist. A comparison of satellite-derived chlorophyll pigment concentrations with the particle abundance in the surface waters led to different results in the two transects. While in the northern transect decreasing chlorophyll concentration corresponds with decreasing particle abundance, this is not the case for the southern transect (Tab. 3). The more or less constant chlorophyll values in the southern transect cannot be correlated with the wide differences in the particle concentrations measured with the camera system. The difference between the transects is curious because the distances from one profile to the other is not more than 30 km and the time difference was always less than 12 h. There are two possible reasons for these differences: either the primary production conditions have changed significantly within hours, or the particle concentrations are not a reflection of the chlorophyll pigment concentrations because of the different measurement methods. To test in how far the latter is the case is not possible from our available datasets, but it has to be taken into account. A connection between chlorophyll and particle abundance was indicated at least for the northern transect. However, the rapidly changing primary production conditions might be another relevant and influencing factor. The presented chlorophyll concentrations were averaged for one month and are therefore not coincident in time with the camera profiles. Because the primary production conditions change dramatically on short temporal and spatial scales, a connection between chlorophyll concentrations and particle abundance cannot be established if the two parameters are not obtained simultaneously. Considering the more or less constant chlorophyll concentrations in the southern transect, the particle abundances in the ocean surface show a wide range of values. The spatial pattern of of particulate matter production is not consistent, but is of a “patchy” nature. There can be small areas of only a few tenths of square kilometres where productivity is higher compared to adjacent regions. This situation leads to high productivity gradients. The differences in particle abundance could be explained by the rapid spatial changes of primary production “patches” in the upwelling belt. Spatial heterogeneity of phytoplankton in the ocean was reported as early as 1957 by Bainbridge (1957). Martin and Richards (2001), modelled complex hot spots of only several tens of kilometres where increased phytoplankton

growth and primary production occurred. Enhanced productivity and small regions of strong upwelling of 5 km-10 km, can be strongly associated with eddies (Martin et al., 2001), which are common in the Cape Blanc area.

However, Gorsky et al.(1992) and Ratmeyer and Wefer (1996) described a connection between the vertical concentration of the integrated chlorophyll biomass in the upper water column, measured with CTD sensors, and the particle concentrations obtained with camera profiles. Thus, a connection between the two parameters apparently exists, but could not be verified in this study due to the temporal differences in the data acquisition.

4.3 Vertical distribution of particulate matter on the middle slope area (Profiles GeoB 7408 and GeoB 7411)

We believe that profiles GeoB 7408 (Fig. 4a) and GeoB 7411 (Fig. 4b, Fig. 5) represent typical, undisturbed particle distribution patterns for high productive areas. With respect to the vertical distribution of particulate matter, the water column can be divided into three parts where significant changes in the particle concentrations occur. First is the upper mixed layer (UML), which is regarded as the most active and dynamic part of the water column (Lampitt, 1996), with high numbers of particles down to a depth of approximately 200 m. At the boundary between the upper mixed layer and the mid-water column there is an abrupt change in the concentration of particles. Their abundance decreases significantly within only few meters at the lower boundary of the UML. The mid-water column is characterised by a constant and continuous decrease of particulate matter down to above the seafloor. In the benthic boundary layer (BBL), which is described as the water layer above the sediment (Thomsen, 2003), the number of particles increases slightly. In the following chapters, we will use the terms UML, mid-water column, and BBL to describe particle distributions within different parts of the water column.

As already mentioned, such a typical distribution pattern can be recognized at the deeper stations GeoB 7408 and GeoB 7411. It might also be inferred for site GeoB 7415 below 800 m depth (Fig. 3a), where a constant decrease down to the seafloor is well documented and the highest numbers of particles are measured in the upper 200 m of the water column. However, the particle maximum at sites GeoB 7408 (Fig. 4a) and GeoB 7411 (Fig. 4b, ~200 m) is located at the border between the upper mixed layer and the mid-water column and not at the ocean surface. The particle concentration increases down to the lower boundary of the UML while the concentration of large, coagulated aggregates decreases (Fig. 5a-b). A possible explanation for this anticorrelation might be the fragmentation of large

aggregates to small, spherically shaped particles while sinking through the upper mixed layer. It appears that particulate matter in the ocean surface layer is primarily bound into large, coagulated aggregates, resulting in reduced abundances of small, spherically shaped particles. Production and turbulent mixing is highest in the surface waters, leading to higher coagulation rates and therefore high numbers of large aggregates. As these fragile aggregates sink through the water, they break apart and the particles forming the aggregate are released back into the water (Alldredge et al., 1990).

The mechanisms responsible for the fragmentation of aggregates are manifold. Properties like the solubility of the organic components responsible for the agglutination of particles to aggregates by bacteria, can affect aggregate stability to a high degree (Smith et al., 1992; Vetter et al., 1998). Other biological processes, such as aggregate fragmentation by feeding activities, influence the distribution of particles and aggregates in the water column. Grazers are reported to remove a large portion of specific particle-size classes with high efficiency rates (Deibel, 1988; Harbison and McAllister, 1979). Apart from biological processes, physical mechanisms cause aggregates to break apart on their descent to the seafloor. Although the fluid shear stress along large particle aggregates has to be high to destroy large aggregates (Alldredge et al., 1990), this is a mechanism, which is not to be underestimated. The total mass of particulate matter within the UML may be fairly constant with depth between the ocean surface and the lower boundary of the UML, with the only difference being the form in which the material is available. While a large portion of the particulate matter near the ocean surface is predominantly available in the form of large aggregates, the fragmentation processes result in a continuous release of small, spherical particles down to the deeper parts of the UML with no overall significant change in total mass.

The distinct particle maximum at the base of the UML at sites GeoB 7408 and GeoB 7411 might be related to another physical mechanism. Particulate matter is reported to accumulate at depths where rapid changes in the density structure of the water column occur. MacIntyre et al. (1995) correlated aggregated particle maxima with density discontinuities in the coastal surface waters off California. Particle profiles published by Gorsky et al. (1992) obtained in the Mediterranean Sea, showed a similar accumulation of particles at density discontinuities in the UML. The reproduction of such accumulation patterns was successfully modelled by Condie (1999) and shows the importance of density discontinuities for the vertical distribution of particles in the surface waters. Due to the lack of CTD data, we are not

able to prove if this mechanism is related to the particle maximum observed at our profiles, but has to be considered as an important possible factor.

The mid-water column, below the UML and above the benthic boundary layer, is characterised by a steady decrease in the abundance of spherical particles with depth. A continuous loss of material with depth can be attributed to the remineralisation and dissolution of particulate matter on its way down to the seafloor (Fig. 4a, 250 m-1800 m; Fig. 4b, 250 m-1100 m). In contrast to the decreasing particle abundances, the size spectrum increases with depth, with particles getting coarser (Fig. 5c). These findings are difficult to explain on the basis of our images. Perhaps a small portion of the spherical particles coagulate to larger particles on their descent to the ocean bottom. To what extent this occurs cannot be resolved by our data. Increased coagulation rates are usually related to high particle concentration. However, the mid-water column is characterised by relatively low particle abundances. If coagulation takes place in the mid-water, it may be caused by differential settlement that is, the collision of particles might result from the vertical impact of a rapidly sinking particle with a slower-moving one. In the UML, increased aggregation does not only occur as a direct result of vertical, gravitational processes, but also by the horizontal movement of particles, for instance, by internal waves, wind driven shear (Lampitt, 1996), or Brownian motion (O'Melia and Bowman, 1984). In the mid-water column, these factors might play an ancillary role, so that coagulation processes in the horizontal direction are more unlikely. A vertical collision of particles by differential settlement in the mid-water column is more likely and could possibly be an explanation for increasing particle sizes with depth. Another explanation might be the release of small particles into the water column that were formerly incorporated into large aggregates. We described an anticorrelation in the abundance of large aggregates and small, spherical particles in the UML and explained these findings with the fragmentation of large aggregates to smaller particles. The same process might be operating to a certain degree in the mid-water column as well. Possibly, particles are released or detach continuously from large aggregates as a result of dissolution processes and/or fluid shear stress. Because large particles are likely to be more resistant to biogeochemical degradation, it might not be surprising that they are predominantly found in the deeper water strata when they detach from large aggregates.

In contrast to the decreasing particle concentrations in the mid-water column, the abundance of large aggregates does not significantly change with increasing depth. Aggregates occur in the entire mid-water column in more or less constant concentrations and for the GeoB 7408 and GeoB 7411 sites we conclude an undisturbed, continuous vertical

transport of material from the ocean surface to the seafloor. Large aggregates sink more rapidly and are more voluminous than small particles and thus, deliver the majority of organic matter originally produced in the surface waters. Correlations between aggregate size and sinking velocities were described by Alldredge and Gotschalk (1988) and Pilskaln et al. (1998). These findings might be supported by the particle orientation dataset (Chapter 3.5). Aggregates are predominantly orientated perpendicular to the ocean surface (Fig. 7b). Video sequences obtained with a video camera mounted on the ParCa frame and the observation of ParCa with a ROV system attached to the ship's wire showed that ParCa is orientated more or less horizontally, despite the drag on the wire and the ship's movement. Therefore, we assume that the orientation of particles as seen on the images is almost equal to their natural orientation in the water column. Due to the high sinking velocities and the resulting shear along the aggregate, the components forming an aggregate, align themselves in the direction of least resistance. As they sink relatively fast, their lateral advection by current activity might be much smaller compared to the spherically shaped particles. Possibly, this results in a more or less autochthonous deposition of the material in the sediment and hence high sediment accumulation rates on the middle slope.

The resuspension of particulate matter from the seafloor occurs mainly by the friction of water masses against the ocean floor and the uplift of particulate matter from the ocean bottom is the direct result of near-bottom current activity (Tengberg et al., 2003). Turbulence along the ocean bottom has been reported to transport resuspended material over long distances (Thomsen, 2003) and to keep a portion of the particles in a state of permanent suspension (McCave, 1986). Thus, the water in the benthic boundary layer is characterised by a higher particle load compared to the mid-water column (Biscaye and Eitrem, 1977). Increased particle concentrations above the seafloor are well documented in our profiles. For the southern profile (Fig. 4a-d), we described a continuous reduction of the numbers of particles with increasing water depth in the BBL. A similar observation was reported by McCave et al. (2001) where particulate material concentration decreased constantly with increasing water depth during summer on the slope and shelf edge of the Goban Spur margin (North Atlantic Ocean). At the deepest station, a benthic nepheloid layer was not as pronounced during winter times. The authors explained this by low current activity in deeper depths, and the same might be true for our particle profiles. Lower current speeds at greater water depths, observed by McCave et al. (2001) and Müller and Siedler (1992) for the North Atlantic, apparently resulted in a reduced uplift of material over the seafloor. Bottom currents measured on the upper slope of the NW European continental margin, for example, reached

velocities up to 37 cm s^{-1} in autumn and winter, while much lower velocities of 2 cm s^{-1} were found at the continental rise at 4500 m depth (Thomsen and van Weering, 1998). The observed particle maxima above the seafloor reflect a permanent uplift of particulate matter from the ocean bottom by low bottom current velocities as compared to the upper slope areas (see following chapter).

4.4 Vertical distribution of particulate matter at the shelf break and upper slope area

The shallower stations (<1000 m depth) are characterised by a large variety of distribution patterns, with no similarities in the progression curves. The typical, tripartite classification of the water column into upper mixed layer, mid-water column, and benthic boundary layer as described for the deeper stations, is difficult to apply here. The fact that no clear differentiation of the water column on the basis of particle distribution is possible could be related to an interplay of the actual water depth, bottom morphology, and current activities. The entire water column of shallow areas is strongly influenced by currents, wave energy in the surface water, and currents along the seafloor. These processes might lead to enhanced turbulent mixing throughout the water column, thus inhibiting a clear structure in the particle distribution (GeoB 7410 – Fig. 4c). Mittelstaedt (1983) and Sarnthein et al. (1981) described several currents along the shelf areas off NW Africa. The southward flow of the Canary current over the shelf, responsible for the upwelling, is underlain by a variety of northward-directed undercurrents and counter currents at the shelf break. The occurrence and intensity of the different current systems can vary depending on the season. However, the interaction of these currents might result in enhanced turbulences and mixing of the water column, and thus influence particle distribution insofar as no coherent distribution patterns occur in profiles obtained at shallower depths.

Particle concentration at site GeoB 7410 varies down to a depth of 530 m, but remains around a mean value of 100 n l^{-1} . There is no clear structure with respect to particle distribution except for the pronounced BBL (Fig. 4c). The influence of strong near-bottom currents and resulting resuspension is well reflected in the distinct thickness of the benthic boundary layer of more than 100 m. It is apparent that this is the result of intense coastal near-bottom current activity. The height of the benthic boundary layer even exceeds 250 m at site GeoB 7413. In comparison to the deeper sites, resuspension intensity might be amplified by the bottom morphology. A steep shelf break at sites GeoB 7410 and GeoB 7413 is likely to support resuspension processes. Strong bottom currents, in connection with steep shelf breaks,

might enhance the resuspension of already settled material in contrast to the deeper stations, where near-bottom current velocities are low and bottom morphology is flat.

McCave et al. (2001) were able to trace intermediate nepheloid layers, detaching from the benthic nepheloid layer on the upper slope, towards deeper slope stations at the Goban Spur. Similar observations were made by Frignani et al. (2002) in the northwest Mediterranean Sea. Such an offshore vectored, mid-water lateral transport is not apparent at either of our ParCa transects. This might be related to the differences in the resolution limits of our camera and the method used by McCave et al. (2001). The authors calculated the mass of material from their transmissiometer profiles and sediment trap data by using estimates of the density of aggregates published by Alldredge and Gotschalk (1988) and McCave (1984). Transmissiometers measure a much smaller particle-size spectrum compared to the particle camera, which obtains particulate matter of $>180\ \mu\text{m}$. The laterally advected material from the slope reported by McCave et al. (2001) might be of a different size range than the particle camera data published in this study. If particulate matter is shifted seaward over the slope in the Cape Blanc region, our camera was not able to detect this process. At least one conclusion can be drawn. There is no evidence of lateral advection of particles larger than $180\ \mu\text{m}$. This, in turn, might support our implication that the vast majority of particulate matter is predominantly deposited in place in the Cape Blanc region.

In addition to the ocean surface waters, the benthic boundary layer is a place of intense aggregation processes. Bottom turbulences due to current activity raises particulate matter from the seafloor (Auffret et al., 1994), and is often accompanied by tidal signatures (Huthnance et al., 2002; Thomsen, 2003). Aggregation rate in the benthic boundary layer is predominantly a function of turbulence, particle stickiness, particle size, particle concentration, and the differences between the sinking velocities of particulate matter (Thomsen and McCave, 2000). Re-aggregation processes in the benthic boundary layer can be derived from our profiles and are observed solely at the shallower stations GeoB 7410 (Fig. 4c) and GeoB 7413 (Fig. 3b). Those profiles in the benthic boundary layer are characterised by an increased abundance of large aggregates, which are coincident with high particle concentrations above the seafloor (GeoB 7410 – Fig. 4c). It is unlikely that the large aggregates observed in the benthic boundary layer originate directly from the surface waters. This is evidenced by the fact that their abundance above the benthic boundary layer is significantly lower than within the BBL. In fact, aggregates in the BBL are most likely to originate from two sources: First, aggregates arrive directly from the ocean surface and, second, aggregates are formed in this particular layer by resuspension and subsequent re-

aggregation. In addition, particle concentrations twice as high in the BBL as compared to the surface water at site GeoB 7410 enhance the probability of the coagulation of small particles to large aggregates.

4.5 A special case: Sinking event at site GeoB 7415

The particle, aggregate and size distributions of site GeoB 7415 (Fig. 6a-c) very likely indicate a rarely observed sinking event, where large amounts of material are transferred on a short temporal scale from the ocean surface to the seafloor.

Ideally, site GeoB 7415 is presumed to possess a particle abundance pattern similar to sites GeoB 7408 and GeoB 7411, with high particle concentrations in the UML. The material from the UML layer starts to sink at higher rates than the particulate matter in the mid-water column, triggered by a mechanism as yet unknown. The particles, falling from the UML, collide preferably with smaller particles from the mid-water column because they are more abundant. The depletion of smaller particle sizes (size classes 1-3, Fig. 6c) above the sinking particle cloud is clearly visible in the size spectrum plot of profile GeoB 7415. In turn, the collision of small particles in the mid-water column with material settling from the UML results in a coarsening of particles in the sinking particle cloud due to scavenging processes. Scavenging processes are important for the growth and removal of particulate matter in the water column (Alldredge and Gotschalk, 1989; Stolzenbach, 1993). This is likewise reflected in the size-distribution plot in the depth range of the particle maximum between 650 m and 800 m depth, where particles of a size >1mm are predominant. It might be suggested that the initial concentration of particulate matter in the middle water before the settling started and the observed concentration during the event are almost identical. The only difference is that the particles are getting larger in size. The aggregate abundance distribution supports our conclusion that the sinking cloud is moving rapidly downwards. The mid-water particle maximum corresponds to increased aggregate concentrations, which are believed to sink at higher rates, as opposed to small particles. In addition, the high concentration of large aggregates indicates intense scavenging and aggregation processes. At this point, the difficulties of the limited resolution of our images become apparent. In the size spectrum plot, we only took into account small, spherical particles. If these particles are increasing in size while sinking through the water column, the conclusion must be drawn that a large portion of these particles are present as aggregates as well. Due to the picture resolution we were not able to identify those spherically shaped particles as aggregates. The smaller size fractions (size classes 1-3, Fig. 6c) dominate the water column below the mid-water maximum. We

suggest that while the particle cloud continues to sink, particles of these size classes will be depleted in a similar way as in the water column above the mid-water maximum. The proposed theory is complicated by the high concentrations of small particles (size class 2 and 3) in the upper 220 m, because we postulated a preferred scavenging of particularly this small size fraction by the settling of the particle cloud. This phenomenon might be explained in the following way: Assuming a sinking velocity for particles between 1 and 2 mm of about 35 m d^{-1} , the cloud requires at least 20 days from the beginning of the event to reach a depth of 700 m. This is a reasonable value when taking into account published sinking speeds. Alldredge and Gotschalk (1988), Shanks and Trent (1980), Pilskaln et al. (1998) and Asper (1987) calculated sinking speeds for particles in this size category of 35 m d^{-1} , 53 m d^{-1} , 22 m d^{-1} and 36 m d^{-1} , respectively. The increased numbers of the small size fraction in the surface waters can be explained by the production of new material. The surface waters are recovering from the “sinking shock”, and while the particle cloud is still on its way down to the seafloor new material is supplied by phytoplankton growth in the upper mixed layer. However, a sinking velocity of 35 m d^{-1} is probably an underestimation. The association of large particles and large aggregates between 650 and 800 m water depth allows the assumption that large aggregates and large particles sink at the same rate. While large, coagulated aggregates are presumed to sink faster than small particles, combined with the assumption that the large, spherically shaped particles also have to be treated as aggregates, a much higher settling speed than 35 m d^{-1} is expected. Because the camera profiles represent a snapshot of the actual particle distribution frozen in time and space, a calculation of the sinking speeds is not possible.

Two triggering processes for such a sinking event can be considered. First, the input of large amounts of dense, wind transported dust from the continent into the investigation area and, second, the mass aggregation and subsequent deposition of phytodetritus after a phytoplankton bloom. The latter has been observed and measured with the aid of sediment traps by several investigators. Berger and Wefer (1990) describe an explosive growth of phytoplankton in the Bransfield strait that resulted in increased particle fluxes at short temporal scales. A similar mechanism was reported by Fischer et al. (1996b) for the Canary Islands region. Short-term sedimentation pulses were observed during late winter and early spring, lasting only a few hours to a few days, and Lampitt (1985) described the arrival of phytodetritus at a water depth of 2000 m one month after a bloom in the Porcupine Sea bight. This supports findings that there is a close temporal coupling between the ocean surface and the deep ocean (Asper et al., 1992a) in the region off Cape Blanc.

Outbreaks of sandstorms over the African continent are strongly coupled with the input of high-density lithogenic material into the Atlantic Ocean (Schütz et al., 1981; Swap et al., 1996). The interaction of marine particulate matter with episodically imported dust from the Sahara leads to so-called “particle loading” (Ramaswamy et al., 1991; Stolzenbach, 1993). Terrigenous grains collide with phytodetritus in the water column, resulting in the forming of high-density aggregates in the surface waters. This, in turn, leads to higher sinking rates and possibly a cleaning of the water column of large amounts of particulate matter. Ratmeyer et al. (1999) reported a rapid vertical flux for the Canary Island region in conjunction with scavenging of lateral advected material, which could be related to the seasonal input of atmospheric dust from the Sahara. However, the investigation area was influenced by an intense sandstorm outbreak during the deployment of the camera system and so no useful SeaWiFS images were obtained during the ParCa deployments. The input of wind-transported dust could be a reasonable mechanism to trigger the postulated sinking event.

5. Conclusions

Although no datasets simultaneous to the images were available, the obtained profiles delivered new insights about the particle distribution and transport processes in the Cape Blanc region. Comparisons of satellite-derived chlorophyll concentrations with the particle abundances measured with the camera system were not highly satisfactory. This is in part due to the temporal differences in the data acquisition of the methods. Nevertheless, an estimation of the particulate matter concentration in the surface water from satellite images might be possible in the future if, first, enough vertical particle distribution data from near the surface, are available and, second, datasets of cameras and satellites are obtained simultaneously.

Our profiles were able to support many findings published in the literature, such as re-aggregation processes in the BBL, the fragmentation of large aggregates, and near-bottom resuspension. On the other hand, processes such as particle accumulation at density discontinuities could not be detected due to the lack of CTD data. Thus, it is crucial to obtain as many datasets as possible, coincident in time and space, for satisfactory explanations of the processes that determine particle distribution patterns.

Particulate matter is often treated as a single unit, but we think that the differentiation of spherical particles and large aggregates is important. The two populations differ decisively in terms of size, sinking velocity, sinking behaviour, and composition, and thus in their roles relating to particle fluxes. Although a certain amount of particulate matter that was allocated to spherical particles turned out to include aggregates as well, the exercise in differentiation

revealed new insights with respect to the size distribution of particulate matter in the water column.

The processes and mechanisms observed in the Cape Blanc region are summarized in Fig. 8a-c.

1.) Sinking events (Fig. 8a)

Occasionally occurring sinking events (Fig. 7a), transfer large amounts of material from the ocean surface to the seafloor, possibly within several days to a few weeks. The sinking cloud preferably scavenges the more abundant small particle sizes, which is reflected in the depletion of small particles in the water column above. The scavenging of the small size fraction results in increasing particle sizes within the particle cloud during its descent through the water column. The occurrence of large, coagulated aggregates in the sinking cloud supports the conclusion that the material sinks quite rapidly through the water column, possibly at rates of more than 35 m d^{-1} . Suggested triggering processes are either the deposition of phytodetritus after a phytoplankton bloom, or the input of high-density lithogenic dust from the continent.

2.) Middle slope areas (Fig. 8b)

The middle slope areas are characterised by a continuous flux of particulate matter from the ocean surface to the seafloor. This conclusion is based on the observation of large, coagulated aggregates in high concentrations throughout the water column. The lateral advection of fast-sinking, large aggregates is presumed to be small compared to that of spherical particles, resulting in a more or less autochthonous deposition of particulate matter on the middle slope areas. The aggregation of particles to large aggregates mainly takes place in the upper ocean layer. Physical fragmentation and solubility processes acting on these aggregates on their way down to the base of the upper mixed layer result in the detachment of small, spherical particles from the large aggregates. Spherical particles accumulate at the base of the UML (around 200 m depth), which might be explained by strong density gradients in this specific part of the water column.

3.) Upper slope areas (Fig. 8c)

The unstructured upper and mid-water column on the upper slope areas is related to the interactions of current flow, water depth, and slope morphology. Intense resuspension and re-aggregation processes are observed in the pronounced benthic boundary layer. Some

aggregates observed in the BBL originates directly from the ocean surface, and a second source are aggregates formed within this particular water layer. A lateral advection of particles >180 μm from the slope towards the open ocean could not be detected. Either there are no advection processes, or it acts only on the small size fractions beyond the camera's resolution limits.

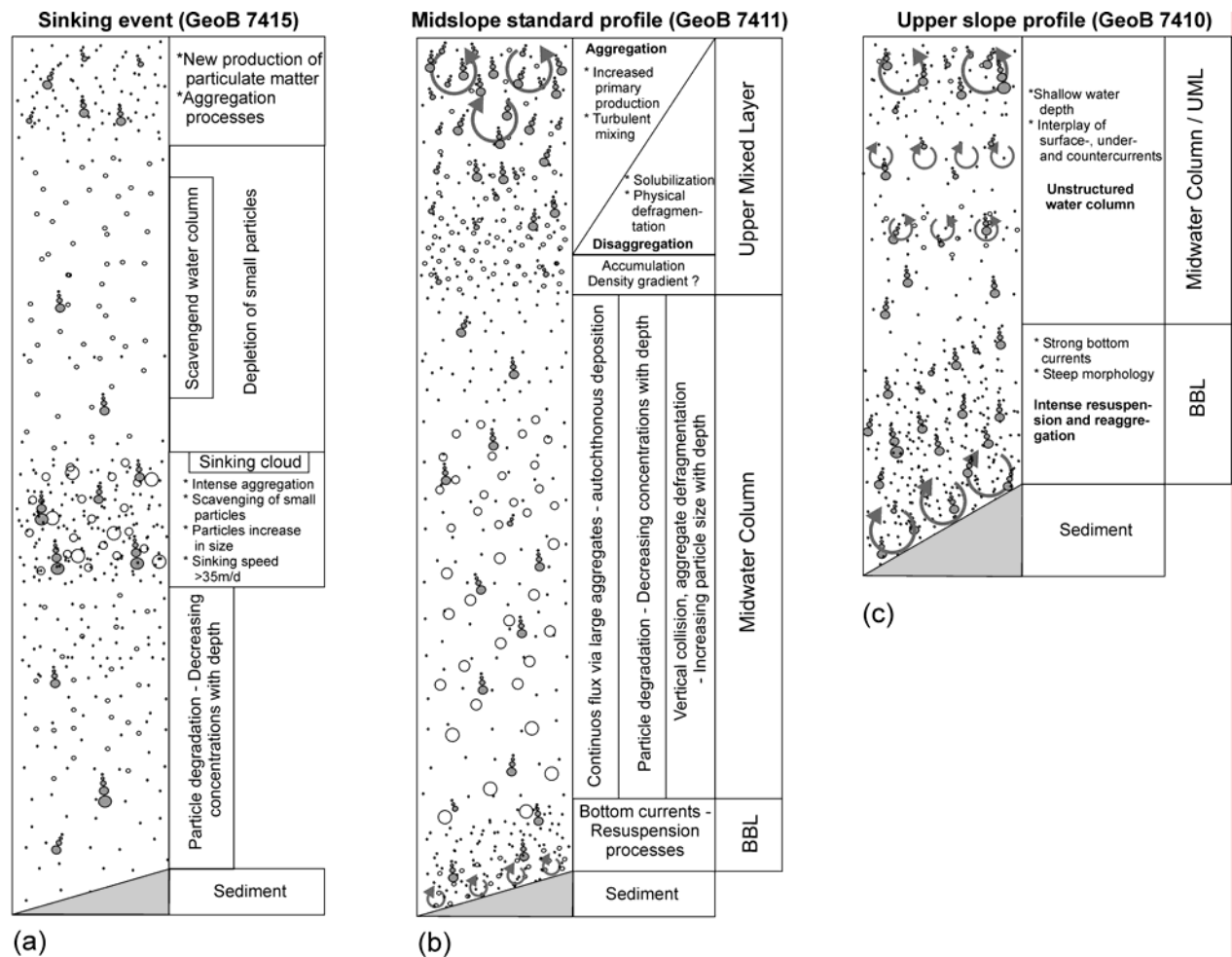


Fig.8a-c: Schematic model of mechanisms that determine particle distribution and transport processes in the Cape Blanc region. In Fig. 8a, the mechanisms of a rarely observed sinking event are presented, where large amounts of material are transferred from the ocean surface to the seafloor on short temporal scales. Fig. 8b shows the standard situation on the midslope areas. A continuous, vertical flux is provided by large particle aggregates observed throughout the water column in high concentrations. The lateral advection of these fast sinking aggregates is small, thus an in-situ deposition of particulate matter is apparent. The upper slope profiles (Fig. 8c) are characterised by an unstructured upper and mid-water column, with no clear trends in the particle distribution. This is related to the interplay of water depth, current activity, and slope morphology. The distinct benthic boundary layer is a site of intense resuspension and re-aggregation processes.

Acknowledgements

We thank the crew of the RV POSEIDON for their help in deploying and recovering the ParCa system. The manuscript greatly benefited from discussions with G. Fischer, U. Passow and T. Freudenthal. Satellite-derived pigment concentrations were provided by the SeaWiFS project, NASA/Goddard Space Flight Centre. We thank P. Helmke for creating the pigment concentration map and the extraction of the chlorophyll concentrations. Many helpful comments from the reviewers helped to improve this manuscript.

The presented datasets are available in the PANGAEA database (<http://www.pangaea.de/>)

This study was funded by the “Deutsche Forschungsgesellschaft” (DFG) within the scope of the DFG Research Center Ocean Margins

References

- Allredge, A.L., 1979, The chemical composition of macroscopic aggregates in two neritic seas: *Limnology and Oceanography*, v. 24, p. 855-866.
- Allredge, A. L. and C. Gotschalk, 1988) In situ settling behaviour of marine snow: *Limnology and Oceanography* **33**(3): 339-351.
- Allredge, A.L., and Gotschalk, C., 1989, Direct observation of the mass flocculation of diatom blooms: characteristics, settling velocities and formation of diatom aggregates: *Deep Sea Research I*, v. 36, p. 159-171.
- Allredge, A.L., 1998, The carbon, nitrogen and mass content of marine snow as a function of size: *Deep Sea Research I*, v. 45, p. 529-541.
- Allredge, A.L., Gotschalk, C., Passow, U., and Riebesell, U., 1995, Mass aggregation of diatom blooms: Insights from a mesocosm study: *Deep Sea Research II*, v. 42, p. 9-28.
- Allredge, A.L., Granata, T.C., Gotschalk, C., and Dickey, T.D., 1990, The physical strength of marine snow and its implications for physical disaggregation in the ocean: *Limnology and Oceanography*, v. 35, p. 1415-1428.
- Allredge, A.L., and McGillivray, P., 1991, The attachment probabilities of marine snow and their implications for particle coagulation in the ocean: *Deep Sea Research*, v. 38, p. 431-443.
- Asper, V.L., 1987, Measuring the flux and sinking speed of marine snow aggregates: *Deep Sea Research I*, v. 34, p. 1-17.
- Asper, V.L., Deuser, W.G., Knauer, G.A., and Lohrenz, S.E., 1992a, Rapid coupling of sinking particle fluxes between surface and deep ocean waters: *Letters to Nature*, v. 357, p. 670-672.
- Asper, V.L., Honjo, S., and Orsi, T.H., 1992b, Distribution and transport of marine snow aggregates in the Panama Basin: *Deep Sea Research I*, v. 39, p. 939-952.
- Auffret, G., Khripounoff, A., and Vangriesheim, 1994, Rapid post-bloom resuspension in the northeastern Atlantic: *Deep Sea Research I*, v. 41, p. 925-939.
- Bainbridge, R., 1957, The size, shape and density of marine phytoplankton concentration: *Biological Review*, v. 32, p. 91-115.
- Berger, W., and Wefer, G., 1990, Export production: seasonality and intermittancy and paleoceanographic implications: *Palaeogeography, Palaeoclimatology, Palaeoecology*, v. 89, p. 245-254.
- Biscaye, P.E., and Eitrem, S.L., 1977, Suspended particulate loads and transport in the nepheloid layer of the abyssal Atlantic Ocean: *Marine Geology*, v. 23, p. 155-172.
- Burdick, H.E., 1997, *Digital Imaging Theory and Applications*: New York, San Francisco, Washington, D.C., Auckland, Bogota, McGraw Hill, 313 p.
- Condie, S.A., 1999, Settling regimes for non-motile particles in stratified waters: *Deep Sea Research I*, v. 46, p. 681-699.
- Conte, M.H., Ralph, N., and Ross, E.H., 2001, Seasonal and interannual variability in the deep ocean particle fluxes at the Oceanic Flux Program (OFP)/Bermuda Atlantic Time Series (BATS) site in the western Sargasso Sea near Bermuda: *Deep Sea Research II*.
- Deibel, D., 1988, Filter feeding by *Oikopleura vanhoeffeni* grazing impact on suspended particles in cold water ocean waters: *Marine Biology*, v. 99, p. 177-186.
- deMenocal, P., Ortiz, J., Guilderson, T., Adkins, J., Sarnthein, M., Baker, L., and Yarusinski, M., 2000, Abrupt onset and termination of the African Humid Period: rapid climate responses to gradual insolation forcing: *Quat. Sci. Rev.*, v. 19, p. 347-361.
- Diercks, A.R., and Asper, V.L., 1997, In situ settling speeds of marine snow aggregates below the mixed layer: Black Sea and Gulf of Mexico: *Deep Sea Research I*, v. 44, p. 385-398.
- Fischer, G., Donner, B., Ratmeyer, V., Davenport, r., and Wefer, G., 1996a, Distinct year-to-year particle flux variations off Cape Blanc during 1988-1991: Relation to $\delta^{18}O$

- deduced sea-surface temperatures and trade winds: *Journal of marine research*, v. 54, p. 73-98.
- Fischer, G., Neuer, S., and Wefer, G., 1996b, Short-term sedimentation pulses recorded with a fluorescence sensor and sediment traps at 900-m depth in the Canary basin: *Limnology and Oceanography*, v. 41, p. 1354-1359.
- Fowler, S.W., and Knauer, G.A., 1986, Role of large particles in the transport of elements and organic compounds through the oceanic water column: *Progress in Oceanography*, v. 16, p. 147-194.
- Frignani, M., Courp, T., Cochran, J.K., Hirschberg, D., and Vitoria i Codina, L., 2002, Scavenging rates and particle characteristics in and near the Lacaze-Duthiers submarine canyon, northwest Mediterranean: *Continental Shelf Research*, v. 22, p. 2175-2190.
- Gardner, W.D., and Walsh, I.D., 1990, Distribution of macroaggregates and fine-grained particles across a continental margin and their potential role in fluxes: *Deep Sea Research I*, v. 37, p. 401-411.
- Gentien, P., M. Lunven, et al. (1995). "In-situ depth profiling of particle sizes." *Deep Sea Research I* **42**(8): 1297-1312.
- Gorsky, G., Aldorf, C., Kage, M., Picheral, M., Garcia, Y., and Favole, J., 1992, Vertical distribution of suspended aggregates determined by a new underwater video profiler: *Annales de l'Institut océanographique*, v. 68, p. 275-280.
- Harbison, G.R., and McAllister, V.L., 1979, The filter-feeding rates and particle retention efficiencies of three species of *Cyclosalpa* (Tunicata, Thaliacea): *Limnology and Oceanography*, v. 24, p. 875-892.
- Hernandez-Guerra, A., and Nykjaer, L., 1997, Sea surface temperature variability off north-west Africa: 1981-1989: *International Journal of Remote Sensing*, v. 18, p. 2539-2558.
- Honjo, S., Doherty, K.W., Agrawal, Y.C., and Asper, V.L., 1984, Direct optical assessment of large amorphous aggregates (marine snow) in the deep ocean: *Deep Sea Research i*, v. 31, p. 67-76.
- Huthnance, J.M., Humphery, J.D., Knight, P.J., Chatwin, G., Thomsen, L., and White, M., 2002, Near-bed turbulence measurements, stress estimates and sediment mobility at the continental shelf edge: *Progress in Oceanography*, v. 52, p. 171-194.
- Jackson, G.A., 1990, A model of the formation of marine algal flocs by physical coagulation processes: *Deep Sea Research*, v. 37, p. 1197-1211.
- Jackson, G.A., 2001, Effect of coagulation on a model planktonic food web: *Deep Sea Research I*, v. 48, p. 95-123.
- Lampitt, R.S., 1985, Evidence for the seasonal deposition of detritus to the deep-sea floor and its subsequent resuspension: *Deep Sea Research I*, v. 32, p. 885-897.
- Lampitt, R.S., 1996, Snow Falls in the Open Ocean, in Summerhayes, C.P., and Thorpe, S.A., eds., *Oceanography - An Illustrated Guide*: London, Manson Publishing, p. 96-112.
- MacIntyre, S., Alldredge, A.L., and Gotschalk, C., 1995, Accumulation of marine snow at density discontinuities in the water column: *Limnology and Oceanography*, v. 40, p. 449-468.
- Martin, A.P., and Richards, K.J., 2001, Mechanisms for vertical nutrient transport within a North Atlantic mesoscale eddy: *Deep Sea Research II*, v. 48, p. 757-773.
- Martin, A.P., Richards, K.J., and Fasham, M.J.R., 2001, Phytoplankton production and community structure in an unstable frontal region: *Journal of Marine Systems*, v. 28, p. 65-89.
- McCave, I.N., 1975, Vertical flux of particles in the ocean: *Deep Sea Research I*, v. 22, p. 491-502.
- McCave, I.N., 1984, Size spectra and aggregation of suspended particles in the deep ocean: *Deep Sea Research*, v. 31, p. 329-352.

- McCave, I.N., 1986, Local and global aspects of the bottom nepheloid layers in the world ocean: *Netherland Journal of Sea Research*, v. 20, p. 167-181.
- McCave, I.N., Hall, I.R., Antia, A.N., Chou, L., Dehairs, F., Lampitt, R.S., Thomsen, L., van Weering, T.C.E., and Wollast, R., 2001, Distribution, composition and flux of particulate material over the European margin at 47°-50°N: *Deep Sea Research II*, v. 48, p. 3107-3139.
- Mittelstaedt, E., 1983, The Upwelling Area Off Northwest Africa - A Description of Phenomena Related to Coastal Upwelling: *Progress in Oceanography*, v. 12, p. 307-331.
- Müller, T.J., and Siedler, G., 1992, Multi-year current time series in the eastern North Atlantic Ocean: *Journal of Marine Research*, v. 50, p. 63-98.
- Neuer, S., Ratmeyer, V., Davenport, R., Fischer, G., and Wefer, G., 1997, Deep water particle flux in the Canary Island region: seasonal trends in relation to long-term satellite derived pigment data and lateral sources: *Deep-Sea Research I*, v. 44, p. 1451-1466.
- Nykjaer, L., and Van Camp, L., 1994, Seasonal and interannual variability of coastal upwelling along northwest Africa and Portugal from 1981 to 1991: *Journal of Geophysical Research*, v. 99, p. 197-207.
- O'Melia, C.R., 1972, An approach to modeling of lakes: *Schweizerische Zeitschrift für Hydrologie*, v. 34, p. 1-33.
- O'Melia, C.R., and Bowman, K.S., 1984, Origins and effects of coagulation in lakes: *Schweizerische Zeitschrift für Hydrologie*, v. 46, p. 64-85.
- Parker, J.R., 1997, *Algorithms for Image Processing and Computer Vision*: New York, Cichester, Brisbane, Toronto, Singapore, Weinheim, Wiley Computer Publishing, 417 p.
- Passow, U., and Alldredge, A.L., 1995, Aggregation of a diatom bloom in a mesocosm: The role of transparent exopolymer particles (TEP): *Deep Sea Research II*, v. 42, p. 99-109.
- Pilskaln, C.H., Lehmann, C., Paduan, J.B., and Silver, M.W., 1998, Spatial and temporal dynamics in marine aggregate abundance, sinking rate and flux: Monterey Bay, central California: *Deep Sea Research II*, v. 45, p. 1803-1837.
- Ramaswamy, V., Nair, R.R., Manganini, S., Haake, B., and Ittekott, V., 1991, Lithogenic fluxes to the deep Arabian Sea measured by sediment traps: *Deep Sea Research I*, v. 38, p. 169-184.
- Ratmeyer, V., Fischer, G., and Wefer, G., 1999, Lithogenic particle fluxes and grain size distributions in the deep ocean off northwest Africa: Implications for seasonal changes of aeolian dust input and downward transport: *Deep Sea Research I*, v. 46, p. 1289-1337.
- Ratmeyer, V., and Wefer, G., 1996, A high resolution camera system (ParCa) for imaging particles in the ocean: System design and results from profiles and a three-month deployment: *Journal of Marine Research*, v. 54, p. 589-603.
- Romero, O.E., Lange, C.B., and Wefer, G., 2002, Interannual variability (1988-1991) of siliceous phytoplankton fluxes off northwest Africa: *Journal of Plankton Research*, v. 24, p. 1035-1046.
- Sarnthein, M., Tetzlaff, G., Koopmann, B., Wolter, K., and Pflaumann, U., 1981, Glacial and interglacial wind regimes over the eastern subtropical Atlantic and North-West Africa: *Nature*, v. 293, p. 193-196.
- Schütz, L., Jaenicke, R., and Pietrek, H., 1981, Saharan dust transport over the North Atlantic Ocean: *Geological Society of America Spec. Pap.*, v. 186, p. 87-100.
- Shanks, A.L., and Trent, J.D., 1980, Marine snow: sinking rates and potential role in vertical flux: *Deep Sea Research I*, v. 27A, p. 137-143.

- Silver, M.W., Coale, S.L., Pilskaln, C.H., and Chavez, F.P., 1998, Exploratory observations of marine aggregates at sub-euphotic depths: *Deep Sea Research II*, v. 45, p. 1839-1861.
- Smith, D.C., Simon, M., Alldredge, A.L., and Azam, F., 1992, Intense hydrolytic enzyme activity on marine aggregates and implications for rapid particle dissolution: *Nature*, v. 359, p. 139-142.
- Stolzenbach, K.D., 1993, Scavenging of small particles by fast-sinking porous aggregates: *Deep Sea Research I*, v. 40, p. 359-369.
- Swap, R., Ulanski, S., Cobbett, M., and Garstang, M., 1996, Temporal and spatial characteristics of Saharan dust outbreaks: *Journal of Geophysical Research*, v. 101, p. 4205-4220.
- Syvitsky, J. P. M., K. W. Asprey, et al. (1995). "In-situ characteristics of particles settling within a deep-water estuary." *Deep Sea Research II* **42**(1): 223-256.
- Tengberg, A., Almroth, E., and Hall, P., 2003, Resuspension and its effects on organic carbon recycling and nutrient exchange in coastal sediments: in situ measurements using new experimental technology: *Journal of Experimental Marine Biology and Ecology*, v. 285-286, p. 119-142.
- Thomsen, J., 2003, The benthic boundary layer, in Wefer, G., Billet, D., Hebbeln, D., Jorgensen, B.B., Schlüter, S., and van Weering, T.C.E., eds., *Ocean Margin System: Berlin Heidelberg New York, Springer Verlag*, p. 143-155.
- Thomsen, L., and McCave, I.N., 2000, Aggregation processes in the benthic boundary layer at the Celtic Sea continental margin: *Deep Sea Research I*, v. 47, p. 1389-1404.
- Thomsen, L., and van Weering, T.C.E., 1998, Spatial and temporal variability of particulate matter in the benthic boundary layer at the N.W. European Continental Margin (Goban Spur): *Progress in Oceanography*, v. 42, p. 61-76.
- Van Camp, L., Nykjær, L., Mittelstaedt, E., and Schlittenhardt, P., 1991, Upwelling and boundary circulation off Northwest Africa as depicted by infrared and visible satellite observations: *Prog. Oceanogr.*, v. 26, p. 357-402.
- Vetter, Y.A., Deming, J.W., Jumars, P.A., and Krieger-Brockett, B.B., 1998, A Predictive Model of Bacterial Foraging by Means of Freely Released Extracellular Enzymes: *Microbial Ecology*, v. 36, p. 75-92.
- Walsh, I.D., and Gardner, W.D., 1992, A comparison of aggregate profiles with sediment trap fluxes: *Deep Sea Research I*, v. 39, p. 1817-1834.

3.2 The abundance and size of marine particles off the NW-African coast (Dakhla, Cape Bojador) and the detection of a massive lateral intrusion

submitted to *Limnology & Oceanography*

Nicolas Nowald, Volker Ratmeyer and Gerold Wefer

University of Bremen, Department of Geosciences, Klagenfurterstrasse, 28359 Bremen

Abstract

With aid of a profiling deep-sea camera system, particle profiles were obtained west off Dakhla and Cape Bojador (NW-Africa) on stations along two transects. The studies were carried out to investigate on particle distribution patterns and transportation pathways of particulate matter.

Particle abundances measured in the ocean surface are strongly coupled to the prevailing primary production conditions. The gradient in the primary production off Dakhla obtained by satellite derived pigment concentrations, is well reflected in decreasing particle abundances with increasing distance from the coast. In contrast, lowest particle concentrations were observed in the low productive areas off Cape Bojador further north.

Both regions are characterised by similar, comparably low particle fluxes. This is reflected in the reduced abundances of large, fast sinking, coagulated aggregates and low particle concentrations in general. However, a significant difference is seen in the sedimentation patterns. The water column off Dakhla shows an erratical and inhomogeneous size distribution compared to the profiles obtained off Cape Bojador. Thus, there are variations in the amount of material simultaneously reaching the seafloor on short temporal scales, resulting in “patchy” sedimentation. In contrast, the region off Cape Bojador shows a homogeneous size distribution in the water column, leading to more even particle sedimentation. The differences are related to the enhanced particle dynamics of aggregation and fragmentation of particulate matter in higher productive, compared to lower productive areas.

The Cape Bojador region is influenced by laterally advected material from the upper slope or shelf areas. Apart from smaller intrusions, a huge laterally advected cloud could be observed in one profile. The intrusion is 700 m in height and characterised by increased particle concentrations in the midwater column. The upper and lower boundaries of the lateral advected cloud could be clearly identified by means of the size distribution. Small particles are accumulated at the upper boundary of the advected cloud, which is related to the sheer processes occurring at the transition zone of two water masses. The small size fraction underlies a longer retention time along the transition zone and the accumulation processes are presumably enhanced by density gradients. In turn, the described sheer process and density gradients prohibit a further supply of the same size fraction below the lower boundary of the advected cloud. Comparable advection processes were not observed in the Dakhla region.

1. Introduction

In comparison to particle flux studies carried out with sediment traps in the worldwide oceans, studies on the in-situ distribution of particulate matter in the water column are considerably rare. In-situ observations on the vertical distribution of macroscopically resolvable particles are in the first instance provided by profiling camera systems. Since the introduction of this method by Honjo et al. (1984), similar systems were developed and deployed in different oceanic regions like the Panama Basin (Asper et al., 1992), on the Louisiana Shelf (Gardner and Walsh, 1990), the Monterey Bay (MacIntyre et al., 1995) or the Mediterranean Sea (Gorsky et al., 1992). Although camera profiles acquire only a snapshot of the actual particle distribution, their advantage lie in their non-destructive nature. Optical methods allow the direct observation and measurement of specific particle characteristics like abundance, size and shape. Particulate matter is not evenly distributed in the water column but is influenced by many processes. Concentrations are usually highest in the ocean surface and strongly coupled to the seasonal and regional conditions of the investigated area (Lampitt, 1996). Other factors like density gradients (Alldredge and Crocker, 1995; MacIntyre et al., 1995), bottom near currents (McCave et al., 2001; Thomsen and van Weering, 1998) or aggregation processes (Alldredge and Gotschalk, 1989; Alldredge and McGillivray, 1991; Jackson, 1990, 2001) influence particle distributions in the water column to a high degree. In particular the aggregation of single particles, to large coagulated aggregates is thought to play a key role in the vertical flux of material from the ocean surface to the deep-sea. Large aggregates, known as “Marine Snow” (Fowler and Knauer, 1986; McCave, 1975), sink considerably faster and are the major transport vehicle for the transfer of elements and nutrients from the euphotic zone to the deep-sea (Asper, 1987; Lampitt, 1996; Shanks and Trent, 1980). The idea of a predominantly vertical flux of material through the water column, which was established past the last decades, has to be modified. Abrantes et al. (2002), Freudenthal et al. (2001), Tanaka (2003) or Gardner and Walsh (1990) showed evidences for the lateral advection of material from the shelf areas into deeper parts of the water column, being an important factor for the flux of particulate matter to the open ocean.

In this study, we present seven high resolution camera profiles, obtained with the deep-sea camera system ParCa (Ratmeyer and Wefer, 1996). Investigation sites are two camera transects on the upper and mid slope areas off Dakhla and Cape Bojador, NW-Africa. We examined differences between the two regions in terms of the distribution of particulate matter in the water column. Of particular interest were the sedimentation patterns and flux of marine particles in both regions. In addition, this study describes in detail the occurrence of a

rarely observed, lateral intrusion. The observed intrusion was acquired on the mid slope areas off Cape Bojador. The probability to detect such an event is considerably low, thus it could improve our knowledge on how lateral intrusions can be characterised and described using vertical camera profile datasets.

2. Methods

2.1 Investigation area

Camera profiles were taken along two transects on the mid and upper slope areas off the NW-African coast (Fig. 1). The camera profiles were obtained during the RV Poseidon 272 cruise in April 2001. The first transect is a cross slope section comprising three camera profiles located ~90 km west of the city of Dakhla. The transect leads from the high productivity areas close to the coast, to the lower productivity regions further offshore. Water depths range between 600 m and 1600 m.

The second transect consists of an array of four camera profiles, obtained parallel to the NW-African coast off Cape Bojador. All profiles are located on the low productivity mid slope areas, offshore from the narrower upwelling belt. Profiling depths are between 900 m and 1800 m. A station list of the evaluated camera profiles is presented in Table 1.

2.2 Camera system and data extraction

The profiling deep-sea camera system ParCa (Ratmeyer and Wefer, 1996) was developed after similar optical devices used by Asper (1987) or Honjo et al. (1984). A detailed camera description and data extraction procedures are presented elsewhere (Nowald et al. submitted). ParCa consists of a modified PHOTOSEA 70 middle format camera and can be deployed to a water depth of 6000 m. The system is lowered at a winch speed of 0.3 m s^{-1} and acquires images from the entire water column in depth intervals of 10 m. The camera is triggered by the pressure sensor of a CTD probe, providing accurate trigger depths. Sample volume of each image is 4.18 litre and the smallest measurable particle size is $180 \text{ }\mu\text{m}$.

Two subsamples of the 6x6 cm sized negatives were digitised and data extraction was provided by the digital image analysis software *OPTIMAS*. We clearly distinguished between spherically shaped particles and prolate, coagulated particle aggregates, described as “Stringers” (Shanks, 2002; Syvitsky et al., 1995). The dataset of the abundance of coagulated particle aggregates was created by manually counting the numbers of aggregates appearing on each image. Manual counting was used because the image analysis software is not able to distinguish between spherically shaped particles and coagulated aggregates.

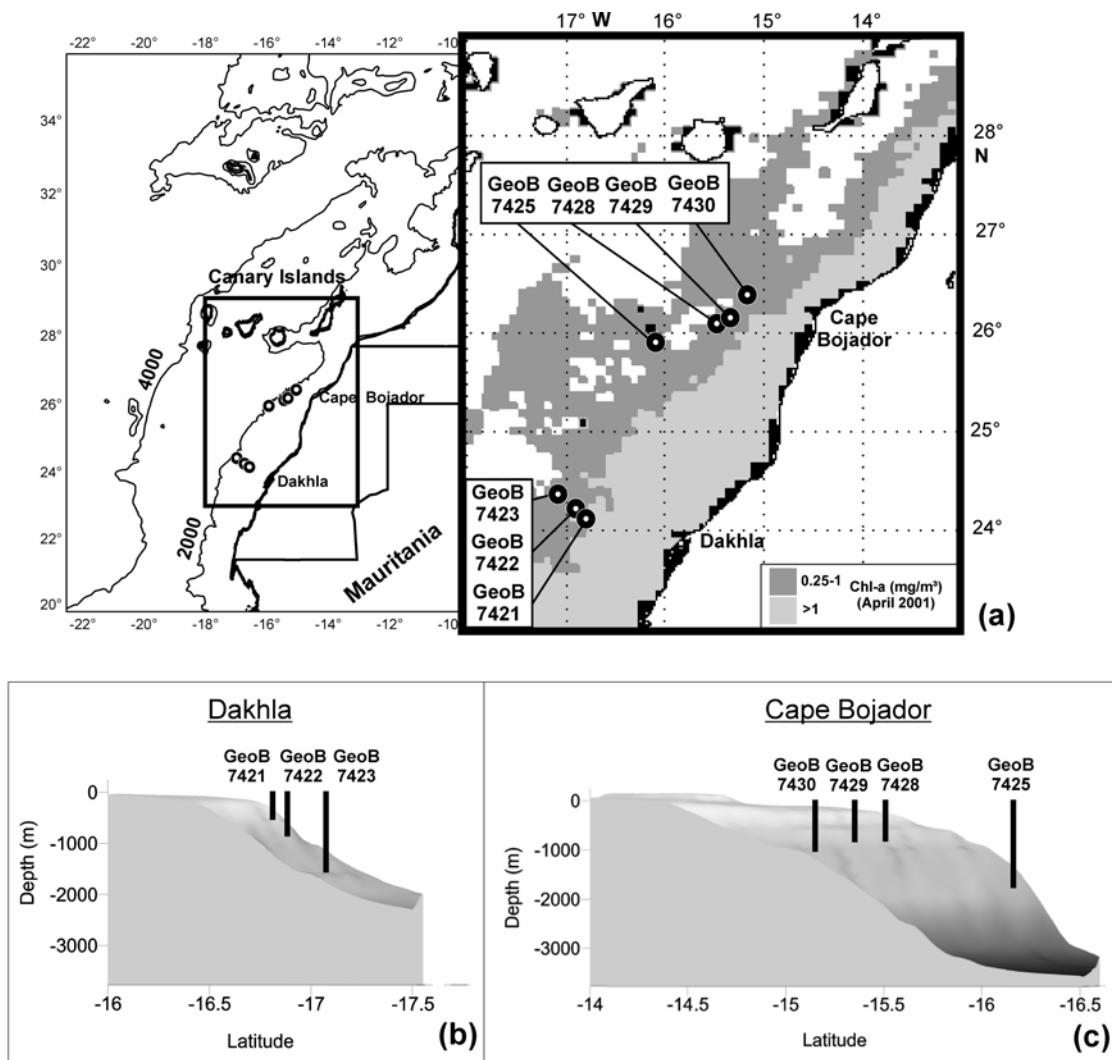


Fig. 1a-c: Map of two camera transects obtained along the NW-African coast and slope morphology off Dakhla and Cape Bojador. Presented chlorophyll pigment concentrations were averaged over the period of April 2001

Table 1: ParCa station list: positions, deployment times and depths

Station	Position		Date	Deploy time		Depths(m)	
	Lat.	Lon.		Time	(UTC)	Water	Profile
GeoB 7421	24°09.8'N	16°46.6'W	10.04.01	23.45	– 01.00	618	618
GeoB 7422	24°12.4'N	16°50.7'W	10.04.01	01.50	– 03.15	1071	1071
GeoB 7423	24°20.2'N	17°04.2'W	10.04.01	04.50	– 06.30	1641	1641
GeoB 7425	25°55.2'N	16°04.9'W	11.04.01	05.20	– 07.20	1813	1813
GeoB 7428	26°06.6'N	15°27.4'W	11.04.01	19.50	– 20.45	880	880
GeoB 7429	26°11.4'N	15°19.4'W	11.04.01	22.40	– 23.50	1010	1010
GeoB 7430	26°23.0'N	15°09.1'W	12.04.01	05.30	– 07.00	1160	1140

We defined aggregates to consist of at least two coherent, macroscopically resolvable particles. To prevent a second measurement of the particles forming an aggregate by the software, aggregates and zooplankton were cut away from the images before measuring the

abundance of spherical particles.

The abundance and size of spherical particles was extracted automatically by the software (Fig. 2). The software computes the Equivalent Spherical Diameter (ESD) of each particle on the image and exports the values to a separate worksheet. The computation of ESD from large aggregates was not done. Most aggregates consisted of a large variety of particles with different sizes and a characterisation of large, coagulated aggregates by means of an ESD is not reasonable. A proper description of such aggregates can only be provided by their abundance and volumes (see below).

To visualize the change of the size distribution of the spherical particles with depth, 24 size classes were generated (Table 2). The frequencies in percent of each size class was averaged over a depth interval of 100 m and encoded in grey values.

A similar approach was done for the particle volumes. Volumes were calculated from the ESD using equation (1) for spheres:

$$(1) \quad V = (4 / 3) * \pi * r^3$$

All volumes calculated from spherical particles were added, resulting in the total particle volume datasets. In addition to the computation of the total particle volume, a similar classification as described for the size distribution was accomplished for the particle volumes. The volumes of particulate matter were allocated to one of four volume classes. These were likewise averaged over 100 m and visualised in grey values. The classification of volumes per size class is given in Table 3.

The volumes of large, coagulated aggregates were calculated by computing the volume of each particle, forming the aggregate. Afterwards, the volumes of each particle were added, resulting in the total volume of a single aggregate. These were added to the total particle volume dataset and subsequently allocated to one of the corresponding volume classes. The measurement did not take into account the organic matter, binding the aggregates. This method may introduce some error in the computation but it was the only possibility to obtain the actual aggregate volumes.

Table 2: Size classifications and ranges for spherically shaped particles

Size Class	1	2	3	4	5	6	7	8	9	10	11	12	13	14	15	16	17	18	19	20	21	22	23	24
Range (µm)	≤ 185	245	269	296	324	356	391	429	471	517	623	684	751	825	905	994	1091	1198	1315	1443	1584	1739	1909	> 2000
Range (mm)	≤ 0,5									> 0,5 - ≤ 1						> 1 - ≤ 2					> 2			

Table 3: Volume classifications

Volume Class	1	2	3	4
Volume Range (mm ³)	> 0 – 0.065	> 0.065 – 0.523	> 0.523 – 14.136	> 14.136
Size Range ESD (mm)	> 0-0.5	> 0.5-1	> 1-3	> 3

To obtain information on water column turbidity, we introduce a new parameter extracted from the 8 bit images, called the “Mean Grey Value”. Each image has a pixel resolution of 1024x1024 resulting in a total of 1048576 pixels. An 8 bit image ($2^8 = 256$) comprises 256 grey values, where the value 0 represents black and 255 white. One of the 256 available grey values is allocated to each pixel, forming the entire image. Thus, the addition of the grey values of each pixel, divided by the total number of pixels determines the mean grey value. However, the images had to be processed, because this procedure would include the grey values of the foreground particles, leading to falsified turbidity measurement of the water column. Hence, the foreground particles had to be separated from the background (Fig. 2a). This was accomplished by the multiple appliance and combination of two morphological filter operations, called “Dilation” and “Erosion”. An “Erosion” followed by a “Dilation” is called “Opening” and a “Dilation” followed by an “Erosion” is called “Closing”. These filters operations blur and etch away boundaries (foreground particles) with aid of a specified structuring element, shifted pixel by pixel over the image. For detailed information on morphological filter operations, we refer to Umbaugh (1998). After the “Opening” and subsequent “Closing” operation on the original image, a new image is generated containing the grey values of the image background (Fig. 2b). The arithmetic division of the original image (Fig. 2a) with the new image of the background information (Fig. 2b) results in a third image, with foreground particles clearly separated from the background (Fig. 2c). Particle characteristics like size and abundance were extracted from the foreground image, the mean grey value from the background image, respectively.

Although we cannot compare the mean grey values with optical backscatter or transmissiometer data in this study, unpublished data from an optical backscatter in comparison with the mean grey value showed a good correlation (Nowald, 1999). In Figure 3, a comparison of both methods is presented from a profile obtained off the Orinoco delta during the Meteor M34-4 cruise in 1996. Progression curves of the mean grey value and the backscatter are almost identical but we are not able to provide information about the resolution limits of the mean grey value or which particle populations are obtained by this method. Differences in the resolution limits might be reflected in the increase of the turbidity

shortly above the seafloor seen in the mean grey values. A similar increase is not observed in the optical backscatter data and thus, differences between both methods are likely to exist but cannot be further quantified.

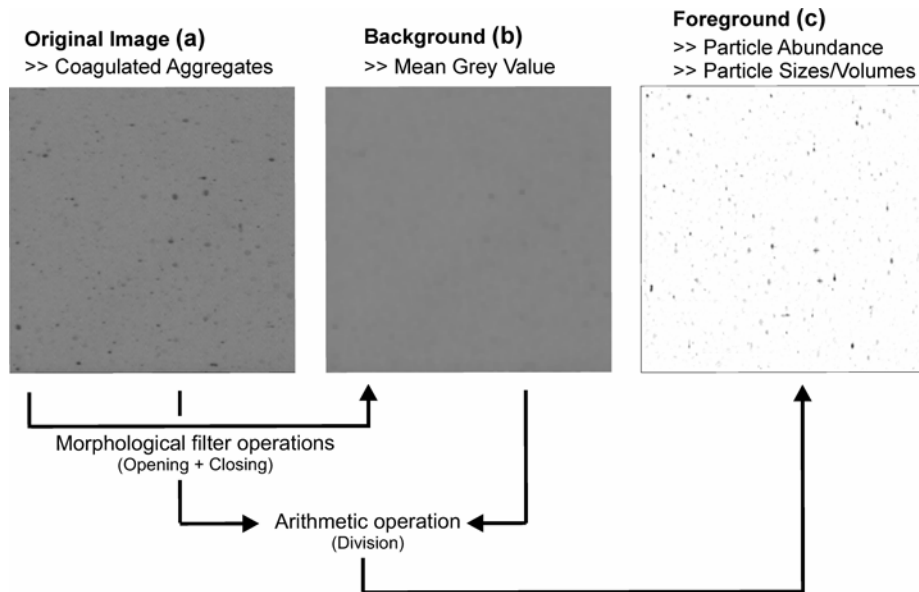


Fig. 2a-c: Diagram of image processing procedures for the extraction of the mean grey value and individual particle and aggregate parameters.

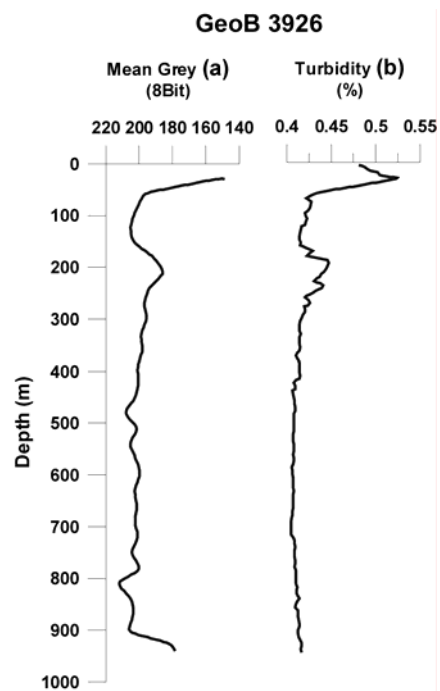


Fig. 3a-b: Comparison of optical backscatter data with the mean grey value obtained during the METEOR cruise M-34 off Venezuela in 1994. These two different methods provide almost similar results measuring the turbidity of the water column.

3. Results

3.1 Dakhla

3.1.1 Particle abundances

The particle abundances within the upper 150 m of the water column show a decreasing trend from the coastal near station to the sites further offshore. Particle concentrations decrease from 110 n l⁻¹ at site GeoB 7421 (Fig. 4a), to 70 n l⁻¹ at site GeoB 7422 (Fig. 5a) down to a minimum value of 30 n l⁻¹ at station GeoB 7423 (Fig. 6a). Profile GeoB 7421 is characterised by a particle minimum between 100 m and 300 m depth, reaching lowest concentrations of 16 n l⁻¹. Below this depth, particle concentrations increase to a depth of ~350 m and remain more or less constant down to the seafloor. A comparable increase beyond the euphotic zone is not observed at the deeper stations GeoB 7422 and GeoB 7423. Below 200 m water depth, no significant changes in the particle concentrations were measured down to the ocean bottom and particle abundances remain more or less constant around 25 n l⁻¹.

3.1.2 Aggregate abundances

Coagulated particle aggregates are predominantly found in high concentrations between the ocean surface and 150 m water depth. Their concentration is very low in comparison to the spherical particles. The maximum concentration of 0.35 n l⁻¹ was found at site GeoB 7421 at 60 m depth (Fig. 4b), which is 30 times less than that of spherical particles at the same depth. Within the euphotic zone, the concentration of large aggregates is almost equal at all profiles evaluated in this study. The major difference between the near-coastal site GeoB 7421 and the profiles located further offshore (GeoB 7422 – Fig. 5b, GeoB 7423 – Fig. 6b), is in terms of the vertical distribution of the large aggregates. Aggregates are almost always present in the entire water column at station GeoB 7421. In contrast at sites GeoB 7422 and GeoB 7423, there are large vertical sections where aggregates are almost non-existent. The largest gap is located between 450 m and 700 m water depth at station GeoB 7422, where no aggregates were observed at all.

3.1.3 Mean grey values

The particle abundance shows a good correspondence with the mean grey values. Where particle concentrations are high, the mean grey values decrease, and vice versa. This is seen throughout the entire camera profile at site GeoB 7421 (Fig. 4a, 4c) and at the stations GeoB 7422 (Fig. 5a, 5c) and GeoB 7423 (Fig. 6a, 6c). In addition, an abrupt change in the mean grey values, reflecting changes in the turbidity of the water column, is observed around

800 m water depth at site GeoB 7422 and 1450 m water depth at site GeoB 7423. The water column becomes less turbid within only a few tenths of meters. However, this change was not seen in the particle abundance data for the corresponding depths.

3.1.4 Size distributions

There is no coherence between the particle abundance and the size distribution. Although the particle abundances at sites GeoB 7422 (Fig. 5a) and GeoB 7423 (Fig. 6a) do not significantly change with depth below 150 m, strong variations and changes in the size distribution of particles are observed (Fig. 5d, Fig. 6d). One would expect a consistent particle size distribution at constant particle concentrations but in fact, size distribution appears erratically. At site GeoB 7421 (Fig. 4a), where changes in the particle concentrations occur even below the euphotic zone, a correspondence between abundance and the particle sizes (Fig. 4d) is likewise missing.

DAKHLA

Figure 4

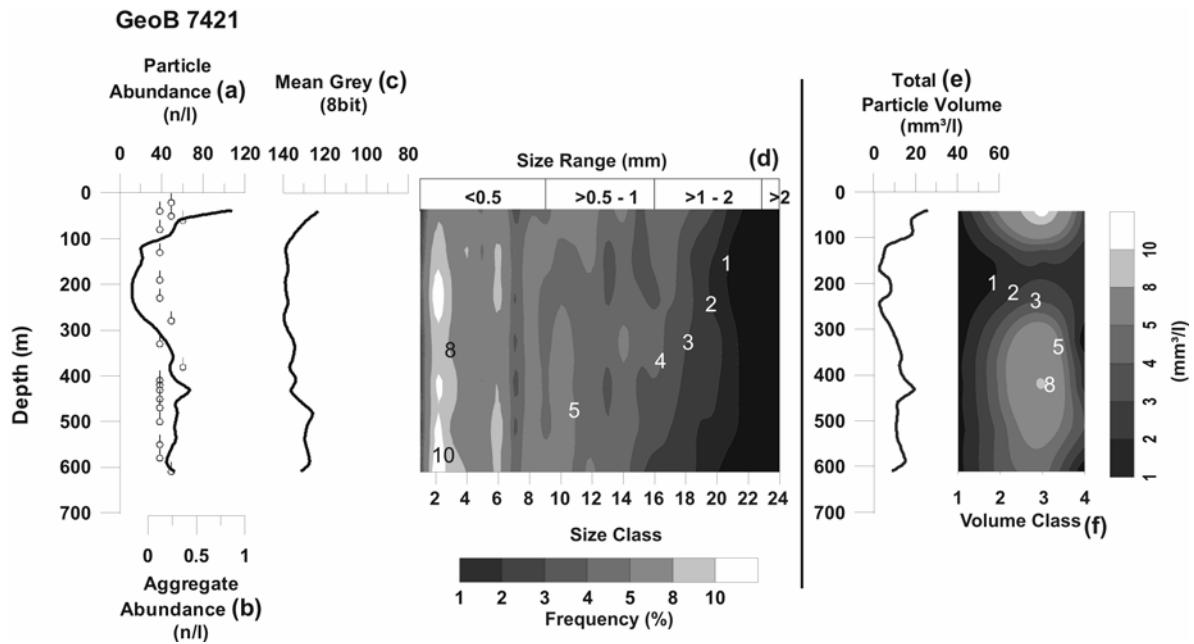


Figure 5

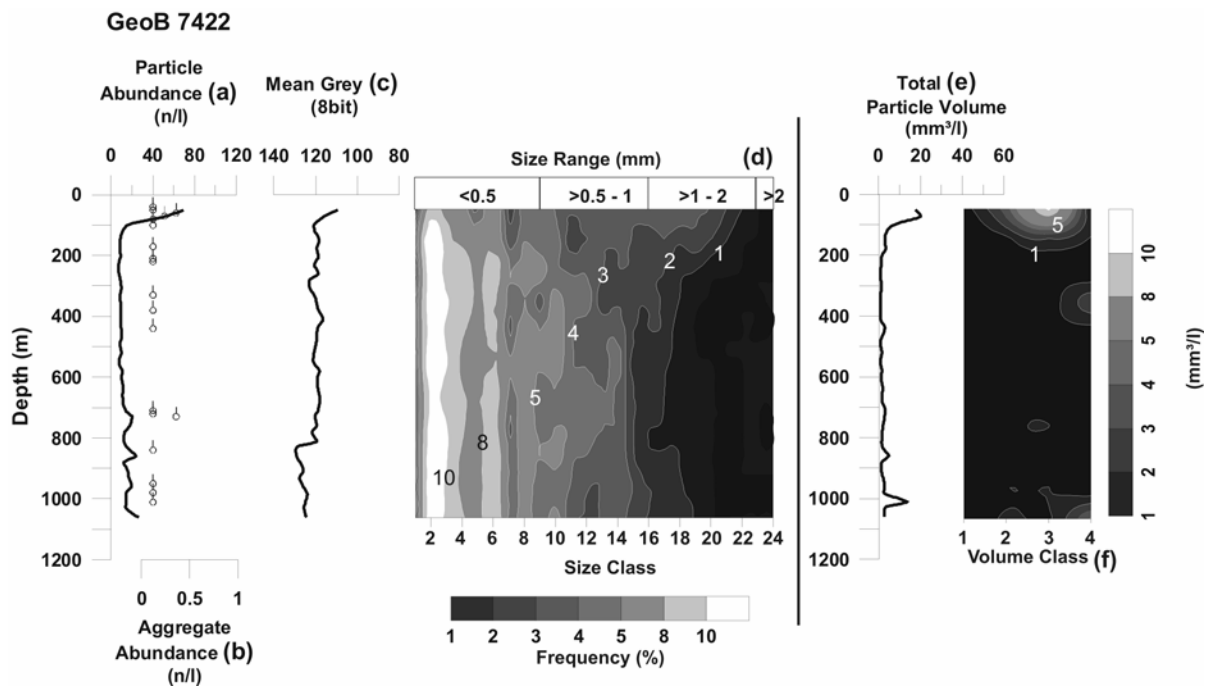


Figure 6

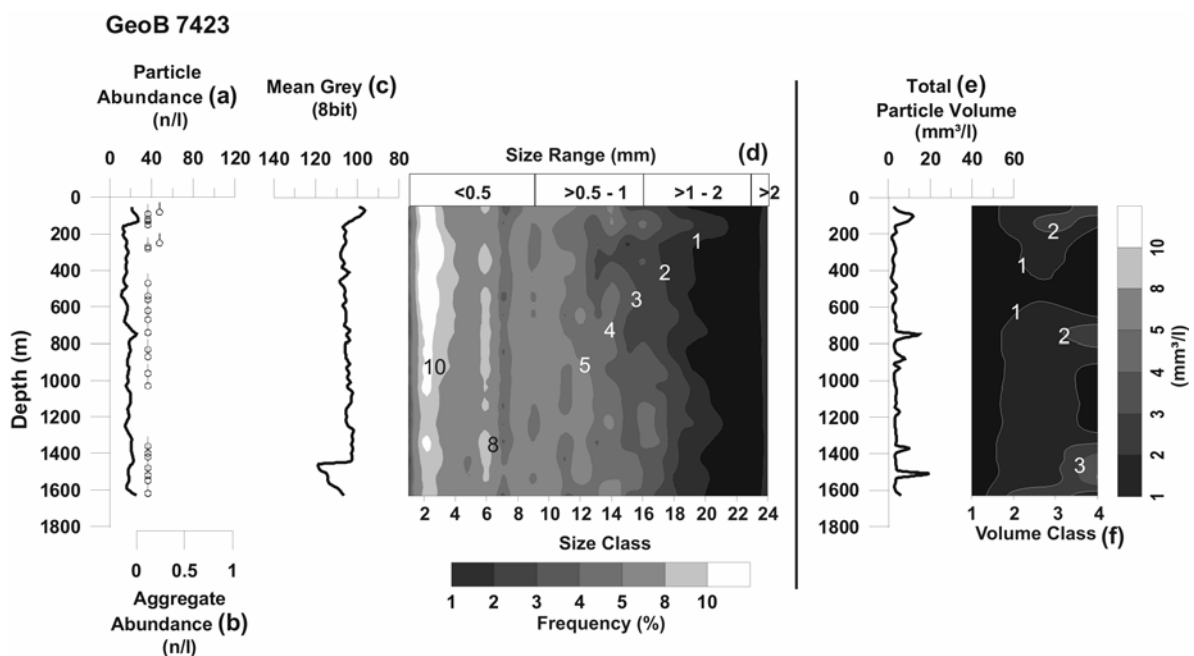


Fig. 4-6: Particle distribution off Dakhla. All lines are fitted with a 5-point running average. Particle concentrations in the surface decrease with increasing distance from the coast (Fig. 4a – 6a), which is related to the decreasing primary production conditions. Site GeoB 7421 is characterised by a huge BBL between 450 m and 600 m, which was not detected at the other transect stations. Note the uneven and erratical size distribution of particles with depth (Fig. 4d – 6d). A possible explanation are intense aggregation and disaggregation processes in the water column.

3.1.5 Particle volumes

Total particle volumes in the upper water column decrease with increasing distance from the coast, corresponding well with the decreasing particle abundances. The values decrease from $30 \text{ mm}^3 \text{ l}^{-1}$ at site GeoB 7421 (Fig. 4e), to $20 \text{ mm}^3 \text{ l}^{-1}$ at site GeoB 7422 (Fig. 5e), down to $13 \text{ mm}^3 \text{ l}^{-1}$ at station GeoB 7423 (Fig. 6e). The majority of the total particle volume in the surface waters at sites GeoB 7421 and GeoB 7422 is provided by particles and aggregates contributing to volume class 3 (Fig. 4f, Fig. 5f). They contribute to at least $8 \text{ mm}^3 \text{ l}^{-1}$ of the total volume of $30 \text{ mm}^3 \text{ l}^{-1}$ at site GeoB 7421 and the total volume of $20 \text{ mm}^3 \text{ l}^{-1}$ at station GeoB 7422. Apart from occasional peaks (GeoB 7423 at 800m and 1500 m), total volumes below the euphotic zone remain more or less constant. Site GeoB 7421 is characterised by an increase in the particle volumes below 300 m depth, reaching concentrations of more than $10 \text{ mm}^3 \text{ l}^{-1}$.

3.2 Cape Bojador

3.2.1 Particle abundances

Lowest particle abundances of 20 n l^{-1} in the upper water column are measured at site GeoB 7425 (Fig. 7a). From the ocean surface down to 780 m depth, concentrations remain almost constant. The midwater column is characterised by a distinct midwater concentration maximum between 780 m and 1450 m water depth, where particle abundances reach values three times higher compared to surface water. Another noticeable particle maximum is located between 1620 m and the ocean bottom. In this depth interval, the highest concentrations of the entire profile were measured, reaching a maximum value of 90 n l^{-1} at 1800 m depth.

The particle distribution patterns of sites GeoB 7428 (Fig. 8a), GeoB 7429 (Fig. 9a) and GeoB 7430 (Fig. 10a) are quite similar. Increased particle concentrations are observed in the euphotic zone, reaching maximum concentrations of more than 30 n l^{-1} at each station. No significant changes in the particle abundances are visible below 150 m. An increase in the particle abundance is observed at site GeoB 7428 at around 70 m above the seafloor. A similar increase in the particle abundance is seen around 700 m at site GeoB 7429 and 950 m at station GeoB 7430. Within these near-bottom maxima, particle concentrations are higher compared to the abundances in the very ocean surface.

3.2.2 Aggregate abundances

Aggregates are predominantly concentrated in the upper 150 m of the water column,

which corresponds with the aggregate distributions in the surface water described for the Dakhla profiles. In the remaining water column, aggregates show a comparable patchy distribution. Large depth intervals with no coagulated aggregates are found in all profiles of the Cape Bojador transect.

3.2.3 Mean grey values

In contrast to the Dakhla profiles, variations between the mean grey value and the particle abundances are observed. At site GeoB 7428, mean grey value and the particle abundance show similar depth profiles (Fig. 8a, 8c). Deviations between the mean grey value and the particle concentrations are found in the midwater column at stations GeoB 7429 (Fig. 9c) and GeoB 7430 (Fig. 10c). At site GeoB 7429, there is an abrupt change to a less turbid water column between 380 m and 690 m depth. A similar midwater anomaly of the mean grey values is observed at site GeoB 7430 between 480 m and 720 m (Fig. 10c).

The most significant differences between the particle abundances and the mean grey values are observed at site GeoB 7425. Particle abundances and mean grey values are comparable within the upper 470 m but below this depth, these parameters deviate. In the midwater column between 470 m and 1480 m, at least four well defined turbidity layers can be observed (Fig. 7c; I-IV). These layers are located above and in the depth range of the particle midwater maximum between 780 m and 1450 m (Fig. 7a). Below this midwater maximum the mean grey values remain almost constant, although there is a particle maximum between 1620 m and the seafloor.

3.2.4 Size distributions

Two major differences in the size distribution of particulate matter between the Dakhla and Cape Bojador profiles are observed. The first difference is the more abundant small particle sizes. Frequencies of size classes 1-4 are higher compared to the profiles in the Dakhla transect. At sites GeoB 7428 (Fig. 8d), GeoB 7429 (Fig. 9d) and GeoB 7430 (Fig. 10d) these size classes are always available in frequencies >5 %. The second difference is a more even size distribution. Small particles predominate and frequencies decrease constantly with increasing particle diameter. Off Dakhla, no such smooth gradients can be observed where a more arbitrary size distribution was described.

Profile GeoB 7425 is the only site where changes in the abundance of particles match changes in the particle size distribution (Fig. 7a, 7d). From the ocean surface to the top of the particle midwater maximum, small particles (size class 1-3) dominate the size spectra. At 720

CAPE BOJADOR

Figure 7 (for description see p. 80)

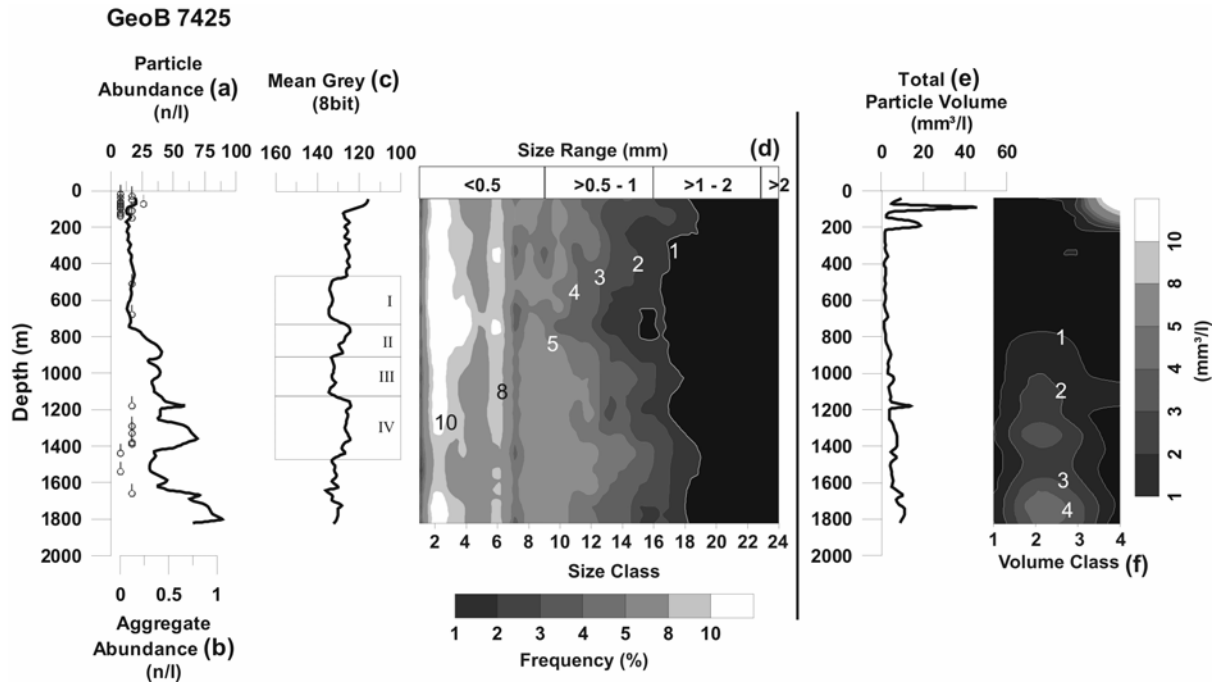


Figure 8

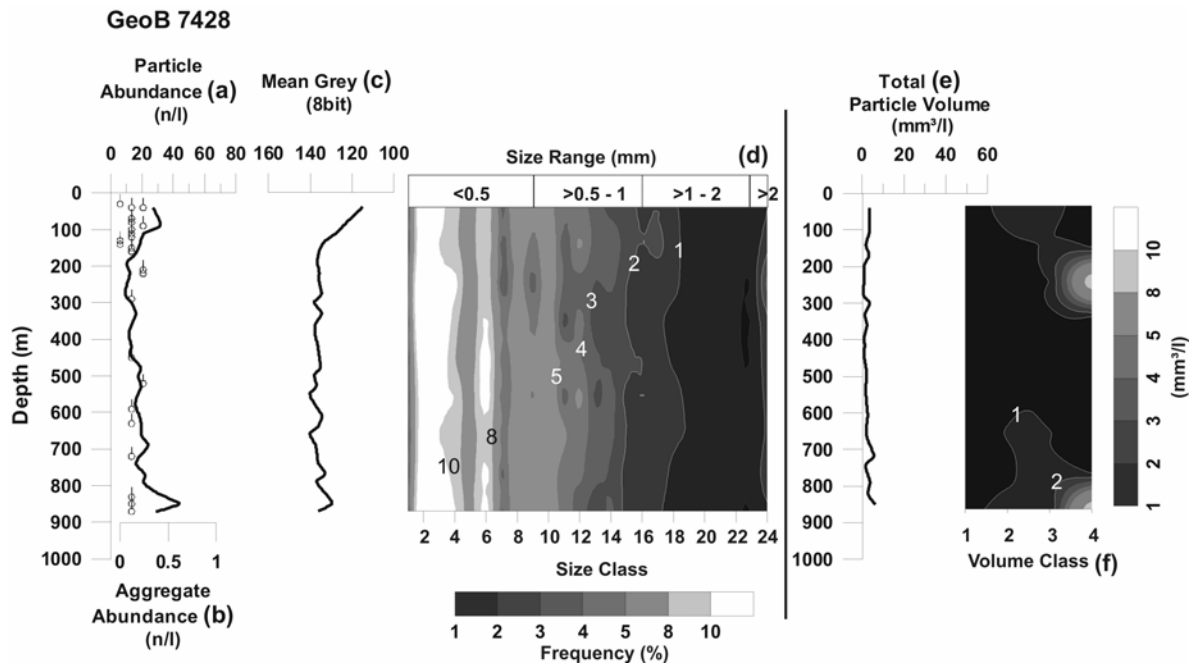


Figure 9

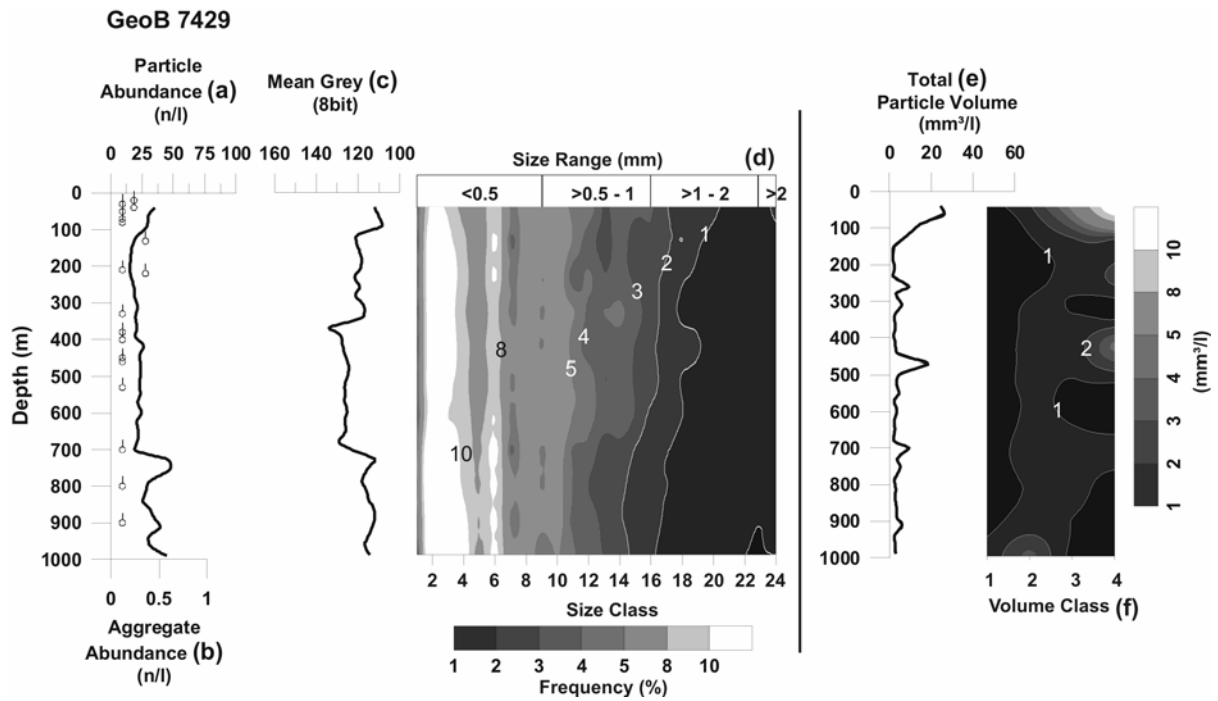
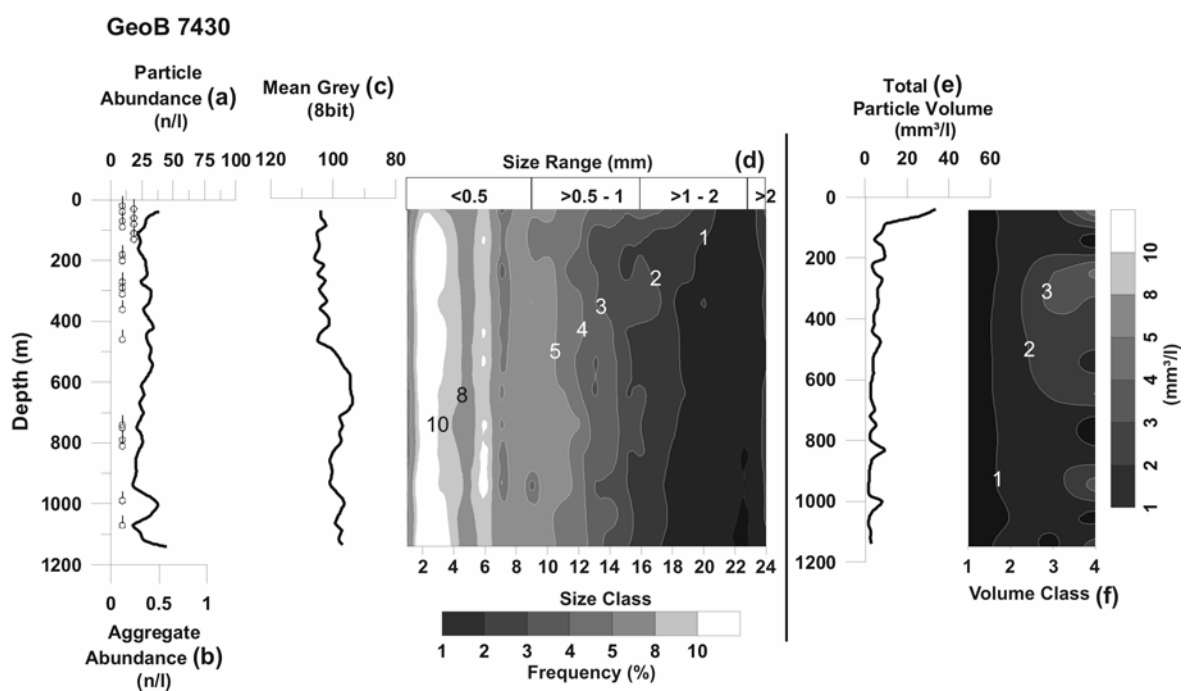


Figure 10



Description of Fig. 7-10 (p. 78/79): Particle distribution off Cape Bojador. All lines are fitted with a 5 point running average. Site GeoB 7425 (Fig.7) reflects a massive lateral intrusion of material from a distant source. This is seen in the particle abundance and size distribution plots (Fig. 7a & 7d). Increased frequencies of size classes 1-4 are found at the upper boundary of the particle maximum, which is related to accumulation processes when external material is shifted into a formerly undisturbed water column. In comparison to the Dakhla profiles, the size distribution with depth appears more evenly (Fig. 7d – 10d), resulting in an evenly pronounced sedimentation pattern off Cape Bojador. Although particle concentrations in the ocean surface are considerably lower compared to the Dakhla profiles, total particle volumes are much higher (Fig. 7e-f – 10 e-f). This might be explained with enhanced growth of large aggregates, which preferred form in areas of lower particle dynamics.

m depth, where the particle concentrations begin to increase, an accumulation of smaller particles is observed. Size class 4 reaches frequencies of 10 % in this specific water depth and the highest concentration of this size class for the entire profile are found at this particular depth. Within the particle midwater maximum, a depletion of size fractions 1-4 is visible compared to the water column above, and in addition, middle sized particles are enriched (size classes 8-10). Below the midwater maximum, in the depth range between 1480 m and 1620 m, the largest particles are found whereas small particles are again reduced in their frequency. Within the near-bottom particle maximum, between 1620 m and the seafloor, an increase of the smaller and a decrease of large and middle sized particles is measured.

3.2.5 Particle volumes

Although particle abundances in the surface waters are comparable, ranging between 20 n l^{-1} and 33 n l^{-1} , total particle volumes are highly variable. Highest volumes are found at site GeoB 7425, reaching almost $50 \text{ mm}^3 \text{ l}^{-1}$ (Fig. 7e). Lowest values are measured at site GeoB 7428 ($\sim 5 \text{ mm}^3 \text{ l}^{-1}$), with almost no changes throughout the entire profile (Fig. 8e). Apart from this specific site, the majority of particulate matter in the remaining profiles is concentrated in the euphotic zone and decrease considerably to volumes $<10 \text{ mm}^3 \text{ l}^{-1}$ at the border to the midwater column at around 150 m water depth. An unexpected observation are the higher total volumes at site GeoB 7425, compared to the near-coastal Dakhla station GeoB 7421 (Fig. 4e). Although particle concentrations at profile GeoB 7425 (Fig. 7e) are 5 times lower, total particle volumes are twice as high in a region of considerably lower primary production.

Apart from single, occasionally occurring peaks, as observed for instance at site GeoB 7429 at 480 m depth (Fig. 9e), no significant changes in the total particle volumes with depth are observed at profiles GeoB 7428, GeoB 7429 and GeoB 7430. Volumes remain constant even if particle abundances increase. This is, for example, clearly seen at site GeoB 7429 between 700 m depth and the ocean bottom (Fig. 9a, 9e). In contrast, site GeoB 7425 is the

only station where total particle volumes increase with depth (Fig. 7e). The volumes begin to increase around 700 m depth, just above the distinct midwater particle maximum in the coincident depth (Fig. 7a).

4. Discussion

4.1 Particulate matter distributions

Carr (2002) and Nixon and Thomas (2001) proposed a chlorophyll boundary value of 1 mg m^{-3} to distinguish between high productivity and low productivity areas. According to this, site GeoB 7421 (Fig. 4a) is located in the higher productivity area close to the coast, a finding confirmed by the highest particle abundances of all stations along this transect. Particle concentrations decrease along the transect further offshore, which coincides with the productivity gradient observed in the chlorophyll concentrations (Fig. 1). The comparably lower primary production conditions off Cape Bojador, ranging between 0.25 mg m^{-3} and 1 mg m^{-3} , are reflected in reduced and more constant particle abundances of around 30 n l^{-1} . All of these profiles were acquired within in a region of similar primary production intensity. Gorsky et al. (1992) and Ratmeyer and Wefer (1996) showed a connection between the integrated chlorophyll biomass, obtained by CTD sensors, and particle data, acquired by camera systems.

In this study a close coupling between satellite derived chlorophyll concentrations and particle abundances was found and this is the first study to conclusively show that primary productivity controls particle abundances in the euphotic zone.

Along both transects particle abundances below the euphotic zone remain more or less constant down to above the seafloor. The only exception is site GeoB 7425 (Fig. 7), which is a special case and discussed in the next section. Although there are only slight changes in the particle concentrations with depth, the vertical size distribution patterns between both transects differ decisively. The Dakhla profiles (Fig. 4d, 5d, 6d) are characterised by an erratical and uneven size distribution. In comparison, the size distribution off Cape Bojador (Fig. 8d, 9d, 10d) appears more even and homogenous. These differences might be related to different particle dynamics in regions of different primary productivity. The variety in the particle sizes as seen off Dakhla, might be due to intense and repetative aggregation and disaggregation of particulate matter. These processes are quite complex and are controlled by a large variety of factors such as particle concentration (Alldredge et al., 1993), particle stickiness (Jackson, 1990), wave energy (Lampitt, 1996) or gravitational processes (Alldredge

and McGillivray, 1991). Faster sinking particles collide with slower sinking ones, resulting in particle growth. The movement and feeding activities of zooplankton may also cause fragmentation of particulate matter. Zooplankton were found to destroy a large portion of aggregates beyond the euphotic zone (Dilling and Alldredge, 2000; Harbison and McAllister, 1979). Most of the processes discussed cannot be observed directly from the images, but in an area influenced by increased primary productivity, coagulation and fragmentation dynamics are probably more intense compared to a lower productive region like Cape Bojador. One question remains though: are the observed particle size distributions off Dakhla a reflection of the exported material from the surface water, or is a certain fraction of the material altered on its descent to the seafloor ?

The particle volumes are another parameter reflecting the different particle dynamics between both study areas. The most striking difference regarding the particle volumes is observed in the surface water. In the midwater column, total particle volumes remain almost constant along both transects, coincident with the particle abundances. In the area off Cape Bojador (Fig. 7e, 8e, 9e, 10e) total particle volumes in the ocean surface are up to five times higher, compared to the Dakhla profiles (Fig. 4e, 5e, 6e). The Cape Bojador region, with considerably lower particle concentrations and primary productivity is characterised by larger particles and aggregates in the surface water than the Dakhla region, which is partly influenced by the high productive, near-coastal upwelling belt. The majority of the total particle volume is provided by particles and aggregates of volume class 4 (Fig. 7f, 9f, 10f), which correspond to an ESD of at least 3 mm. Comparable particle size could not be measured along the Dakhla transect. This paradoxum might again be explained by the differences in the aggregation and disaggregation dynamics between low and high productive areas. The profiles obtained off Dakhla are as mentioned above, under the influence of high primary productivity and hence, increased coagulation rates. While coagulation and aggregation rates are high, disaggregation and fragmentation of particulate matter might have a comparable significance, prohibiting the growth of aggregates above a certain size. In the low productive areas off Cape Bojador these dynamics possibly play a minor role as seen in the particle size spectra. Reduced coagulation and disaggregation rates could enable the growth of much larger aggregates. It is possible, that the retention time of particles in the euphotic zone is higher in low productive areas, compared to regions with an increased primary production and enhanced aggregation/disaggregation dynamics.

Many profiles show increased particle abundances above the seafloor. The near-bottom maximum, described here as the Benthic Boundary Layer (BBL), is considerably well

pronounced at the near-coastal Dakhla site GeoB 7421 (Fig. 4a). The height of the BBL is almost 200 m, indicating intense uplift and resuspension processes. The resuspension intensity is dependent on many factors, for instance current velocities and the resulting shear stress along the seafloor (Tengberg et al., 2003; Thomsen and Gust, 2000), or particle sizes and characteristics (Thomsen, 2003). Bottom currents are usually highest close to the coast and decrease in intensity further offshore (McCave et al., 2001; Müller and Siedler, 1992; Thomsen et al., 2002). It is difficult to assess whether the increased particle concentrations above the seafloor observed at stations GeoB 7429 (Fig. 9a) and GeoB 7430 (Fig. 10a) are generated by similar processes. They are located further offshore, where current velocities are thought to be lower. Perhaps these anomalies can be related to Intermediate Nepheloid Layers (INL), which are reported to detach from the BBL (McPhee-Shaw and Kunze, 2002) and are advected towards the open ocean. Such layers were observed and described for instance by McCave et al. (2001) in the North Atlantic Ocean, McPhee-Shaw et al. (submitted) along the California continental margin or Frignani et al. (2002) in the Mediterranean Sea. Another mechanism for increasing concentrations above the seafloor in the Cape Bojador region might be the prevailing morphology. Weaver et al. (2000) published a map showing large canyons and a heavily furrowed ocean floor on the slope off Cape Bojador, close to the camera locations. The continuously changing bottom morphology at Cape Bojador, comprising steeper and flatter parts, could also enhance particle uplift in this region.

4.2 Particle flux and sedimentation patterns:

It has become established that large, coagulated aggregates are major transport vehicle of elements and nutrients to the deep-sea (e.g. Fowler and Knauer, 1986, Alldredge, 1998, Walsh and Gardner, 1992, Asper et al., 1992). Apart from the near-coastal site Geo 7421 (Fig. 4), there are large gaps in their vertical distribution. A previous study carried out within the highly productive upwelling belt off Cape Blanc further south (Nowald et al. submitted), showed high concentrations of these large aggregates in the entire water column. This gives a continuous supply of large amounts of material to the ocean bottom. Hence, we conclude that comparably lower vertical transfer rates of material occur in the Dakhla and Cape Bojador region compared to Cape Blanc. The exception is site GeoB 7421 (Fig. 4) where high numbers of these aggregates are seen. Site GeoB 7421 is still influenced by the increased primary production conditions close to the coast, implying higher particulate matter production and export rates.

The low flux rates in the Dakhla (exception is site GeoB 7421) and Cape Bojador

region are reflected likewise seen in the particle abundance and volume data. Particle volumes are usually below $5 \text{ mm}^3 \text{ l}^{-1}$ and particle abundances are around 20 n l^{-1} below the euphotic zone. Particle abundance and volumes do not significantly change down to the seafloor. Based on this observation, comparable export and flux rates of material from the surface to the seafloor are expected in both study areas.

However, we think that there is a major difference in the way the material reaches the ocean bottom. The erratical and inhomogenous particle size distributions off Dakhla must result in fluctuations in the amount of particulate matter reaching the seafloor simultaneously. By assuming a relationship between size and sinking rate (Alldredge and Gotschalk, 1988; Pilskaln et al. 1998) and allocating a sinking velocity to each particle class, the result must be a “patchy sedimentation” of particles. In comparison, the Cape Bojador stations are characterised by a uniform size distribution, which must result in an even sedimentation of particles. We don't think that the observed differences in the sedimentation patterns have larger effects on the total flux in the Dakhla and Cape Bojador region. The difference is only seen in the way the material is delivered to the ocean bottom.

4.3 Lateral intrusion at site GeoB 7425

We believe that site GeoB 7425 (Fig. 7a) reflects a massive lateral intrusion of particulate matter. This can be inferred from the particle abundance and the size distribution datasets. Particle concentrations are significantly increased between 700 m and 1400 m in comparison to the water column above. In addition, changes in the particle abundances coincide with changes in the particle size distribution (Fig. 7d). The water column above the midwater maximum shows increased frequencies of the smaller size classes (classes 1-3) and lower frequencies of the middle sized particles (classes 7-11). The opposite is the case within the midwater maximum. Smaller particles are depleted while the middle-sized particles are increased in frequency. Furthermore, the increased abundances of small particles of size class 4 and 5 at the upper limit of midwater maximum around 700 m depth (Fig. 7d), suggest that this midwater maximum is related to the lateral advection of particulate matter. We infer that the increased frequencies in this specific water column depth are related to accumulation processes at the border of two different water masses with different, physical characteristics. The first process is possibly strong gradients in the density structure. Small particles are reported to accumulate in depths, where strong gradients in the density structure occur (MacIntyre et al., 1995; Pilskaln et al., 1998). The second factor is differences in the current velocities and directions of two specific water masses. It is likely that the lateral advected

cloud is characterised by a higher current velocity in comparison to the water column above and below. These differences might result in turbulences occurring along the transition zone and thus, leading to increased retention times of the smaller particle size fraction. These processes are considered to be the key factors controlling accumulation, and the definition of the upper border of the lateral advected cloud around 700 m depth. Although we cannot provide any additional data to substantiate this theory, we propose that these processes are the most likely explanation for the increased frequencies of small particles.

MacIntyre et al. (1995) suggested that particulate matter accumulation was related to changes in the speed and direction of currents. The lower boundary of the intrusion is likewise defined by the abundance and size of particulate matter. It is located around 1400 m depth and characterised by an abrupt loss of the particle concentration and a significant loss of small particles in size class 1-3. The lateral advected cloud appears as a consolidated water mass with well defined borders, which can be clearly deduced from changes within the particle size spectra. The density gradients and higher current velocities can likewise explain the depletion of size classes 1-3 beyond the lower boundary of the advected cloud. Both factors prohibit the further supply of smaller particles below 1400 m. The increasing frequencies of these size classes above the seafloor (between 1620 m and the seafloor) are related to near-bottom resuspension processes and decoupled from the lateral advection.

These kinds of advection processes must have a major influence on the offshore vectored particle transport and are certainly a significant source for the delivery of biogenic material into deeper parts of the oceans. While camera profiles obtain the particulate matter distribution to a certain time at a certain place, two questions arise. First, is the lateral advection a temporal event or is it a consistent phenomenon? Second, what is the spatial extension of the advected cloud? Freudenthal et al. (2001) concluded from their sediment trap studies a continuous, annual lateral advection of material with varying intensity from the Cape Ghir towards their trap site located in the Canary Islands region. On the other hand, (McCave et al., 2001) reported the occurrence of INL from the slope off the Goban Spur margin, which were characterised by distinct temporal variability. All profiles of the Cape Bojador transect were obtained within 24 h and the distance between site GeoB 7425 to the adjacent profile GeoB 7428 is not more than 60 km. Thus, the spatial extension of this lateral advected cloud towards the north and south must be less than 60 km, because the remaining Cape Bojador profiles show no similar particle distribution patterns.

Possible source of the lateral advected material might be the upper slope areas.

Gardner and Walsh (1990) report the lateral advection from the upper slope in the Gulf of

Mexico observed in their St 25 particle profile (Fig. 11a). There is a striking similarity between the St 25 particle profile and the Cape Bojador profile GeoB 7425 (Fig. 11b). Water depth is only 1000 m and particle abundances are considerably lower at St 25, however the similarity of both profiles suggests that both abundance patterns are created by the same processes. The material within the lateral advected cloud is unlikely to have originated directly from the ocean surface. In a previous study, also using the ParCa camera system, we observed a sinking event on the midslope areas off Cape Blanc, further south (Nowald et al., submitted). The sinking cloud scavenges preferably the smaller size fractions because the small size fractions are more abundant. This results in a depletion of small particles above the cloud and a coarsening of the material within the sinking cloud.

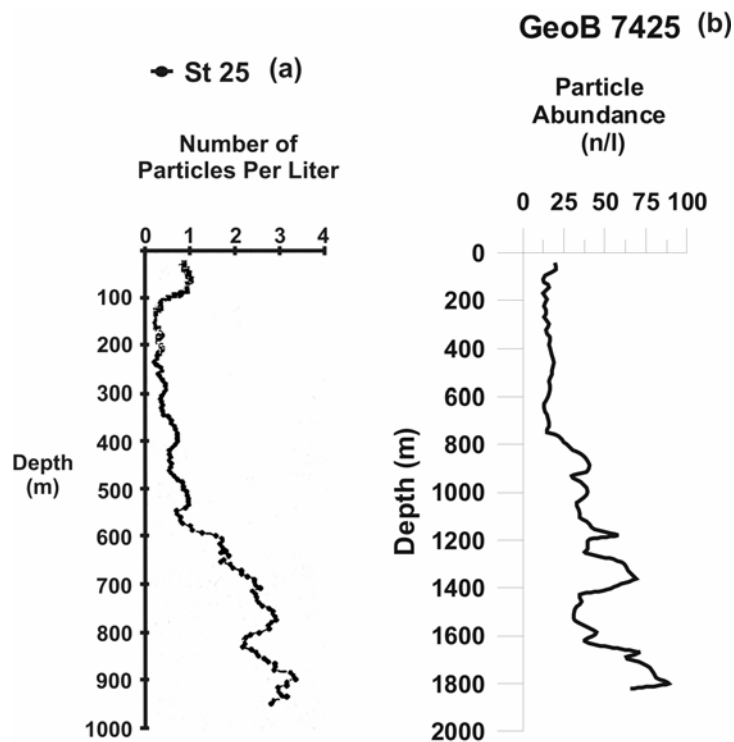


Fig. 11a-b: Comparison of site GeoB 7425 and St.25 obtained on the Louisiana shelf by Gardner and Walsh (1990). Although concentrations and profiling depths differ, the particle distribution patterns show a significant similarity.

At site GeoB 7425 a similar size distribution is not observed. The water column above the advected cloud is neither depleted in small particles nor is a significant coarsening of material visible within the cloud. The particle volumes provide further evidence for the lateral shift of material into the midwater column. Site GeoB 7425 is the only station, where total particle volumes increase with depth (Fig. 7e). Volumes begin to increase around 700 m, which

coincides with the depth where particle concentrations also begin to increase. Particle volumes are more or less constant above the advected cloud and it is unlikely that the material originates directly from the ocean surface or was formed in the midwater column. Thus, it is presumably shifted into the midwater from a different source other than the surface waters.

The mean grey values of the GeoB 7425 profile show several, well defined layers containing the smallest suspended material in the midwater column. At least 4 layers are observed above and within the midwater particle maximum (Fig. 7c), which are not observed in the particle abundance data for the coincident depths. The particle abundances in the advected cloud appear “finger-like” (Fig. 7a) and such distribution patterns likely result from very dynamic processes in the water column.

The lateral advection of material probably plays an important role in the Cape Bojador region. Apart from the large lateral intrusion, smaller intrusions processes can be seen in the mean grey values in the midwater column at sites GeoB 7429 (Fig. 9c) and GeoB 7430 (Fig. 10c). Assuming the mean grey value is a reasonable proxy for measuring the turbidity of the water column, no indications for similar processes are observed off Dakhla.

Table 4: Proposed taxonomy of particulate matter in the ocean on the basis of camera images

Class	Name	Size	Description
1	Smallest suspended particles	< eye resolution	These particles are responsible for the turbidity of the water column. Obtainable by transmissometers, optical backscatter and mean grey value.
2	Small spherical particles	200-400 μ m	Presumably available as single particulates and unaffected by coagulation processes, which is related to their evenly distribution in the water column. This particle class is found in increased concentrations above the seafloor.
3	Small spherical aggregates	400-1000 μ m	A large portion of this class is probably available in the form of aggregates, consisting of more than one component. Their uneven distribution in the water column lead to the conclusion that they underlie intense aggregation and disaggregation.
4	Large spherical aggregates	>1000 μ m	These aggregates are predominantly seen in the euphotic zone. Most of them are already destroyed in the upper water column, thus their abundance below this depth is significantly reduced.
5	Strings and Floccs	all sizes	Prolate or floccose habitus. Consist of many, macroscopically resolvable particles. They are likewise observed in high concentrations in the surface water and are considerably reduced in abundance below the euphotic zone.

The discussion shows that an appropriate description of the observed processes is complicated, because there is no detailed taxonomy for particles in the ocean. Although Alldredge (1998), Pilskałn et al. (1998), Silver et al. (1998) and others could identify several aggregate classes, a distinct differentiation is missing. The classification published by these

authors regards large, coagulated aggregates, which might not be accounted to a large portion of particles present in the ocean. This is related to the fact, that the available methodologies are not able to obtain characteristics of individual particles. Mostly, particulate matter is just divided into smaller “Marine Snow” and “Marine Snow”. This differentiation is dependant on the size and gives no information whether the particulate matter consists of single particles or coagulated aggregates. More differentiated particle classes are necessary, because different particle population own different characteristics. The role of coagulated aggregates and their contribution to the total particle volume would not have become visible if they were allocated to the common particle abundance datasets. On the basis of the presented particle profiles and images, we propose a more detailed taxonomy for particulate matter in the ocean (Table 4).

5. Conclusions

The results of this study are summarised as follows:

- 1.) Particulate matter distribution in the surface water is directly related to the primary production conditions in the euphotic zone. This was shown off Dakhla by the decreasing particle concentrations with increasing distance from the coast, following the productivity gradient seen in the satellite derived pigment concentrations. In a region of similar primary productivity conditions, particle concentrations are almost identical as shown for the Cape Bojador area.
- 2.) The areas of investigations, Dakhla and Cape Bojador show low, though similar particle fluxes and export rates. Differences are seen in the sedimentation patterns. Dakhla is characterised by a “patchy” sedimentation pattern compared to the uniform sedimentation of material off Cape Bojador.
- 3.) The area off Cape Bojador is strongly influenced by lateral intrusions. These intrusions have a significant effect on the offshore vectored particle transport. Similar processes are not observed off Dakhla.

Although vertical camera profiles acquire a snapshot of the actual particle distribution in the water column, this method is useful for observing processes, responsible for particle distribution patterns in the ocean. This study shows the potential application of vertical camera profiles and shows that the images provide more than particle counts. The high resolution particle size distribution datasets proved to be valuable for the detection of particle fluxes and transportation pathways. The lateral advection of material at site GeoB 7425 for instance, could only have been deduced from the particle abundances. But the processes

occurring in the water column when foreign particulate matter is shifted into an undisturbed water column could only be seen in the size distribution. The size distribution data also showed sedimentation variabilities between Dakhla and Cape Bojador. The particle volume and abundances data showed that there are no great differences in the total amount of material reaching the seafloor at both sites. However, the size distribution data revealed more uniform sedimentation off Cape Bojador, whereas the Dakhla region is characterised by a patchy particle sedimentation. Particle volumes and abundances are two parameters that have to be combined for a proper display and comprehension of particulate matter distributions in the oceans. Most studies present either particle volumes or the particle abundance. The significance of a comparison and combination of both parameters became visible in the distribution of particulate matter in the ocean surface. On the basis of the particle abundances one would have never expected larger particles and aggregates in a region of lower primary productivity, compared to areas where primary production is comparably higher. These differences with respect to the particle distribution in the euphotic zone between the Dakhla and Cape Bojador profiles reflects the complexity of aggregation and disaggregation processes, which are still not sufficiently understood.

The good correspondences between particle abundances and the mean grey value suggests that this parameter is an appropriate method for obtaining the turbidity of the water column. The detections of smaller intrusions of suspended material showed that from this method it is possible to obtain the same information as the more traditional optical backscatter or transmissiometers methodologies.

Acknowledgements

We thank the crew of the RV POSEIDON for their help in deploying and recovering the ParCa system. The manuscript greatly benefited from discussions with G. Fischer, U. Passow, H. Meggers and T. Freudenthal. Satellite derived pigment concentration was provided by the SeaWiFS project, NASA/Goddard Space Flight Centre. We thank P. Helmke for creating the pigment concentration map and the extraction of the chlorophyll concentrations. Many helpful comments from the reviewers helped to improve this manuscript.

The presented datasets are available in the PANGAEA database (<http://www.pangaea.de/>)

This study was funded by the “Deutsche Forschungsgesellschaft” (DFG) within the scope of the DFG Research Center Ocean Margins.

References

- Abrantes, F., Meggers, H., Nave, S., Bollman, J., Palma, S., Sprengel, C., Henderiks, J., Spies, A., Salgueiro, E., Moita, T., and Neuer, S., 2002, Fluxes of micro-organisms along a productivity gradient in the Canary Islands region (29°N): implications for paleoreconstructions: *Deep Sea Research II*, v. 49, p. 3599-3629.
- Allredge, A.L., 1998, The carbon, nitrogen and mass content of marine snow as a function of size: *Deep Sea Research I*, v. 45, p. 529-541.
- Allredge, A.L., and Crocker, K.M., 1995, Why do sinking mucilage aggregates accumulate in the water column?: *The Science of the Total Environment*, v. 165, p. 15-22.
- Allredge, A.L., and Gotschalk, C., 1988, In situ settling behaviour of marine snow: *Limnology and Oceanography*, v. 33, p. 339-351.
- Allredge, A.L., and Gotschalk, C., 1989, Direct observation of the mass flocculation of diatom blooms: characteristics, settling velocities and formation of diatom aggregates: *Deep Sea Research I*, v. 36, p. 159-171.
- Allredge, A.L., and McGillivray, P., 1991, The attachment probabilities of marine snow and their implications for particle coagulation in the ocean: *Deep Sea Research*, v. 38, p. 431-443.
- Allredge, A.L., Passow, U., and Logan, B.E., 1993, The abundance and significance of a class of large, transparent organic particles in the ocean: *Deep Sea Research I*, v. 40, p. 1131-1140.
- Asper, V.L., 1987, Measuring the flux and sinking speed of marine snow aggregates: *Deep Sea Research I*, v. 34, p. 1-17.
- Asper, V.L., Honjo, S., and Orsi, T.H., 1992, Distribution and transport of marine snow aggregates in the Panama Basin: *Deep Sea Research I*, v. 39, p. 939-952.
- Carr, M.-E., 2002, Estimation of potential productivity in Eastern Boundary Currents using remote sensing: *Deep-Sea Research Part I*, v. 49, p. 59-80.
- Dilling, L., and Allredge, A.L., 2000, Fragmentation of marine snow by swimming macrozooplankton: A new process impacting carbon cycles in the sea: *Deep Sea Research I*, v. 47, p. 1227-1245.
- Fowler, S.W., and Knauer, G.A., 1986, Role of large particles in the transport of elements and organic compounds through the oceanic water column: *Progress in Oceanography*, v. 16, p. 147-194.
- Freudenthal, T., Neuer, S., Meggers, H., Davenport, R., and Wefer, G., 2001, Influence of lateral particle advection and organic matter degradation on sediment accumulation and stable nitrogen isotope ratios along a productivity gradient in the Canary Islands region: *Marine Geology*, v. 177, p. 93-109.
- Frignani, M., Courp, T., Cochran, J.K., Hirschberg, D., and Vitoria i Codina, L., 2002, Scavenging rates and particle characteristics in and near the Lacaze-Duthiers submarine canyon, northwest Mediterranean: *Continental Shelf Research*, v. 22, p. 2175-2190.
- Gardner, W.D., and Walsh, I.D., 1990, Distribution of macroaggregates and fine-grained particles across a continental margin and their potential role in fluxes: *Deep Sea Research I*, v. 37, p. 401-411.
- Gorsky, G., Aldorf, C., Kage, M., Picheral, M., Garcia, Y., and Favole, J., 1992, Vertical distribution of suspended aggregates determined by a new underwater video profiler: *Annales de l'Institut océanographique*, v. 68, p. 275-280.
- Harbison, G.R., and McAllister, V.L., 1979, The filter-feeding rates and particle retention efficiencies of three species of *Cyclosalpa* (Tunicata, Thaliacea): *Limnology and Oceanography*, v. 24, p. 875-892.
- Honjo, S., Doherty, K.W., Agrawal, Y.C., and Asper, V.L., 1984, Direct optical assessment of large amorphous aggregates (marine snow) in the deep ocean: *Deep Sea Research I*, v.

- 31, p. 67-76.
- Jackson, G.A., 1990, A model of the formation of marine algal flocs by physical coagulation processes: *Deep Sea Research*, v. 37, p. 1197-1211.
- Jackson, 2001, Effect of coagulation on a model planktonic food web: *Deep Sea Research I*, v. 48, p. 95-123.
- Lampitt, R.S., 1996, Snow Falls in the Open Ocean, in Summerhayes, C.P., and Thorpe, S.A., eds., *Oceanography - An Illustrated Guide*: London, Manson Publishing, p. 96-112.
- MacIntyre, S., Alldredge, A.L., and Gotschalk, C., 1995, Accumulation of marine snow at density discontinuities in the water column: *Limnology and Oceanography*, v. 40, p. 449-468.
- McCave, I.N., 1975, Vertical flux of particles in the ocean: *Deep Sea Research I*, v. 22, p. 491-502.
- McCave, I.N., Hall, I.R., Antia, A.N., Chou, L., Dehairs, F., Lampitt, R.S., Thomsen, L., van Weering, T.C.E., and Wollast, R., 2001, Distribution, composition and flux of particulate material over the European margin at 47°-50°N: *Deep Sea Research II*, v. 48, p. 3107-3139.
- McPhee-Shaw, E.E., and Kunze, E., 2002, Boundary layer intrusions from a sloping bottom: A mechanism for generating intermediate nepheloid layers: *Journal of Geophysical Research*, v. 107, p. 3-1 - 3-15.
- McPhee-Shaw, E.E., Sternberg, R.W., Mullenbach, B., and Ogston, A.S., submitted, Observation of intermediate nepheloid layers on the Northern California continental margin: *Continental Shelf Research*.
- Müller, T.J., and Siedler, G., 1992, Multi-year current time series in the eastern North Atlantic Ocean: *Journal of Marine Research*, v. 50, p. 63-98.
- Nixon, S., and Thomas, A., 2001, On the size of the Peru upwelling ecosystem: *Deep-Sea Research Part I*, v. 48, p. 2521 -2528.
- Nowald, N., 1999, Die Erfassung der vertikalen Verteilung partikulären Materials im Ozean mit Hilfe von Kamerasystem und digitaler Bildanalyse [Diploma thesis]: Bremen, University of Bremen.
- Nowald, N., Ratmeyer, V., and Wefer, G., submitted, The vertical distribution of particulate matter in the upwelling system off Cape Blanc (NW-Africa) and implications for rapid, vertical mass transfer.
- Pilskaln, C.H., Lehmann, C., Paduan, J.B., and Silver, M.W., 1998, Spatial and temporal dynamics in marine aggregate abundance, sinking rate and flux: Monterey Bay, central California: *Deep Sea Research II*, v. 45, p. 1803-1837.
- Ratmeyer, V., and Wefer, G., 1996, A high resolution camera system (ParCa) for imaging particles in the ocean: System design and results from profiles and a three-month deployment: *Journal of Marine Research*, v. 54, p. 589-603.
- Shanks, A.L., 2002, The abundance, vertical flux, and still-water and apparent sinking rates of marine snow in a shallow coastal water column: *Continental Shelf Research*, v. 22, p. 2045-2064.
- Shanks, A.L., and Trent, J.D., 1980, Marine snow: sinking rates and potential role in vertical flux: *Deep Sea Research I*, v. 27A, p. 137-143.
- Silver, M.W., Coale, S.L., Pilskaln, C.H., and Chavez, F.P., 1998, Exploratory observations of marine aggregates at sub-euphotic depths: *Deep Sea Research II*, v. 45, p. 1839-1861.
- Syvitsky, J.P.M., Asprey, K.W., and Leblanc, K.W.G., 1995, In-situ characteristics of particles settling within a deep-water estuary: *Deep Sea Research II*, v. 42, p. 223-256.
- Tanaka, Y., 2003, Coccolith fluxes and species assemblages at the shelf edge and in the Okinawa Trough of the East China Sea: *Deep Sea Research II*, v. 50, p. 503-511.
- Tengberg, A., Almroth, E., and Hall, P., 2003, Resuspension and its effects on organic carbon

- recycling and nutrient exchange in coastal sediments: in situ measurements using new experimental technology: *Journal of Experimental Marine Biology and Ecology*, v. 285-286, p. 119-142.
- Thomsen, J., 2003, The benthic boundary layer, *in* Wefer, G., Billet, D., Hebbeln, D., Jorgensen, B.B., Schlüter, S., and van Weering, T.C.E., eds., *Ocean Margin System: Berlin Heidelberg New York, Springer Verlag*, p. 143-155.
- Thomsen, L., and Gust, G., 2000, Sediment erosion thresholds and characteristics of resuspended aggregates on the western European continental margin: *Deep Sea Research I*, v. 47, p. 1881-1897.
- Thomsen, L., and van Weering, T.C.E., 1998, Spatial and temporal variability of particulate matter in the benthic boundary layer at the N.W. European Continental Margin (Goban Spur): *Progress in Oceanography*, v. 42, p. 61-76.
- Thomsen, L., van Weering, T.C.E., and Gust, G., 2002, Processes in the benthic boundary layer at the Iberian continental margin and their implication for carbon mineralization: *Progress in Oceanography*, v. 52, p. 315-329.
- Umbugh, S.E., 1998, *Computer vision and image processing*: Upper Saddle River, NJ 07458, Prentice-Hall, Inc., 504 p.
- Walsh, I.D., and Gardner, W.D., 1992, A comparison of aggregate profiles with sediment trap fluxes: *Deep Sea Research I*, v. 39, p. 1817-1834.
- Weaver, P.P.E., Wynn, R.B., Kenyon, N.H., and Evans, J., 2000, Continental margin sedimentation, with special reference to the north-east Atlantic margin: *Sedimentology*, v. 47, p. 239-256.

**3.3 Observation of accumulation of marine particulate matter
at the lower boundary of the mixed layer off
NW-Africa (20°49'N / 17°58'W)**

submitted to Marine Geology

Nicolas Nowald, Volker Ratmeyer and Gerold Wefer

University of Bremen, Department of Geosciences, Klagenfurterstrasse, 28359 Bremen

Abstract

A profiling camera system and ROV mounted video devices were used for observations on the sinking behaviour and distribution of marine particles at a station off Cape Blanc (NW-Africa). The horizontal distribution of marine particles was obtained along short transects (8 - 20 m) in a particle minimum zone around 100 m and in a particle maximum layer at 175 m depth. No significant changes with respect to the horizontal distribution of spherically shaped particles were observed along the transects in the depths of investigation. In contrast, the abundance of large, coagulated aggregates known as “Stringers”, was of a distinct patchy nature. Thus, the conditions for the formation of large aggregates in the same water depth must differ on short spatial scales. We observed significant differences in the sinking behaviour and speed of particles in different water depths. Particles observed in the concentration minimum around 100 m, showed a clear vertical settling direction. In contrast, particles observed in the maximum layer around 175 m showed almost no motion or vertical sinking. Aggregates of different sizes showed a neglectable vertical offset during the observation period. Hence, particulate matter is accumulated in this specific water depth by factors, which significantly reduced the settling speed of marine aggregates. Gradients in the density structure are a possible mechanism, but could not be clearly identified as accumulation cause.

1. Introduction

In-situ observations of marine particulate matter in the oceans are primarily undertaken with aid of optical methods such as camera systems. The advantages of optical methods lie in their non-destructive nature, enabling investigators to study marine particles in their natural environment. Studies on marine aggregates using for instance profiling camera systems were carried out in almost any part of the worlds oceans like the Monterey Bay (Honjo et al., 1984), the Equatorial Pacific (Walsh et al., 1997) or the Mediterranean Sea (Gorsky et al., 1992). One of the major results of these studies is the fact that particulate matter is not evenly distributed in the water column. Highest concentrations are usually found in the upper water column and are related to the primary production conditions in the surface waters. However, lateral advected material from the upper slope areas towards the open ocean was reported to be an important factor increasing particle concentrations in the midwater column significantly (Gardner and Walsh, 1990). The processes generating particle abundance patterns in the oceans are still not clearly understood.

The rates, at which marine particles settle through the water column, are of special importance. The necessity of knowing accurate sinking rates are important for the quantification of the amount of organic matter transferred from the upper ocean surface to the deep-sea. With the deployment of sediment traps, sinking velocities could be estimated by the time the material needs to settle from the upper trap to the lower ones. The calculated settling rates underlie strong variations. Shanks and Trent (1980) estimated sinking rates of 60 m day^{-1} while for instance Wefer and Fischer (1993) calculated speeds to up to 2000 m day^{-1} . In-situ measurements of settling velocities were accomplished by Scuba dives. Mean settling velocities of $74 \pm 39 \text{ m d}^{-1}$ and $117 \pm 56 \text{ m d}^{-1}$ were observed by Alldredge and Gotschalk (1988) and Alldredge and Gotschalk (1989) in the Monterey Bay, respectively. Studies below depths accessible for divers were presented by Pilskaln et al. (1998) using Remotely Operated Vehicle (ROV) technologies.

In this study, we deployed a vertically profiling camera system in combination with a 1000 m depth diving ROV. Apart from the vertical distribution, horizontal transects were accomplished with the ROV to obtain information about the horizontal abundances of marine particles. Another focus was laid on observations of the settling behaviour of particles. These observations were likewise made using the ROV.

2. Methods

2.1 Study site

Camera system and ROV were deployed during the RV METEOR M58-2b cruise in May 2003. The presented datasets are from station GeoB 8630, located approximately 70 km off Cape Blanc/Mauritania at $20^{\circ}49'N/17^{\circ}58'W$ (Fig. 1). The investigation site is located within the highly dynamic and complex upwelling belt at a water depth of 1322 m on the midslope. The area is characterised by intense upwelling throughout the year (Nykjaer and Van Camp, 1994) with chlorophyll concentrations far above 1 mg m^{-3} , classifying it as a high productivity area (Carr, 2002; Nixon and Thomas, 2001).

2.2 Deep-sea particle camera ParCa

ParCa was developed after similar, profiling camera systems used by Honjo et al. (1984) or Asper (1987) to obtain the vertical distribution of particulate matter in the entire water column. A perpendicular to the camera system mounted strobe fires a collimated lightbeam, illuminating a known sample volume. In addition ParCa is equipped with a

SeaBird SBE 19 CTD probe. A detailed system description is given in Ratmeyer and Wefer (1996).

Data extraction was provided by digital image analysis software and particulate matter on the images was divided into two classes. The first class are comparably small, spherically shaped particles and the second class are large coagulated aggregates, known as “Stringers” (Shanks, 2002; Syvitsky et al., 1995). Both categories were regarded as two different particle populations. We refer to Nowald et al. (submitted) for detailed description of extractable particle parameters and classifications.

The camera system was deployed during nighttimes before the ROV dive. After recovery of the camera, images were evaluated and particle datasets extracted from the frames. On basis of the particle concentration profile, depths of interest were determined in which the ROV should operate.

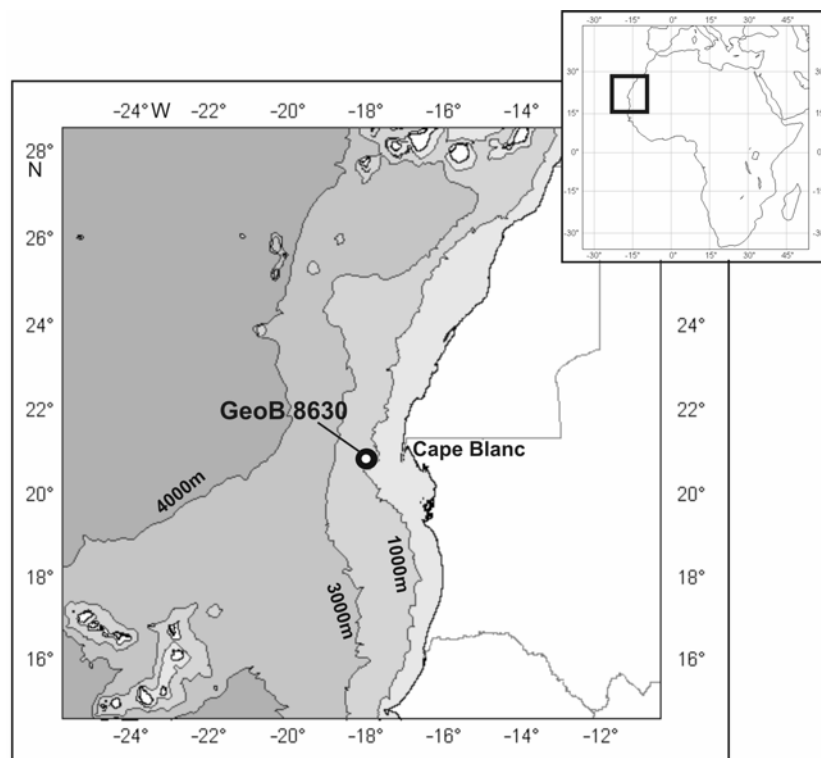


Fig. 1: Map of the study site GeoB 8630, located in ~1300 m water depth off Cape Blanc / Mauritania

2.3 Remotely Operated Vehicle “Cherokee”

The “Cherokee” ROV is a commercially available vehicle, with a maximum diving depth of 1000m (Fig. 2). Dimensions are 140 x 90 x 80 cm (L x W x H) and weight in air is ~250 kg. The ROV has a payload 50 kg and is equipped with common devices such as

hydraulic manipulators and sonar systems. In addition to a standard TV camera, two pencil cameras were mounted onto a second pan & tilt unit, providing real 3D vision via a “Head Mounted Display”. Although no absolute distances and sizes were measured with the 3D system, it proved to be very valuable in observing 3D spatial distribution of particles in the field of view. Video images of the camera systems were stored on MiniDV tapes.

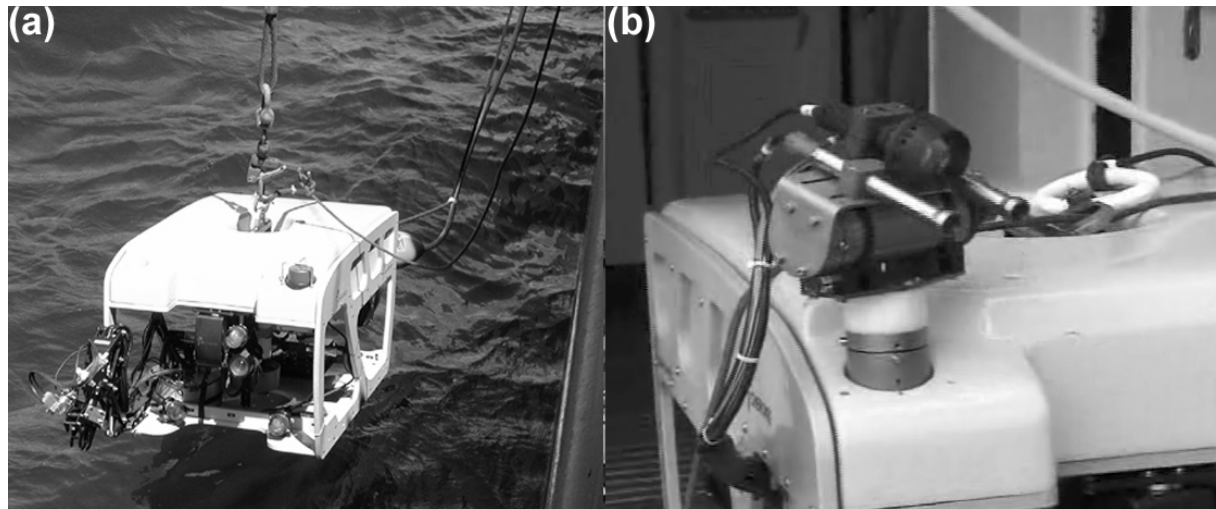


Fig. 2: The Cherokee ROV during deployment (a) and the stereoscopic camera system mounted onto a pan & tilt unit with additional headlight on top (b)

2.3.1 Horizontal distribution of marine particles

To obtain the horizontal distribution of particulate matter, the ROV was manoeuvred horizontally at low speeds in several depths of interest. The pan & tilt unit of the 3D cameras was positioned that camera heading was approximately 25° from ROV heading. This setup turned out to be the best way, tracking particles from a moving platform. Cruising velocity was around 0.5 m s^{-1} . Transect lengths varied according to the cruising speed between 8 m and 20 m. Single frame grabs from the video sequences were made in one second intervals along the transect. Afterwards, a region of interest (ROI) was determined within the frames, in which particle and aggregate abundances were measured. The ROI was identical within all frame grabs for all presented horizontal transects to provide comparable results (Fig. 3).

2.3.2 Observations on the sinking behaviour of particulate matter

We applied two methods for investigations on the sinking behaviour of particulate matter. In the first method, particles were observed along the transects and the relative change in X and Y coordinates on the frames with time was tracked. Frame grabs were made in $\frac{1}{4}$

second intervals from the video sequences. ROV speed was estimated to be around 0.5 m s^{-1} . Quantitative measurements of sinking velocities and size calibrations were not possible with the described system configuration, however differences in the sinking trajectories between different particles could be measured. While no information about the sample volume was available, each frame was divided into 28 X-axis and 24 Y-axis units. Apart from tracking the particles X-Y coordinates, their contours as well as their apparent diameters were extracted by the image analysis software from each frame and transferred to a new image (Fig. 4). The idea behind extracting the apparent diameter was to confirm that some particles sink relatively faster than others. A particle moving straight towards the camera should increase more rapidly in size with time, than particles sinking predominantly vertically.

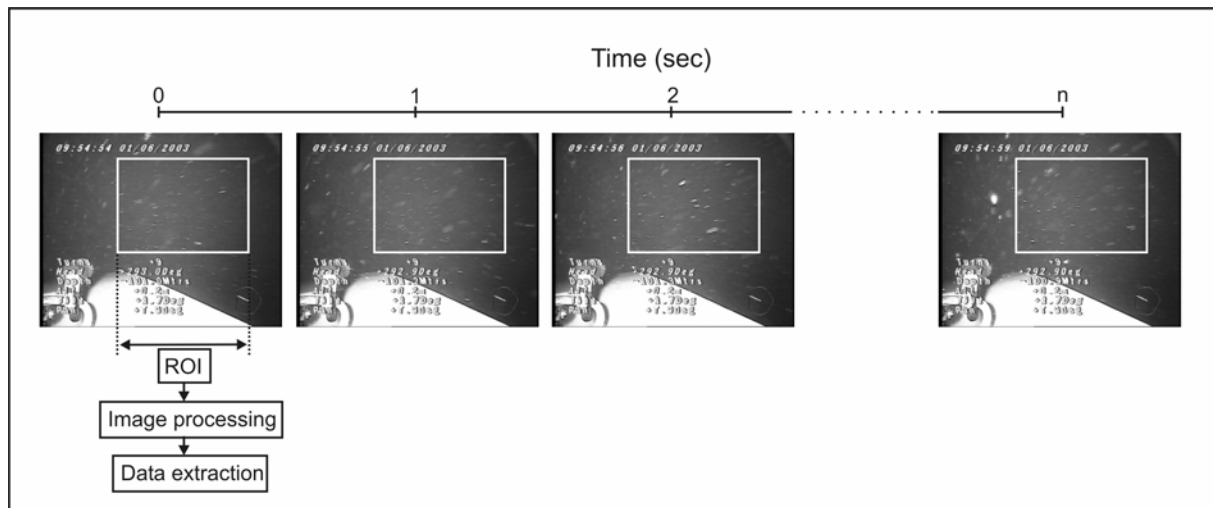


Fig. 3: Extraction of particle abundances along the horizontal transects. Single frames were grabbed in 1 second intervals from the video sequences. The numbers of particles were extracted from a region of interest (white square) within the frame

In a second method, the ROV was approaching several aggregates at very low speeds. Although the vehicle is equipped with an Auto-Depth function, smaller undulations and movements of the ROV in the vertical and horizontal could not be prevented. We tracked large aggregates, which distances to the 3D cameras were almost identical. Each aggregate was marked with one predicate point, for instance the lower boundary of a spherical particle forming the aggregate. In the next step, the X and Y coordinates of these predicate points of both aggregates were extracted. The difference in vertical of the frame (Y-Axis) between the two points is called ΔY . ΔY should change with time in case one of the aggregates sinks relatively faster compared the other (Fig. 5). Due to the lack of an accurate size calibration,

we tried to use the ROV frame, other parts of the vehicle and our experiences with aggregates to estimate the size of the observed aggregates. The error in these size estimations might be considerably high but however, a changing ΔY with time can definitely be measured. Thus, even without a correct size calibration, statements concerning the sinking behaviour of the observed aggregates are possible.

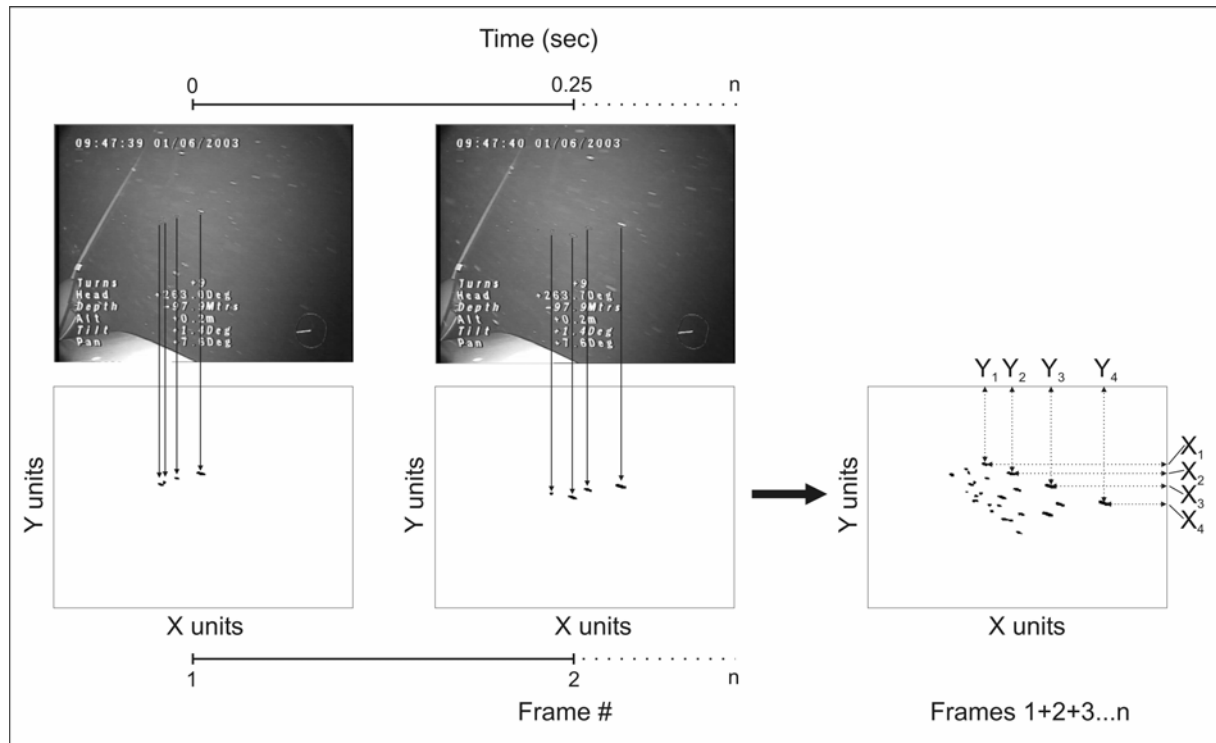


Fig. 4: Particle trajectories, for observations on the sinking behaviour of particulate matter, were created by extracting the X and Y coordinates of several particles of interest from frames obtained in 1/4 second intervals. The X and Y coordinates of all tracked particles from each frame were transferred to a new image while size and shape of the tracked particles were extracted as well.

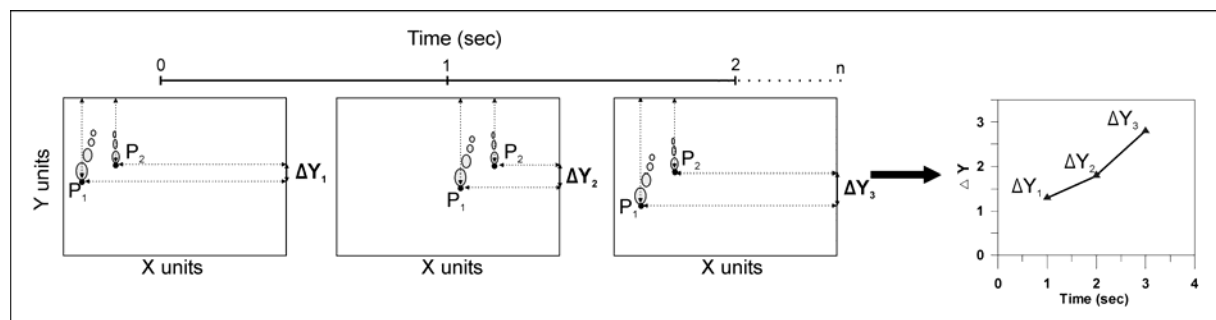


Fig. 5: A second method for studying the sinking behaviour of particulate matter was applied by measuring the distance between two predicate points (P1 and P2) of two neighbored aggregates over several seconds. The distance between P1 and P2, called ΔY , should increase or decrease with time, in case one of the two aggregates sinks faster or slower, respectively.

3. Results

3.1 Vertical distribution of particulate matter (Particle Camera)

The upper 200 m of the water column are characterised by significant changes with respect to the abundance of spherically shaped particles. Concentrations of 200 n l^{-1} are found in the very ocean surface around 40 m depth. Lowest particle concentrations are observed at 100 m depth with abundances of less than 30 n l^{-1} , which we will refer to as the particle minimum zone in the following chapters. Highest numbers of particles are measured at 175 m reaching more than 250 n l^{-1} , which we called the particle maximum zone or layer. Below this particle maximum particle abundances decrease constantly down to 1200 m and begin to increase in the benthic boundary layer 100 m above the seafloor, reaching concentrations of 125 n l^{-1} .

Highest abundances of large, coagulated aggregates (4 n l^{-1}) were observed around 175 m depth, which coincides well with the particle maximum (Fig. 6 a-b). A surprising result is that large, coagulated aggregates are not abundant above 175 m, although they can be found anywhere below this depth. In the remaining water column aggregates are detected with concentrations between 1 and 2 n l^{-1} .

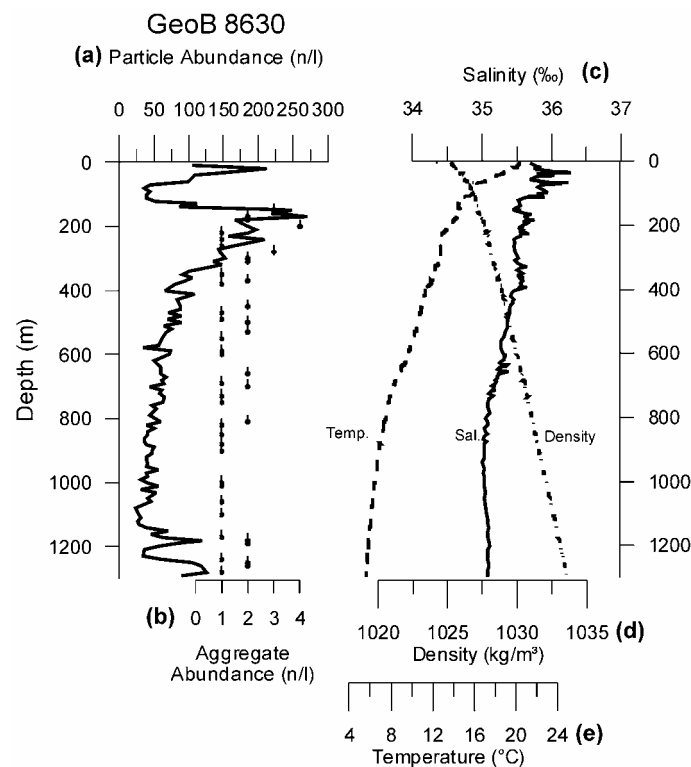


Fig. 6: Camera and CTD profile from site GeoB 8630. Particle concentrations underlie significant changes in the upper 200 m of the water column (a). Large, coagulated aggregates (Stringers) are not observed above this depth (b). The ROV was deployed in 100 m, in the particle minimum zone and around 175 m, in the particle maximum layer.

3.2 CTD Data

The temperature (Fig. 6e) and density (Fig. 6d) profiles show typical progression curves. Between 20 m and 80 m depth temperature is reduced from 20° C down to 15° C. Below 80 m temperature decreases constantly reaching a minimum value of 5° above the seafloor. Distinct changes in the density especially below 100 m are not visible. The salinity profile however (Fig. 6c), is characterised by several areas where the salt content of the ocean water is significantly changing. Changes in the salinity are well visible between 20 m and 100 m water depth and vary between 35,7 ‰ and 36,6 ‰. Two more anomalies are observed between 160 m and 230 m and between 320 m and 400 m with salinities around 35,7 ‰.

3.2 Horizontal distribution of particulate matter (ROV)

We present data from 4 transects (T-I – T-IV) obtained in two different water depths. Transect length are estimated to range between 8 – 20 m. Transects I and II are from 100 m depth located in the particle minimum, while transects T-III and T-IV are from 175 m within in the particle maximum zone.

The concentration of spherically shaped particles along transects T-I and T-II obtained in the minimum are between 55 n ROI⁻¹ [means 55 particles per Region Of Interest] and 15 n ROI⁻¹ (Fig. 7 a-b). Both transects show comparable mean concentrations between 30 n ROI⁻¹ and 25 n ROI⁻¹, respectively. Increased numbers of spherical particles were observed at for instance second #26 (52 n ROI⁻¹) or #34 (45 n ROI⁻¹) along transect T-I while comparable concentrations peaks could not be observed along transect T-II. While the vertical camera profile did not acquire any large, coagulated aggregates above 175 m water depth, a total of three aggregates could be counted along transect T-I. Transect T-II however, is characterised by an absence of any of these large aggregates.

Abundances of spherically shaped particles along transect T-III and IV obtained in the concentration maximum at 175 m depth are twice as high compared to those in the minimum (Fig. 7 c-d). The increased abundances in this water depth, coincides well with the observed increased concentrations obtained with the profiling camera system. Mean concentrations are around 60 n ROI⁻¹ along both transects. Transect T-IV shows a peak at second #4, which is related to a huge aggregate, composed of at least 60 single particles (Fig. 7 d). We would estimate the diameter of this huge aggregate to at least 40 cm. Large, coagulated aggregates are found in increased numbers along transect T-IV. A total of 7 aggregates were observed along the 14 second lasting transect T-IV. In comparison only 5 large aggregates were observed along transect T-III although observation time is three times higher.

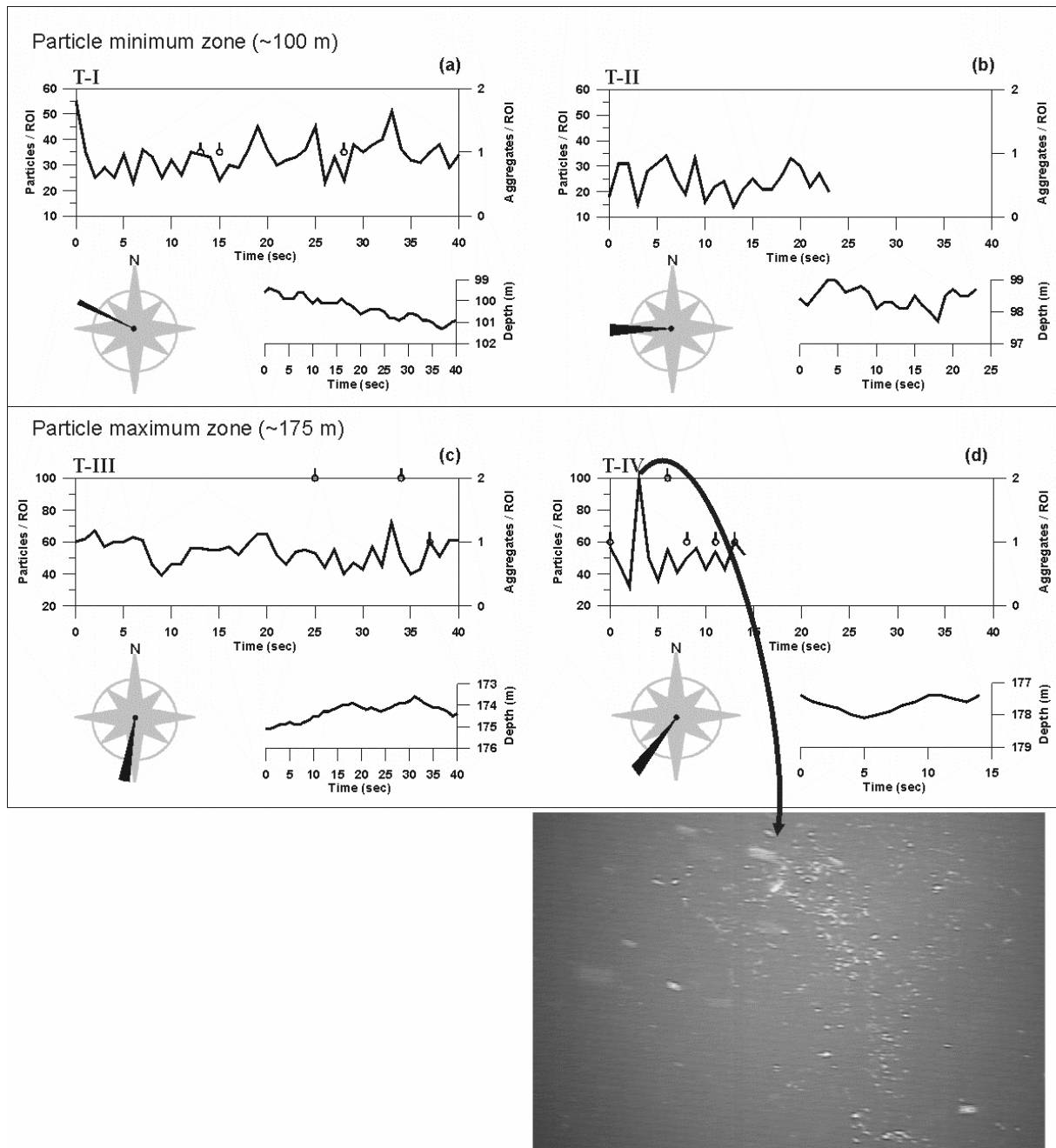


Fig. 7: Abundance of spherically shaped particles (solid lines) and large, coagulated aggregates (drops) along 4 transects in 100 m and 175 m depth. While no significant changes are observed in the horizontal distribution of spherically shaped particles, the abundance of large coagulated aggregates is of a distinct patchy nature. An extremely huge aggregate of ~40 cm in length was observed along transect T-IV. ROV heading and depth are shown for each transect below the abundance plots.

3.3 Sinking behaviour of particulate matter (ROV)

3.3.1 Particle minimum zone (100 m)

Fig. 8 a-b show particle trajectories from the particle minimum zone at 100 m depth. The trajectories of slow sinking particles (dashed lines) are more or less parallel. This is

expected when objects pass a camera and thus, these particles are sinking at more or less the same rate. The consistent changes in the vertical axis of the trajectories (Y) are not related to a

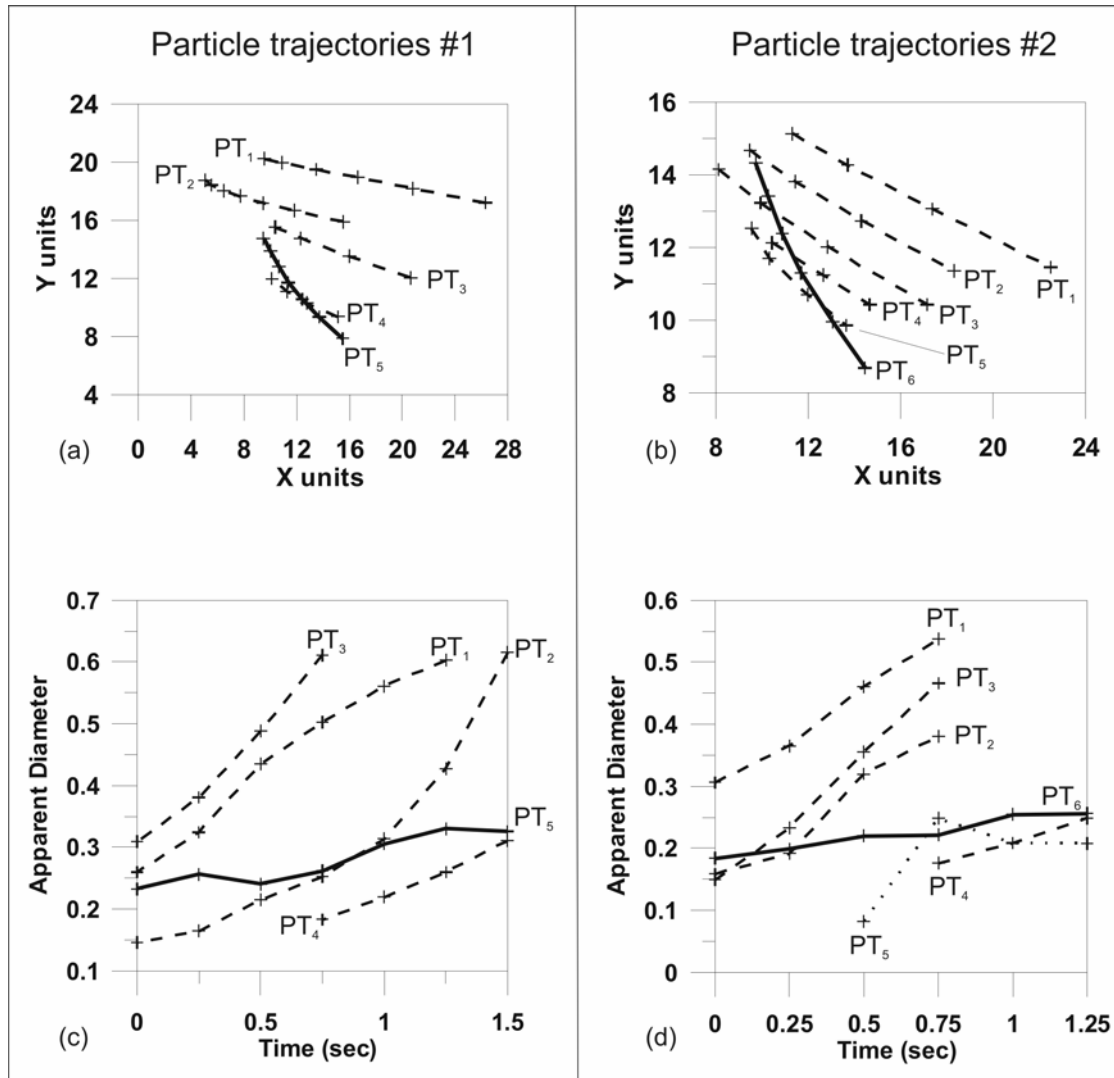


Fig. 8: Particle trajectories from the particle minimum zone at 100 m depth. Most particle trajectories run parallel (dashed lines) which means, they sink at more or less the same rate. Particle trajectories in solid lines are sinking relatively faster, crossing the trajectories of the remaining particles (a-b). This is underlined by the increasing apparent diameters of the tracked particles with time. The apparent diameters of particles with a preferred vertical sinking direction (solid lines), should increase in time more slowly (c-d).

real sinking of the single particles, but to the slight vertical movement of the ROV. However, there are particles, which sink relatively faster than others. This is shown in Fig. 8 a-b. The trajectories of the faster sinking particles (Fig. 8 a-PT₅, Fig. 8 b-PT₆) plotted in solid lines, cross the trajectories of the slower settling particles. The different trajectories are related to different settling speeds. They are not the result of a perspectival or optical effects, as shown when plotting the apparent diameter versus time (Fig. 8 c-d). Particles moving towards

the camera are supposed to increase in size with time. This is applicable for the slow sinking particles (Fig. 8 c-PT₁₋₄, Fig. 8d-PT₁₋₄) plotted in dashed lines. Particles with a predominantly vertical sinking direction should increase in size significantly slower. The apparent diameters of the fast, predominantly vertically sinking particles (Fig. 8 c-PT₅, Fig. 8d-PT₆) increase slower than those of the slower settling ones. There is one exception in Fig. 8 d. The apparent diameter of particle PT₅ shown in dotted lines appears to remain constant above the time stamp of 0.75 seconds. A closer look at the images of this sequence revealed that this particular particle obviously rotated along its Y-axis. The dimensions of this particle along its X-axis turned out to be irregular and above 0.75 seconds, a shorter extension of the X-axis faced the camera. This explains why the apparent diameter of this particle is not increasing in size in the same way as the remaining particles.

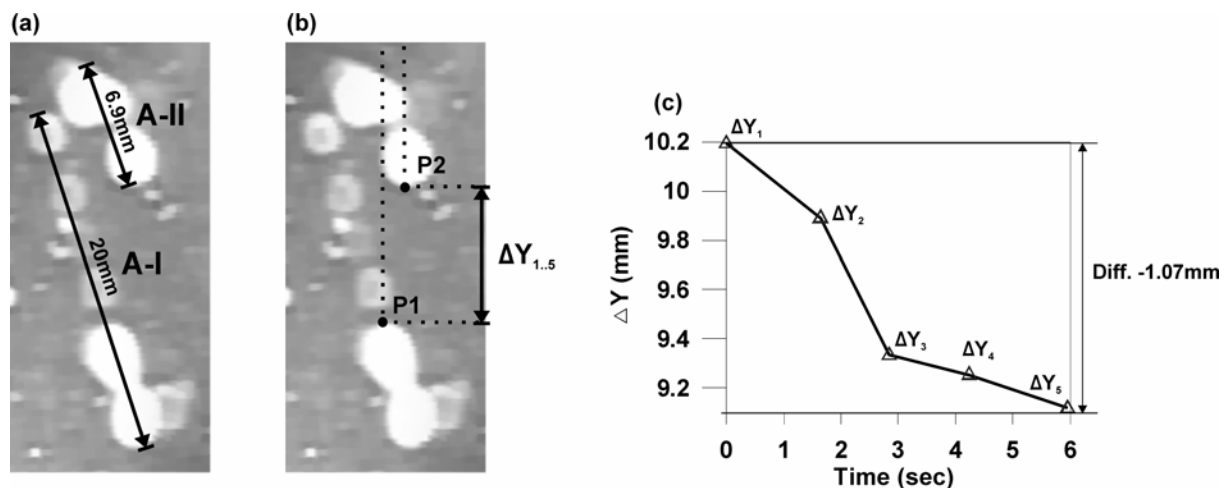


Fig. 9: This aggregate observation from the particle maximum layer (175 m depth) shows a small aggregate (A-II), settling relatively faster than a large aggregate (A-I). The distance between the two predicate points P1 and P2 (ΔY) decreases during the observation period.

3.3.2 Particle maximum zone (175 m)

In the previous section, we described that we were able to track sinking trajectories of particulate matter in the particle minimum zone. In contrast, similar observations of sinking particles could not be made in the particle maximum layer around 175 m. The first impression of all observers present in the ROV control room was that particles were absolutely motionless compared to the particle minimum zone. The massive accumulation of material in this specific part of the water column might imply that differences in the settling speeds of particles of different sizes must be considerably low or maybe equal. One example is shown in Fig. 9 a-b. We estimated the size of Aggregate I (A-I) to 20 mm, resulting in a length of 6.9

mm for Aggregate II (A-II). This size calibration was accounted to all 5 frames, grabbed from the video sequence in a time window of ~6 seconds. The X and Y coordinates of the predicate points P1 and P2 were extracted from all frames for the duration of the observation. The vertical differences between P1 and P2 (ΔY) with time are presented in Fig. 9 c. From second 0 to second 2.84, ΔY decreases from 10.19 mm to 9.88 mm, down to 9.33 mm. ΔY remains almost constant between second 2.84 and 5.96 mm. Overall, the distance between P1 and P2 is reduced by 1.07 mm within the 6 second observation period.

4. Discussion

Since the introduction of profiling camera systems, several studies were carried out in the world's ocean and improved our knowledge regarding the distribution of marine particles in the water column (Asper, 1987; Gardner and Walsh, 1990; Honjo et al., 1984; Ratmeyer and Wefer, 1996). One of the major outcoming of these studies is that particulate matter is not evenly distributed in the water column and a large variety with respect to the vertical distribution of marine particles was reported. The vertical distribution of particulate matter obtained with the profiling camera system off Cape Blanc, coincides well with previous findings published in a previous paper (Nowald et al. submitted). The water column shows a tripartite classification, which is typical for this area. The upper mixed layer down to 200 m is characterised by rapid changes concerning the particle abundances with several, distinct particle maxima and minima. Below this depth, the numbers of particles decrease constantly down to above the seafloor where concentrations begin to increase again due to bottom near resuspension processes.

Little is known about the horizontal distribution of particles in specific water depths. Recent studies using AUV technology allowed horizontal transects at the kilometre scale. For example Cunningham et al. (2003) observed variations in the numerical density of common phytoplankton taxa south of the Isles of Scilly, located southwest off the British Islands. Along a 6 km transect in 9 m depth, an inversion in the abundances of phytoplanktonic organisms was observed approximately 2 km away from the initial deployment site of the AUV. The distribution of the phytoplankton community appeared quite erratical before and became more evenly after the point of inversion. Another AUV-based study from the Cape Cod Bays published by Yu et al. (2002) showed strong variations in the backscattering and chlorophyll fluorescence along different transects of >2 km length. These results show that differences in the horizontal distribution of for instance, the phytoplankton community or the abundance of suspended particles can underlie distinct changes in the kilometre scale.

Observations reported from transects in this study however, are in the range of several metres and can certainly not be compared with large distance transects. The described variations in the horizontal abundance of spherically shaped particles presented in this study (Fig. 7 a-d), might not be interpreted as signals but are presumably in the range of natural variations within this particle population.

While this conclusion is applied to the abundance of spherically shaped particles, this finding cannot be accounted to the distribution of large, coagulated aggregates. The distribution of these aggregates is of a distinct patchy nature. The profiling camera system did not acquire any aggregates above 175 m depth; nevertheless we found 3 aggregates along ROV transect T-I (Fig. 7 a) in 100 m water depth. This kind of inhomogeneous distribution becomes visible in the particle maximum zone at 175 m. The 40 second long transect T-III (Fig. 7 c) shows a smaller number of these aggregates than the 14 second long transect T-IV (Fig. 7 d). In this much shorter transect, we counted 6 stringers and one huge aggregate of probably 40 cm in diameter. While the spherically shaped particles are distributed more or less evenly on short spatial scales, large, coagulated aggregates appear in comparably large numbers within small areas along the horizontal transects.

It has become established that the production of particulate matter and phytoplankton growth in the surface water does not occur evenly (Bainbridge, 1957; Martin and Richards, 2001; Martin et al., 2001). Dense aggregation is often associated with increased particle abundances, which enhance the collision probability of particulate matter (Alldredge et al., 1993). Thus, it is surprising that no aggregates were observed with aid of the profiling camera system within the subsurface particle maximum around 40 m depth (Fig. 6 a). Although the particle abundance within the second particle maximum at 175 m is just 50 n l^{-1} higher, we measured far higher aggregate concentrations between $3\text{-}4 \text{ n l}^{-1}$ (Fig. 6 b). An explanation could be that there are no large aggregates in the surface particle maxima at 40 m, or the camera simply “missed” them because of their inhomogeneous distribution. The first case appears very unlikely because previous studies (Nowald et al., submitted) show that large stringers are ubiquitous in the surface waters in the Cape Blanc region. In addition, the presence of large aggregates above 175 m was proven along horizontal transect T-1 in 100 m depth, where a total of three large aggregates were observed (see above). Thus, the observed intermittencies in the abundance of large coagulated aggregates down to 175 m are probably related to their patchy distribution.

The particle maximum layer around 175 m is of special interest. Highest particulate matter concentrations are observed in this subeuphotic depth and not in the surface waters,

where particulate matter is usually formed. Such an increase in the particle and large aggregate concentrations below the euphotic zone cannot be explained by phytoplanktonic growth. A more suitable explanation for such a distinct particle maximum is the accumulation of particulate matter in this specific depth. Accumulation is preferably achieved by processes, which significantly reduce the sinking velocities of particles. The presented datasets show that particles sink with different velocities in different water depths. Within the particle minimum zone around 100 m we observed particles sinking relatively faster compared to the remaining particles in the video sequence (Fig. 8 a-d). At 175 m water depth however, a vertical movement of the material could hardly be measured (Fig. 9 a-c). There are only a few studies, which describe a relationship between size and settling speed. Such functions were published for instance by Alldredge and Gotschalk (1988, 1989) or Pilskaln et al. (1998). As a “back of the envelope” calculation, we applied these functions to the sizes of our observed aggregates in 175 m depth. The results are presented in Table 1 and Fig. 10. The distance between P1 and P2 (ΔY) measured in this study decreases constantly. The resulting total vertical difference between P1 and P2 during the observation time of 5.96 seconds is -1.07 mm. According to Alldredge and Gotschalk (1989), ΔY would increase with time to a total difference of 6.35 mm between P1 and P2 within the observation period. Comparable size/sinking rates were computed after Alldredge and Gotschalk (1988) and Pilskaln et al. (1998). ΔY increases likewise with time, resulting in a difference between P1 and P2 of 1.78 mm and 1.84 mm respectively. Compared to these calculations, we observed a smaller aggregate sinking faster than a large aggregate.

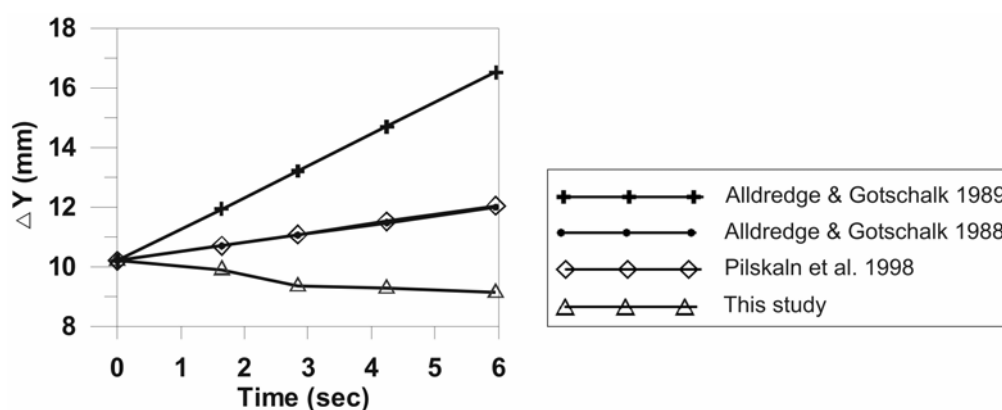


Fig. 10: According to size/sinking rate relationships from the literature, ΔY is supposed to increase with time. Our in-situ observations from the particle maximum zone at 175 m depth show the opposite trend (see also Fig. 9).

Different sinking velocities of particles of same sizes was reported by Pilskaln et al. (1998). Particles of sizes classes 0.5 - < 1.0 mm for instance, sank at a rate of 0.12 mm s^{-1} in a water depth of 200 m and with 0.26 mm s^{-1} at 500 m. The authors relate the differences in the sinking velocities to gradients in the density structure of the water column. Marine particles settling from a lower dense layer into a higher dense pycnocline were reported to accumulate

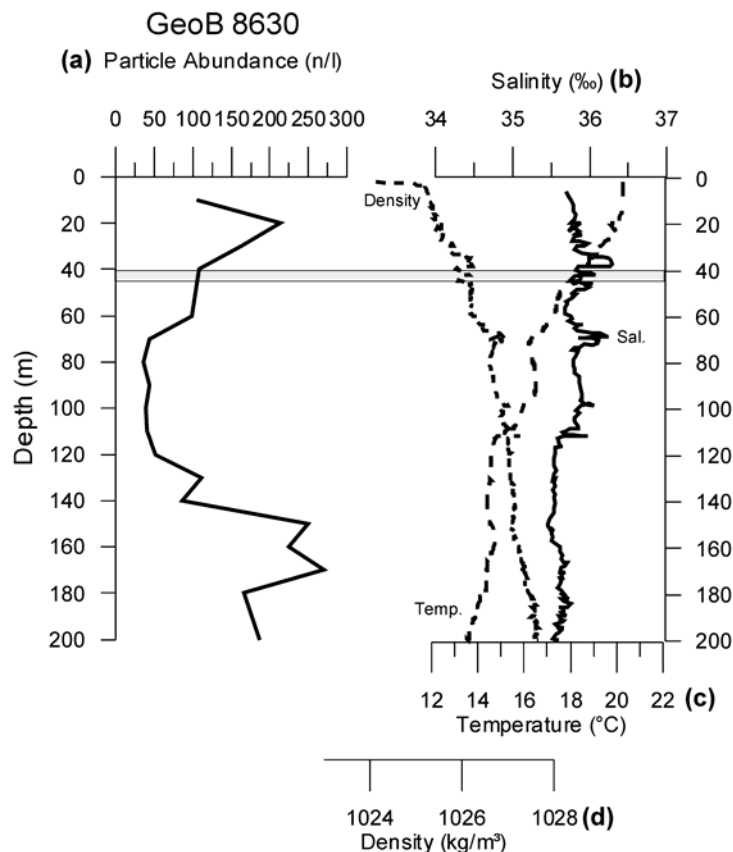


Fig. 11: Accumulation of marine particles is often associated with changes in the density structure of the water column. This might be accounted to the upper particle maximum at 20 m depth. An abrupt change in the density is observed 20 m below this maximum. Similar can not be accounted to the second particle maximum layer at 175 m depth, where changes in the density can not be observed.

within the transition zone (Gorsky et al., 1992; MacIntyre et al., 1995), especially if these particles are occupied by certain amounts of mucus (Alldredge and Crocker, 1995). Different density layers are predominantly found in the upper water strata in comparison to the midwater column (Pilskaln et al., 1998). The authors explained the higher sinking velocities around 500 m by the absence of such distinct density layers below 200 m. On the basis of the CTD profile obtained at site GeoB 8630, it is difficult to assert in how far this can be accounted to our observations. An increase in the density can be observed around 40 m depth

(Fig. 11 d, shaded area) below the first particle maximum. There might be a connection between the physical properties of the water column and the increased particle concentrations around 20 m. Similar cannot be observed for the particle maximum zone around 175 m depth and a connection is not clearly visible. Perhaps the measurement resolution of the CTD probe used in this study is not sufficient to detect comparable density layers as for instance described by MacIntyre et al. (1995).

Table 1: Size/Sinking rate relationships from the literature applied to aggregates of different sizes (A-I, A-II) as observed around 175 m depth. According to these functions, large aggregates sink faster than small ones and the vertical difference (Vertical diff.) between the aggregates increase with time. This does not coincide with our in-situ observations. The smaller aggregate A-II sinks faster than aggregate A-I, resulting in a decreasing vertical distance between the aggregates (see also Fig. 9).

Study /Author	Function A-I X = 20 A-II X = 6.9	Sinking Speed A-I (mm/s)	Sinking Speed A-II (mm/s)
		/ Settling distance during 5.96 seconds (mm)	/ Settling distance during 5.96 seconds (mm)
(a) Alldredge & Gotschalk (1988)	$50 \cdot X^{0.26}$	1.26	0.96
		/	/
(b) Alldredge & Gotschalk (1989)	$8.4 \cdot X^{0.95}$	7.5	5.72
		/	/
(c) Pilskaln et al. (1998)	$2.09 \cdot X + 17.12$	1.67	0.61
		9.95	3.63
		0.68	0.37
		/	/
		4.05	2.2

Study	(a) Alldredge & Gotschalk (1988)	(b) Alldredge & Gotschalk (1989)	(c) Pilskaln et al. (1998)	This study
Vertical diff.	1.78	6.35	1.84	-1.07

The accumulation of material in specific water depths might enhance the forming of large, coagulated aggregates via differential settlement. It is likely to assume that fast settling particles collide with the more or less motionless particles in the maximum zone. This process could result in increased abundances of large, coagulated aggregates as observed within the maximum layer at 175 m depth. Hence, the large, coagulated aggregates, which were acquired by our optical devices, are probably of two origins. The first population is formed in the very ocean surface and accumulated in the particle maximum zone on its descent to the sea floor. The second population is formed directly in the particle maximum zone by the vertical collision of material arriving from the ocean surface and already accumulated particles in the

maximum layer. This process might create huge aggregates as observed along the horizontal transect T-IV (Fig. 7 d).

It appears unlikely that aggregates of such size (40 cm in diameter) produced in the surface water, survive a descent of almost 200 m without being seriously fragmented by the physical, biological and chemical properties of the water column. We infer that these very large aggregates are preferably formed in the accumulation zone because of the excellent conditions for aggregation in these depths. Their role regarding the vertical flux is difficult to determine. It is questionable whether these extremely huge aggregates ever reach the sea floor as one formation. Possibly, these aggregates just bound large amounts of particles for an unknown period of time until they are fragmented, releasing the particles of which they formerly consisted of back to the ocean. We assume that they are a temporal apparition with no great significance for the vertical flux. Little is known about aggregates of such size. However, they might be compared with respect to their size, with discarded houses of larvaceans. As reported by Pilskaln et al. (1991), *Bathochordaeus* housings in the Monterey Bay can reach lengths of more than 90 cm. Their role in delivering organic matter to the deep-sea is discussed widely. While authors like Hamner and Robison (1992) report these housings to be a significant source, datasets presented by Silver et al. (1998) do not support similar assumptions.

5. Conclusions

The major outcomings of these studies can be summarised the following:

- 1.) With respect to their horizontal abundance, large, coagulated aggregates are distributed in a distinct patchy manner, while the abundance of small, spherically shaped particles do not significantly change.

- 2.) Marine particulate matter settles at changing rates in different water depths.

Our results show that the mechanisms, responsible for the vertical settling of marine particulate matter are not sufficiently understood. Pilskaln et al. (1998) and this study showed that particles can sink with different velocities in different water depths, other studies show a clear size/sinking rate relationship (Alldredge and Gotschalk, 1988, 1989) , no relationship between these two parameters at all (Diercks and Asper, 1997), or even ascending particulate matter (Azetsu-Scott and Passow, in press).

- 3.) The reduction of the settling speeds in the particle maximum zone results in an accumulation of material and enhanced aggregation processes due to differential settlement.

The process responsible for the accumulation of large amounts of material might be identified as changes in density gradients of the water column.

4.) In-situ sampling of individual aggregates in the water column and examinations on density, composition and sinking speeds in the future are inevitable for a better comprehension of particle dynamics in the oceans.

The presented datasets could be improved by better quantification methods. Unfortunately, we were not able to measure the sinking velocities in terms of distance per time unit. This is also true for the horizontal distribution of marine, particulate matter. We measured the abundance of particles in a region of interest (ROI) within the images but were not able to describe the concentration as numbers per litre. This can be achieved by modifications on the ROV in the future. However, the ROV deployments show the potential and possibilities of in-situ studies on marine aggregates in combination with vertically profiling systems, which will be continued in future field studies.

Acknowledgements

We thank the crew of the RV METEOR for their help in deploying and recovering the ParCa and ROV system. The manuscript greatly benefited from discussions with G. Fischer, U. Passow and T. Freudenthal. Many helpful comments from the reviewers helped to improve this manuscript.

The presented datasets are available in the PANGAEA database (<http://www.pangaea.de/>)

This study was funded by the “Deutsche Forschungsgesellschaft” (DFG) within the scope of the DFG Research Center Ocean Margins

References

- Allredge, A.L., and Crocker, K.M., 1995, Why do sinking mucilage aggregates accumulate in the water column?: *The Science of the Total Environment*, v. 165, p. 15-22.
- Allredge, A.L., and Gotschalk, C., 1988, In situ settling behaviour of marine snow: *Limnology and Oceanography*, v. 33, p. 339-351.
- Allredge, A.L., and Gotschalk, C., 1989, Direct observation of the mass flocculation of diatom blooms: characteristics, settling velocities and formation of diatom aggregates: *Deep Sea Research I*, v. 36, p. 159-171.
- Allredge, A.L., Passow, U., and Logan, B.E., 1993, The abundance and significance of a class of large, transparent organic particles in the ocean: *Deep Sea Research I*, v. 40, p. 1131-1140.
- Asper, V.L., 1987, Measuring the flux and sinking speed of marine snow aggregates: *Deep Sea Research I*, v. 34, p. 1-17.
- Azetsu-Scott, K., and Passow, U., in press, Ascending marine particles: Significance of transparent exopolymer particles (TEP=) in the upper ocean: *Limnology and Oceanography*.
- Bainbridge, R., 1957, The size, shape and density of marine phytoplankton concentration: *Biological Review*, v. 32, p. 91-115.
- Carr, M.-E., 2002, Estimation of potential productivity in Eastern Boundary Currents using remote sensing: *Deep-Sea Research Part I*, v. 49, p. 59-80.
- Cunningham, A., McKee, D., Craig, S., Tarran, G., and Widdicombe, C., 2003, Fine-scale variability in phytoplankton community structure and inherent optical properties measured from an autonomous underwater vehicle: *Journal of Marine Systems*, v. 43, p. 51-59.
- Diercks, A.R., and Asper, V.L., 1997, In situ settling speeds of marine snow aggregates below the mixed layer: Black Sea and Gulf of Mexico: *Deep Sea Research I*, v. 44, p. 385-398.
- Gardner, W.D., and Walsh, I.D., 1990, Distribution of macroaggregates and fine-grained particles across a continental margin and their potential role in fluxes: *Deep Sea Research I*, v. 37, p. 401-411.
- Gorsky, G., Aldorf, C., Kage, M., Picheral, M., Garcia, Y., and Favole, J., 1992, Vertical distribution of suspended aggregates determined by a new underwater video profiler: *Annales de l'Institut océanographique*, v. 68, p. 275-280.
- Hamner, W.M., and Robison, B.H., 1992, In situ observations of giant appendicularians in Monterey Bay: *Deep Sea Research*, v. 39, p. 1299-1313.
- Honjo, S., Doherty, K.W., Agrawal, Y.C., and Asper, V.L., 1984, Direct optical assessment of large amorphous aggregates (marine snow) in the deep ocean: *Deep Sea Research I*, v. 31, p. 67-76.
- MacIntyre, S., Allredge, A.L., and Gotschalk, C., 1995, Accumulation of marine snow at density discontinuities in the water column: *Limnology and Oceanography*, v. 40, p. 449-468.
- Martin, A.P., and Richards, K.J., 2001, Mechanisms for vertical nutrient transport within a North Atlantic mesoscale eddy: *Deep Sea Research II*, v. 48, p. 757-773.
- Martin, A.P., Richards, K.J., and Fasham, M.J.R., 2001, Phytoplankton production and community structure in an unstable frontal region: *Journal of Marine Systems*, v. 28, p. 65-89.
- Nixon, S., and Thomas, A., 2001, On the size of the Peru upwelling ecosystem: *Deep-Sea Research Part I*, v. 48, p. 2521-2528.
- Nowald, N., Ratmeyer, V., and Wefer, G., submitted, The vertical distribution of particulate matter in the upwelling system off Cape Blanc (NW-Africa) and implications for rapid, vertical mass transfer.

- Nykjaer, L., and Van Camp, L., 1994, Seasonal and interannual variability of coastal upwelling along northwest Africa and Portugal from 1981 to 1991: *Journal of Geophysical Research*, v. 99, p. 197-207.
- Pilskaln, C.H., Lehmann, C., Paduan, J.B., and Silver, M.W., 1998, Spatial and temporal dynamics in marine aggregate abundance, sinking rate and flux: Monterey Bay, central California: *Deep Sea Research II*, v. 45, p. 1803-1837.
- Pilskaln, C.H., Silver, M.W., Davis, D.L., Murphy, K.M., Gritton, B., Lowder, S., and Lewis, L., 1991, A quantitative study of marine aggregates in the mid-water column using specialised ROV instrumentation: *Proceeding Oceans*, v. 2, p. 1175-1182.
- Ratmeyer, V., and Wefer, G., 1996, A high resolution camera system (ParCa) for imaging particles in the ocean: System design and results from profiles and a three-month deployment: *Journal of Marine Research*, v. 54, p. 589-603.
- Shanks, A.L., 2002, The abundance, vertical flux, and still-water and apparent sinking rates of marine snow in a shallow coastal water column: *Continental Shelf Research*, v. 22, p. 2045-2064.
- Shanks, A.L., and Trent, J.D., 1980, Marine snow: sinking rates and potential role in vertical flux: *Deep Sea Research I*, v. 27A, p. 137-143.
- Silver, M.W., Coale, S.L., Pilskaln, C.H., and Steinberg, D.R., 1998, Giant aggregates: Importance as microbial centers and agents of material flux in the mesopelagic zone: *Limnology and Oceanography*, v. 43, p. 498-507.
- Syvitsky, J.P.M., Asprey, K.W., and Leblanc, K.W.G., 1995, In-situ characteristics of particles settling within a deep-water estuary: *Deep Sea Research II*, v. 42, p. 223-256.
- Walsh, I.D., Gardner, W.D., Richardson, M.J., Chung, S.P., Plattner, C.A., and Asper, V.L., 1997, Particle dynamics as controlled by the flow field of the eastern equatorial Pacific: *Deep Sea Research II*, v. 44, p. 2025-2047.
- Wefer, G., and Fischer, G., 1993, Seasonal patterns of vertical particle flux in equatorial and coastal upwelling areas of the eastern Atlantic: *Deep-Sea Research I*, v. 40, p. 1613-1645.
- Yu, X., Dickey, T.D., Bellingham, J., Manov, D., and Streitlien, K., 2002, The application of autonomous underwater vehicles for interdisciplinary measurements in Massachusetts and Cape Bays: *Continental Shelf Research*, v. 22, p. 2225-2245.

4. Summary of research

Manuscript 1

The vertical distribution of particulate matter in the upwelling system off Cape Blanc (NW-Africa) obtained by high-resolution camera profiles, and implications for rapid, vertical mass transfer

The deep-sea camera system ParCa was deployed on 6 occasions along 2 transects within the highly dynamic upwelling belt off Cape Blanc. Although all examined profiles show high particle abundances in the surface water ($\sim 100 \text{ n l}^{-1}$), differences in distribution and abundances are observed between the shallower profiles on the upper slope ($< 1000 \text{ m}$ depth) and the profiles on the midslope ($> 1000 \text{ m}$ depth).

Highest concentrations found at the midslope profiles are not observed in the very ocean surface as expected, but around 200 m depth ($\sim 200 \text{ n l}^{-1}$). The increased abundances of spherically shaped particles at the lower boundary of the mixed layer are related to the fragmentation of large coagulated aggregates. At the ocean surface, particulate matter is primarily bound into aggregates. On their descent, these aggregates disaggregate, releasing their components back into the water column, causing this peak around 200 m. The midslope profiles are characterised by a constant decrease of the particle concentration with depth, which are a direct result of the degradation and solubilisation processes in the midwater column.

Although the upper slope profiles show similar particle concentrations in the ocean surface as the midslope profiles, highest concentrations are observed above the seafloor in the benthic boundary layer. Current velocities on the upper slope are far more intense, compared to the deeper areas, resulting in an enhanced uplift of material from the ocean bottom. In comparison to the midslope profiles, the upper slope stations show far more complex distribution patterns, which is related to the interplay of shallower depth and intense current activity.

On the basis of the acquired profiles, two major transport mechanisms could be described. The standard situation is a continuous flux of material from the ocean surface to the seafloor. It is driven in the first instance by large, coagulated aggregates, which are found in the entire water column. Due to their size and relatively fast sinking rates, they deliver the majority of particulate matter to the seafloor. The second transport process are sinking events, where large amounts of material is delivered at once from the ocean surface to the deep-sea. This process is well visible in the alteration of the particle sizes. The sinking cloud scavenges

preferably small particles, because they are more abundant. The result is a depletion of the small size fraction above and a coarsening of the material within the sinking cloud. Discussed trigger processes are either the mass extinction after a phytoplankton bloom, or the input of higher dense wind transported dust from the continents.

Manuscript 2

The abundance and size of marine particles off the NW-African coast (Dakhla, Cape Bojador) and the detection of a massive lateral intrusion

In this study, the camera was deployed along two transects off Dakhla and Cape Bojador. The Dakhla transect is partly influenced by NW-African upwelling system. The Cape Bojador profiles are located outside, but parallel to the upwelling belt in a lower productive area.

Particles in the surface water decrease with increasing distance from the coast off Dakhla (110 n l⁻¹ coastal near, down to 30 n l⁻¹ further offshore). This is related to the decreasing primary production intensity with increasing distance from the coast, which is well reflected in the satellite derived chlorophyll pigment concentration. Along the Cape Bojador transect, particle concentrations in the ocean surface are similar around 30 n l⁻¹. Particle concentrations below the euphotic zone remain more or less constant along both transect.

Differences are found in the sedimentation patterns between Dakhla and Cape Bojador. The erratical and uneven particle size distribution in the water column off Dakhla are related to intense aggregation and disaggregation of the sinking material. This in turn, leads to differences regarding the total amount of material reaching simultaneously the ocean bottom, which is described as *patchy sedimentation*. In contrast, the Cape Bojador stations are characterised by an evenly pronounced sedimentation, which is seen in the even and homogenous, vertical size distribution. Particle fluxes and export rates are comparably low along both transects. The observed differences in the sedimentation patterns have no larger effect on the total flux in the Dakhla and Cape Bojador region. The difference is only seen in the way the material is delivered to the ocean bottom.

A paradoxum was found in the size and volumes of particulate matter in the surface water between both transects. Coagulated aggregates are significantly larger off Cape Bojador compared to Dakhla. In an area of increased primary production, smaller aggregates are found in comparison to a lower productive environment. This contradictory finding was explained by the longer retention time of the material in the ocean surface and reduced particle dynamics in lower productive parts of the ocean.

The manuscript focuses in detail on the intrusion of lateral advected material observed at site GeoB 7425. The intrusion was observed between 800 m and 1400 m depth at a total profile length of 1800 m. Particle concentrations within the lateral advected cloud are twice as high (60 n l^{-1}) compared to the surface concentration. Apart from this observation, the processes taking place when foreign material is shifted into a formerly undisturbed water column can be deduced from the size distribution. At the upper boundary of the intrusion, small particles are accumulated. This accumulation is related to the sheer processes occurring at the transition zone of water masses of different velocities. Additionally, the accumulation above the transition zone might be enhanced by differences in the density structure. An important transport process, which was often described on the basis of sediment trap studies, could be detected directly in the water column with aid of the ParCa system.

Manuscript 3

Observation of accumulation of marine particulate matter at the lower boundary of the mixed layer off NW-Africa ($20^{\circ}49'N / 17^{\circ}58'W$)

A ROV was used to study the horizontal distribution and sinking behaviour of marine particulate matter at a station off Cape Blanc.

The ParCa system was deployed before the ROV dive, to obtain the current particle distribution. On the basis of these data, depths of interest were determined in which the ROV should operate. The ROV was deployed in a particle minimum zone at 100 m and in a particle maximum around 175 m water depth. Horizontal transect were applied in both depth, showing lower concentrations in the particle minimum zone, compared to the maximum. This supports the profiling camera data to produce representative results. The horizontal variations in the particle abundances in both depths do not underlie significant changes on short spatial scales (8 – 20 m transect length).

The in-situ observations of the sinking behaviour of marine aggregates revealed that particles sink with different velocities in different depths. In the particle minimum zone around 100 m, particle trajectories showed particles sinking much faster than others. In comparison, almost no motion of any aggregate could be observed in the particle maximum zone around 175 m. Either, the aggregates sink at the same rate or the sinking velocities are significantly reduced. The latter is more obvious. The tracking of two aggregates of different sizes clearly showed a minor vertical offset during the time of the observation. When applying size/sinking rate relationships from the literature to the observed aggregates, the vertical offset should be much larger as measured with aid of the ROV cameras. The reason

for the reduction of the sinking velocities and thus, the accumulation of particulate matter could not be determined. We suggest density gradients but unfortunately the evaluated CTD data did not support this suggestion.

5. Conclusions and outlook

The research presented in this PhD thesis entitled “*Distribution and transportation pathways of marine particulate matter off Northwest Africa*” was carried out in the frame of the *DFG-Research Center Ocean Margin (RCOM)* subproject C5 “*Balance of particle transport to the deep-sea*” and *DFG-Researchproject “Marine Aggregates and transportation”*.

Addressing the scientific goals described in Chapter 1.1, the following conclusions can be drawn:

The vertical distribution of particulate matter differs substantially between the three areas of investigation (Cape Blanc, Dakhla, Cape Bojador) but is comparable within each area. Apart from the regional, oceanographic settings like water depth, water chemistry and physics or current activities, the most influencing factor are the primary production conditions. Particle concentrations in the water column are in the first instance related to the amount of material, produced in the surface waters. For instance, within the highly dynamic upwelling belt off Cape Blanc, concentrations in the euphotic zone are up to 4 times higher compared to the lower productive region off Cape Bojador. This connection could be seen in the comparison of the particle concentrations in the surface waters and the satellite derived pigment concentrations.

Low productivity areas (Dakhla/Cape Bojador) are characterised by more or less constant particle concentrations below the euphotic zone to above the seafloor. The export of material from the euphotic zone is much smaller and occurs much slower compared to the high productive area off Cape Blanc. Here, the exceeding particle dynamics of aggregation and increased flux by rapidly sinking aggregates clearly show a very close coupling between the sea surface and the sediment. Large, coagulated aggregates continuously transfer large amounts of material to the seafloor. Additionally, the in-situ detection of a sinking event as described here within the water column, confirms the close link between the ocean surface and seafloor in this highly dynamic upwelling region. Comparable transport processes could not be detected in the remaining areas of investigation off Dakhla or Cape Bojador.

While off Cape Blanc particulate matter is transferred on short temporal scales to the deep-sea, the region off Cape Bojador is more likely influenced by huge lateral intrusions.

This offshore-vectored mechanism transfers large amounts of material from the shelf or upper slope areas, towards the open ocean. Particle concentrations within the advected cloud are three times higher compared to the ocean surface and the cloud is several hundred metres in height. No indications for a similar input of lateral advected material were observed off Cape Blanc. A simplified model of the described processes is shown in Figure 9.

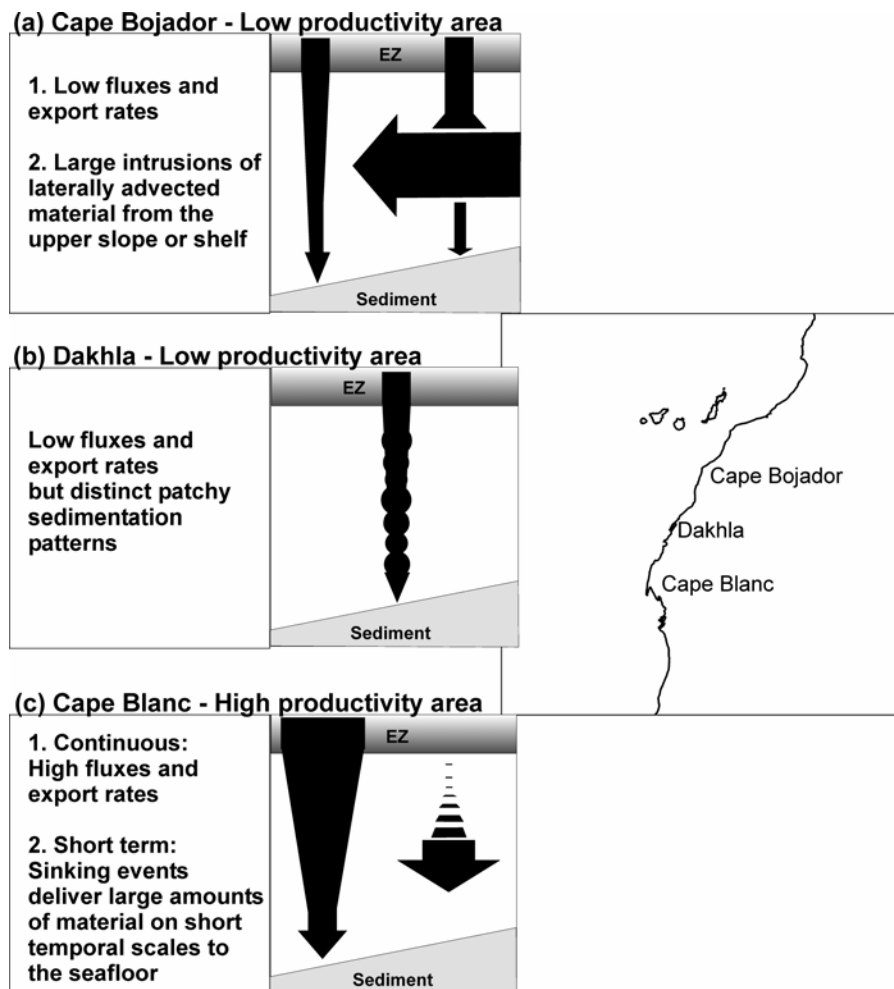


Fig. 9: Simplified transport models of the investigation areas.

(a) The Cape Bojador stations are located in a low productivity area with comparably low flux rates. The amount of material exported from the euphotic zone (EZ) and the amount finally reaching the seafloor does not considerably differ. The even size distribution in water column leads to an evenly sedimentation of particles. The region is influenced by huge intrusions (700 m in height) of laterally advected material from the upper slope or shelf areas. Small particles are accumulated along the upper boundary of the intrusion, which is related to the resulting shear stress between the intrusion and the remaining water column. In addition, this process prohibits a further supply of material below the intrusion.

(b) The Dakhla sites are likewise located in an area of low productivity. Flux rates are comparable with the Cape Bojador region. The difference is seen in the patchy sedimentation patterns, caused by the uneven particle size distribution. The observed, erratical size distribution is related to higher aggregation and disaggregation processes.

(c) Cape Blanc is the region with the closest coupling between surface water and seafloor. Large amounts of material are continuously delivered to the seafloor by fast sinking, large aggregates. Approximately 1/4 of the material produced in the euphotic zone reaches the seafloor. In addition, sinking events transfer large amounts of material from the euphotic zone to the deep-sea on short temporal scales (few weeks to several days).

The major goal of this work was to obtain particle distributions in the water column and to detect particle transport processes in-situ. The transport processes and particle distributions could be characterised and described by the high-resolution size distribution datasets. This parameter proved to be valuable for acquiring the alteration of particle sizes in the water column. More attention will be paid to the particle volumes in future studies. This parameter possibly reflects alterations of particles in a similar way, because it is directly deduced from the particle sizes.

A more detailed differentiation of particles in the ocean is necessary. The classification into smaller *Marine snow* and *Marine snow* is not sufficient for the description of complex particle dynamics. The distinction of large, coagulated aggregates, from spherically shaped particles and suspended material shows the different roles and characteristics of different particle populations in terms of distribution and flux. Hence, a detailed nomenclature of particles in the ocean was proposed in manuscript 2 (p. 65).

Although the profiles have a huge potential to acquire important processes in the water column, simultaneously obtained datasets like CTD, turbidity, oxygen, etc., are necessary to examine the accumulation processes of particles. The accumulation of small particles at the upper boundary of the lateral intrusion at site GeoB 7425 (Manuscript 2, p. 65) was related to changes in the density structure, however this relationship could not be proved due to the unfortunate lack of additional data. The conclusiveness of particle data is enhanced, when they can be compared with datasets obtained with other devices. For future studies, it is inevitable to use optical datasets in combination with methods such as sediment traps and other in-situ data. A complete image of the vertical flux can only be drawn when there are sufficient simultaneous data on the temporal variability of camera profiles, satellite data, trap fluxes and in-situ measurements of aggregate settling velocities.

Since then, accurate sinking velocities and the knowledge of individual particle characteristics, like density or composition, are of major interest. Unfortunately, quantitative measurements of sinking velocities could not be provided in this thesis due to the methodical complexity and technical difficulties in measuring sinking speeds. However, the different results with respect to sinking speeds and behaviour published in the literature and in manuscript 3 (p. 95), emphasize the importance of further studies on this subject. With modifications of the ROV, discrete measurements of the settling velocities of individual aggregates can be carried out. In addition, the sampling of individual aggregates with the ROV might play a key role for more accurate estimates on the vertical flux. The information about composition, settling speeds and density can be used to develop a particle catalogue,

providing characteristics of different particle classes or populations. With aid of vertical profiles, the abundance of each particle class might be determined and a differentiated flux calculation for each particle class could be applied.

To track short term transport events such as rapid sinking clouds or lateral intrusions, it might be reasonable to deploy the camera in time intervals of several days at one site during a cruise. A for instance sinking event could be tracked on its way through the water column until it finally reaches the seafloor. This deployment strategy might increase our understanding of these transport processes.

Moreover, modelling becomes an important branch with respect to particle flux studies. Modellers are dependent on information about the spatial distribution of particles, their sizes and sinking speeds. The obtained datasets might contribute to more detailed models in the near future.

Danksagung

Ich möchte mich sehr herzlich bei Prof. Dr. Gerold Wefer für das geschenkte Vertrauen bedanken, meine Partikelstudien mit Hilfe von optischen Systemen über die Diplomarbeit hinaus fortzusetzen zu können. Insbesondere bedanke ich mich für die einmalige Möglichkeit, mit dem neuen Tauchrobotersystem gearbeitet haben zu dürfen. Die ROV Einsätze an Bord waren stets ein echtes Highlight und werden mir ewig in Erinnerung bleiben. Bei Frau Dr. habil. Uta Passow bedanke ich mich herzlich für die spontane Übernahme des Zweitgutachtens und die zahlreichen, äußerst fruchtbaren Treffen im AWI-Bremerhaven. Ihr Interesse an den Ergebnissen der Arbeit, war für mich eine große Motivation über den gesamten Zeitraum.

Dr. Volker Ratmeyer ist während der letzten Jahre immer wieder Motor für die Weiterentwicklung von ParCa gewesen. Abgesehen von der unermüdlichen, technischen Betreuung, waren die Gespräche und Treffen auch über das Berufliche hinaus, eine große Hilfe und Stütze. Sein Wirken hat maßgeblich an der Fertigstellung dieser Arbeit beigetragen.

Ein großes Dankeschön geht an meine Kollegen Tim Freudenthal, Gerhard Fischer, Helge Meggers, Helen McGregor und Oscar Romero für die vielen, konstruktiven Gespräche. Außerdem möchte ich mich für das exzellente Arbeitsklima an der Uni, und im Marum bedanken: Gerrit Meinecke, Christoph Waldmann, Markus Bergenthal, Götz Ruhland, Steffen Klar, Jens Renken, Thorsten Klein sowie Eberhard Kopiske. An die diversen Feierabendtreffen mit Peer Helmke und Holger Kuhlmann erinnere ich mich immer wieder gern. Für die ausgezeichnete technische Unterstützung bedanke ich mich bei der Geo-Werkstatt: Klaus Dehning, Felix Schewe, Daniel Hüttig und Sebastian Spilker. Desweiteren bei den *Außendienstmitarbeitern* Uwe Rosiak und Werner Schmidt.

Bei der internationalen Forschergemeinschaft möchte ich mich für die unkomplizierte Hilfe und Beantwortung von Anfragen meinerseits bedanken. Diese sind Alice Alldredge, Wilford Gardner, Cynthia Pilskaln und William Hamner.

Die Erhebung der hier präsentierten Daten wäre ohne die Mithilfe der Besatzungen von RV Meteor und RV Poseidon nicht möglich gewesen. Das ausgesprochen kollegiale Miteinander und das Leben an Bord, haben mich immer wieder aufs Neue beeindruckt.

Für den privaten Rückhalt bedanke ich mich bei meinen Brüdern Alexis und Jérôme, den vermutlich weltweit größten Fans der Bremer Tauchrobotersysteme außerhalb der Uni, sowie meinen Eltern Peter und Lina für das rege Interesse an der Meeresforschung und meiner Arbeit. Mein abschließender Dank geht an meine Freundin Alexandra, für die unermüdliche Unterstützung und Aufmunterung während der letzten 3 Jahre.